PB81-196560

The Effects of a Squat Building on Short Stack Effluents: A Wind Tunnel Study

(U.S.) Environmental Sciences Research Lab.
Research Triangle Park, NC

Dec 80

U.S. Department of Commerce
National Technical Information Service
NTIS

United States
Environmental Protection
Agency

Environmental Sciences Research
Laboratory
Research Triangle Park NC 27711

EPA-600/4-80-055
December 1980

Research and Development

PB81-156560

EPA

The Effects of a Squat Building on Short Stack Effluents

A Wind Tunnel Study

PRODUCT OF:
NATIONAL TECHNICAL
INFORMATION SERVICE
U.S. DEPARTMENT OF COMMERCE
SPRINGFIELD, VA. 22161

RESEARCH REPORTING SERIES

Research reports of the Office of Research and Development, U.S. Environmental Protection Agency, have been grouped into nine series. These nine broad categories were established to facilitate further development and application of environmental technology. Elimination of traditional grouping was consciously planned to foster technology transfer and a maximum interface in related fields. The nine series are:

1. Environmental Health Effects Research
2. Environmental Protection Technology
3. Ecological Research
4. Environmental Monitoring
5. Socioeconomic Environmental Studies
6. Scientific and Technical Assessment Reports (STAR)
7. Interagency Energy-Environment Research and Development
8. "Special" Reports
9. Miscellaneous Reports

This report has been assigned to the ENVIRONMENTAL MONITORING series. This series describes research conducted to develop new or improved methods and instrumentation for the identification and quantification of environmental pollutants at the lowest conceivably significant concentrations. It also includes studies to determine the ambient concentrations of pollutants in the environment and/or the variance of pollutants as a function of time or meteorological factors.

This document is available to the public through the National Technical Information Service, Springfield, Virginia 22161.

TECHNICAL REPORT DATA
(Please read Instructions on the reverse before completing)

1. REPORT NO.	2.	3. RECIPIENT'S ACCESSION NO.
EPA-600/4-80-055		PB81 196560

4. TITLE AND SUBTITLE
THE EFFECTS OF A SQUAT BUILDING ON SHORT STACK EFFLUENTS
A Wind Tunnel Study

5. REPORT DATE
December 1980

6. PERFORMING ORGANIZATION CODE

7. AUTHOR(S)
Alan H. Huber, William H. Snyder
Roger S. Thompson, and Robert E. Lawson, Jr.

8. PERFORMING ORGANIZATION REPORT NO.
Fluid Modeling Report No. 8

9. PERFORMING ORGANIZATION NAME AND ADDRESS
Environmental Sciences Research Laboratory
Office of Research and Development
U.S. Environmental Protection Agency
Research Triangle Park, NC 27711

10. PROGRAM ELEMENT NO.
1AA603

11. CONTRACT/GRANT NO.

12. SPONSORING AGENCY NAME AND ADDRESS
Environmental Sciences Research Laboratory - RTP,NC
Office of Research and Development
U.S. Environmental Protection Agency
Research Triangle Park, NC 27711

13. TYPE OF REPORT AND PERIOD COVERED
In-house

14. SPONSORING AGENCY CODE
EPA/600/09

15. SUPPLEMENTARY NOTES

16. ABSTRACT

In a wind tunnel study, the influence of the highly turbulent region found in the lee of a model building upon plumes emitted from short stacks was examined through smoke visualization and tracer gas concentration mappings. The study was conducted in the Meteorological Wind Tunnel of the EPA Fluid Modeling Facility. A thick, simulated atmospheric boundary layer was used to provide background dispersion. A rectangular shaped building with its length equal to twice its height and width was oriented perpendicular to the approaching wind. In all phases of this study each situation was repeated with the building removed. This allowed for a simple demonstration of the building wake effects. A simple mathematical model provided good estimates of concentrations in the building wake. The building influence was found to be reduced with increases in the effective source height. Application of the "2 1/2 times rule," that is, an effective source height greater than 2 1/2 times the height of the building, avoids significant influence by the building on the maximum ground-level concentration.

17. KEY WORDS AND DOCUMENT ANALYSIS

a. DESCRIPTORS	b. IDENTIFIERS/OPEN ENDED TERMS	c. COSATI Field/Group
Air pollution		13B
* Wind tunnels		14B
* Chimneys		13M
* Height		20D
* Downwash		04A
* Atmospheric Diffusion		

18. DISTRIBUTION STATEMENT	19. SECURITY CLASS (This Report)	21. NO. OF PAGES
RELEASE TO PUBLIC	UNCLASSIFIED	
	20. SECURITY CLASS (This page)	22. PRICE
	UNCLASSIFIED	

EPA Form 2220-1 (9-73)

EPA-600/4-80-055
December 1980

THE EFFECTS OF A SQUAT BUILDING ON SHORT STACK EFFLUENTS A Wind Tunnel Study

by

Alan H. Huber
Monitoring and Data Analysis Division
Office of Air Quality Planning and Standards
Research Triangle Park, North Carolina 27711

William H. Snyder
Roger S. Thompson
Meteorology and Assessment Division
Environmental Sciences Research Laboratory
Research Triangle Park, North Carolina 27711

and

Robert E. Lawson, Jr.
Northrop Services, Inc.
Research Triangle Park, North Carolina 27711

ENVIRONMENTAL SCIENCES RESEARCH LABORATORY
OFFICE OF RESEARCH AND DEVELOPMENT
U.S. ENVIRONMENTAL PROTECTION AGENCY
RESEARCH TRIANGLE PARK, NORTH CAROLINA 27711

DISCLAIMER

This report has been reviewed by the Environmental Sciences Research Laboratory, U.S. Environmental Protection Agency, and approved for publication. Mention of trade names or commercial products does not consitute endorsement or recommendation for use.

AFFILIATION

William H. Snyder is a physical scientist in the Meteorology and Assessment Division, Environmental Sciences Research Laboratory, U.S. Environmental Protection Agency, Research Triangle Park, North Carolina. He is on assignment from the National Oceanic and Atmospheric Administration, U.S. Department of Commerce.

ABSTRACT

In a wind tunnel study, the influence of the highly turbulent region found in the lee of a model building upon plumes emitted from short stacks was examined through smoke visualization and tracer gas concentration mappings. The study was conducted in the Meteorological Wind Tunnel of the EPA Fluid Modeling Facility. A thick, simulated atmospheric boundary layer was used to provide background dispersion. A rectangular-shaped building with its length equal to twice its height and width was oriented with the length perpendicular to the approaching wind. In all phases of the study each smoke or tracer release from the stack was repeated with the building removed. This allowed for a simple demonstration of the building wake effects.

Through smoke visualization, a region of recirculating flow was found to extend four building heights downwind from the leading edge with a maximum height and halfwidth of 1.5 building heights. As the highly turbulent flow from this region was transported downstream, it was observed to decay rapidly.

A stack emitting an air-methane mixture was placed midway along the leeward side of the building to examine dispersion in the wake for a variety of source heights. Oscillations of the flow in the immediate wake of the building caused an unsteadiness in the plume that greatly enhanced the vertical dispersion. For the ground source situation, where the plume was emitted directly into the cavity, rapid horizontal spreading also occurred. A convergence of the ground-level concentration to values measured in the absence of the building was found to occur in the far wake region where only a residual influence of the building wake was found. A simple mathematical model provided good estimates of concentrations in the building wake. The building influence was found to be reduced with increases in the effective source height. Application of the "2.5 times rule", that is, an effective source height at 2.5 times the height of the building, resulted in maximum ground-level concentration in the wake being 20 percent higher than found in the absence of the building. A stack 1.5 times the height of the building resulted in maximum ground-level concentrations in the wake being 250 percent higher, which is a far more significant effect.

CONTENTS

ABSTRACT..... iii
FIGURES..... vi
TABLES..... viii
ABBREVIATIONS AND SYMBOLS..... ix
ACKNOWLEDGEMENTS..... x

1. INTRODUCTION..... 1
2. CONCLUSIONS AND RECOMMENDATIONS..... 4
3. DESIGN OF EXPERIMENT..... 6
   - Experimental equipment..... 6
   - Similarity criteria..... 7
   - Experimental plan..... 14
     - Phase I: Flow visualization..... 14
     - Phase II: Concentration measurements..... 16
     - Phase III: Measurements farther downstream..... 17
4. RESULTS..... 18
   - Phase I: Observations of smoke plumes..... 18
   - Phase II: Concentration fields..... 21
     - Plume rise..... 21
     - Characterization of wind tunnel dispersion..... 23
     - Isolated stack data compared with Gaussian Plume Model.... 27
     - The effects of the building..... 31
     - Modified Gaussian Model..... 31
   - Phase III: Measurements to 30 building heights downstream.. 35

REFERENCES..... 46

APPENDIX..... 49

Preceding page blank

LIST OF FIGURES

Number	TITLE	Page
1	Diagrammatic outline of the envelope and cavity regions in the wake of a building (vertical section).....	2
2	Diagrammatic sketch of the wind tunnel and experimental arrangement.....	9
3	Velocity and turbulence intensity measurements, U_r=2.34 m/s..	10
4	Velocity and turbulence intensity measurements, U_r=4.34 m/s..	11
5	Vertical wake cavity and envelope measurements.....	19
6	Lateral wake cavity and envelope measurements.....	20
7	Lateral concentration profiles taken through the plume centerline; Case No. 17(1.5,0.042,1.5,1.0), isolated stack...	25
8	Vertical concentration profiles taken through the plume centerline; Case No. 17(1.5,0.042,1.5,1.0), isolated stack...	26
9	Estimated wind tunnel dispersion parameters compared with standard Pasquill-Gifford values (Turner, 1970).....	28
10	Vertical concentration profiles for isolated stack.....	29
11	Longitudinal ground-level concentration measurements downwind from isolated stacks.....	30
12	Longitudinal ground-level concentration measurements in the lee of the building; neutrally buoyant sources with $H_s/H_b \leq 1.5$.....	32
13	Longitudinal ground-level concentration measurements in the lee of the building; slightly buoyant sources with $H_s/H_b \leq 1.5$.....	33
14	Longitudinal ground-level concentration measurements in the lee of the building; $H_s/H_b \geq 1.5$.....	34

Number	TITLE	Page
15	Longitudinal ground-level concentration measurements for ground source; Case No. 1	36
16	Vertical concentration measurements for ground source; Case No. 1	37
17	Lateral ground-level concentration measurements for ground source; Case No. 1	38
18	Longitudinal ground-level concentration profiles for elevated sources based on the Gaussian model using an adjusted vertical σ from Case No. 1	39
19	Vertical concentration measurements; Case No. 17 (1.5,0.042,1.5,1.0)	40
20	Lateral concentration profiles; Case No. 17(1.5,0.042, 1.5,1.0)	41
21	Longitudinal ground-level concentration measurements; Phase III	42
22	Vertical concentration measurements for ground-source; Case No. 1, Phase III	44
23	Lateral ground-level concentration profiles for ground source; Case No. 1, Phase III	45

LIST OF TABLES

Number	Title	Page
1	Experimental Cases	15
2	Plume Rise From the Isolated Stacks	22
3	Summary of Effect of Building on Plume Rise	24

LIST OF ABBREVIATIONS AND SYMBOLS

B -- building width (in streamwise direction)
D_s -- stack diameter
F -- buoyancy flux
Fr -- stack Froude number
g -- gravitational constant
H_b -- building height
H_e -- effective plume height
H_s -- stack height
K -- constant
L -- building length (in cross-streamwise direction)
Q -- pollutant emission rate
Re_b -- building Reynolds number
Re_s -- stack Reynolds number
S -- virtual source location
$\overline{(u^2)}^{1/2}$ -- standard deviation of velocity fluctuations
U -- average velocity in x-direction
U_r -- average velocity in x-direction at reference height
U_s -- average velocity in x-direction at height of stack
W_s -- stack effluent exit velocity
x -- cartesian coordinate (streamwise)
y -- cartesian coordinate (cross-streamwise)
z -- cartesian coordinate (vertical)
β -- plume entrainment coefficient
Δh -- plume rise
ρ_a -- ambient air density
ρ_s -- stack effluent density
σ' -- enhanced dispersion parameter (with building effects)
σ_y -- horizontal dispersion parameter
σ_z -- vertical dispersion parameter
ν -- kinematic viscosity
χ -- pollutant concentration
$(\ )_F$ -- field value
$(\ )_M$ -- model value

ACKNOWLEDGMENTS

We are grateful to David Lombardi and Robert Flemming, both of Northrop Services, Inc., for their great care in collecting and filing the measured data.

SECTION 1

INTRODUCTION

The entrainment of plumes emitted from short stacks into the wakes of buildings can result in maximum ground-level concentrations that are significantly greater than those found for similar sources in the absence of buildings. The complex flow patterns introduced by the buildings prohibit accurate determination of air quality concentrations close to buildings through the use of the basic Gaussian plume model and associated dispersion parameters (Turner, 1970) without substantial modifications.

The presence of the building creates surface friction and adverse pressure gradients that result in separation of the flow from the building surface. In the classical "cavity" (also termed "bubble") of Halitsky (1968), the separation line from the top upwind edge of the building reattaches to the ground downstream of the building to enclose a zone of recirculating flow. Mean velocities within this cavity are generally weak, but the turbulence is vigorous, resulting in wild oscillations of the size and shape of the instantaneous cavity boundary. This conceptual cavity of Halitsky (1968) has been contested, however, by Britter, et al. (1976) for a three-dimensional building. A practical definition of such a cavity is shown by the boundary ABCDEA in Figure 1 and is further discussed under "Experimental Plan" in Section 3.

The far wake (region downstream of the reattachment point) is characterized by enhanced dispersion rates, which progressively diminish to background levels downwind. The upper bound of the wake displacement region will in this presentation be called the "envelope". A general outline of the building wake regions is presented in Figure 1.

The extent of the wake region is undoubtedly a function of building shape and size as well as the turbulence levels in the approach flow. The downwind extent of the cavity increases when the building length (perpendicular to the wind direction) is increased. This fact, as well as many intricacies, was examined by Evans (1957). For further discussion of the flow in the wakes of buildings, see, for example, Halitsky (1968), Meroney (1971), Meroney and Yang (1971), and Robins and Castro (1977a,b). These papers report on experiences gained from extensive wind tunnel studies. Mathematical models for predicting concentrations in different parts of the flow field near buildings can be found in Britter, et al. (1976).

Since, for each situation, the building effects are somewhat unique, fluid modeling is ideally suited. Detailed concentration mappings around models can be made with little time and expense in comparison with those involved in full-scale studies. Plume behavior resulting from aerodynamic effects induced by

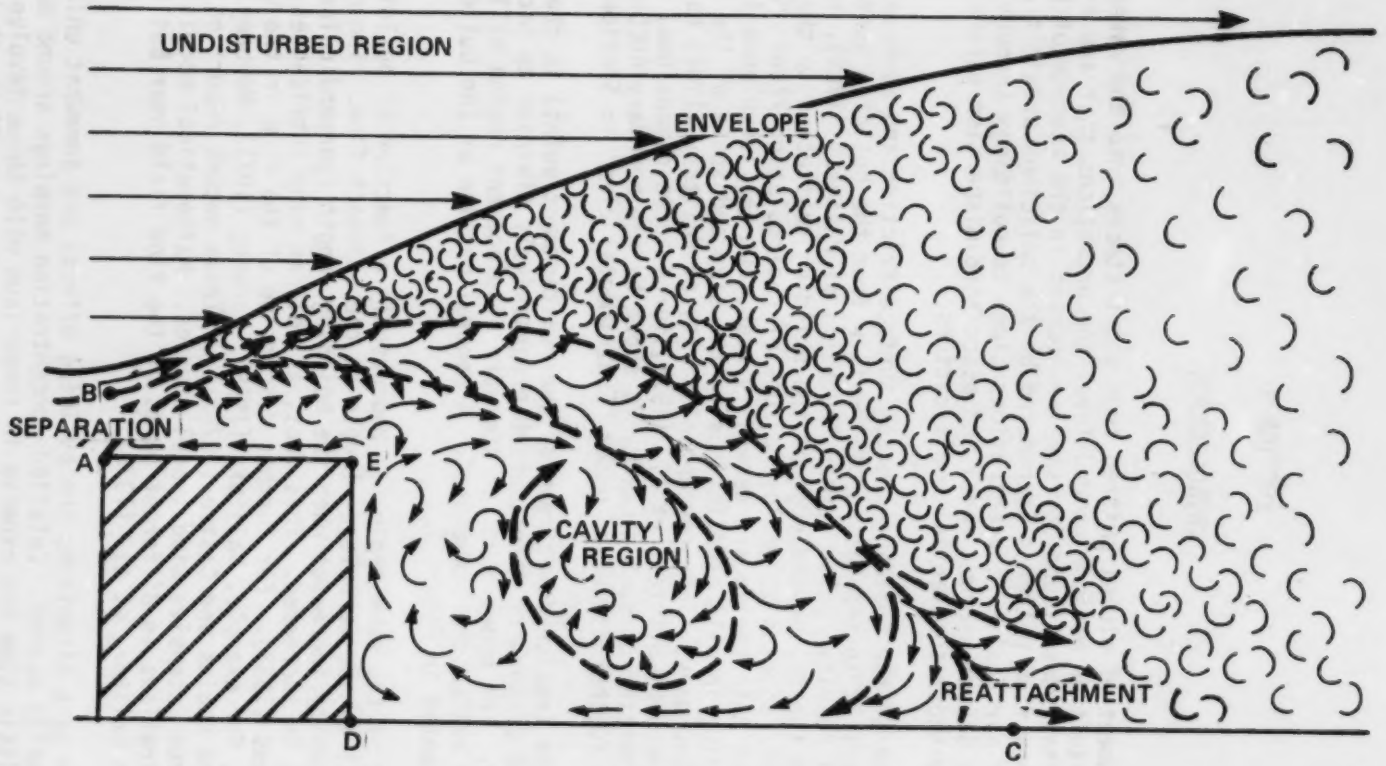

Figure 1. Diagrammatic outline of the envelope and cavity regions in the wake of a building (vertical section).

the buildings can be simulated with essential variables controlled and examined at will.

Many studies and discussions concerning the dispersion of stack effluents into the wakes of buildings are found in the literature. No attempt is made to report on these papers. The general engineering "rule of thumb" for avoiding plume downwash into the wake of a building is to keep the height of the stack "2.5 times" the height of the building. The rule apparently arose in the early part of this century as a working rule used by the British electricity industry to determine chimney heights. Years of practice have substantiated this rule as generally sufficient, but it is not always necessary. The rule, in particular, is not applicable to tall, thin buildings (Snyder and Lawson, 1976).

There is a need for study and clarification of the rather complex effects that buildings can have on plume entrainment. There is little consensus as to the best way to estimate ground-level concentrations for plumes that are entrained within building wakes. This wind tunnel study was conducted to examine building wake effects upon short stack effluents and to provide data for evaluating models used to estimate concentrations there.

In this study the general features of plume dispersion in the wake of a squat building (a building with its height less than either its width or length) were examined. A rectangular-shaped building with its length equal to twice its height and width was selected. The long side of the building was oriented perpendicular to the approaching wind. The stack was placed midway along the leeward side of the building. A variety of combinations of the ratios of stack height to building height, stack diameter to building height, stack effluent speed to wind speed at the top of the stack, and the stack effluent density to ambient air density were modeled.

The study consisted of three major phases. Phase I involved smoke visualization of the plumes and the cavity and wake envelope leeward of the building. In phases II and III, tracer gas concentration measurements were made to define plume dispersion downwind of the building. In all phases of this study, each case was repeated with the building removed. This allowed for a simple demonstration of the wake effects.

SECTION 2

CONCLUSIONS AND RECOMMENDATIONS

The turbulent wake in the lee of the model building was found through smoke visualization and tracer gas concentration mappings to be roughly axisymmetric. The cavity region immediately leeward of the building was found to be highly turbulent. The downwind extent of the cavity region, characterized by a recirculating flow, was found to extend four building heights downwind from the leading edge of the building. The maximum depth and half-width of the cavity region were found to be 1.5 building heights and to occur midway between the windward edge of the building and the leeward end of the cavity. This is in general agreement with measurements of the depth and extent of the cavity reported in the literature for similar buildings. In the lee of a two-dimensional obstruction, the cavity region was reported to extend up to 10 heights downwind (Huber, et al. 1976) with a maximum depth of 1.8 heights. The lateral air motion that was able to flow around the three-dimensional building resulted, as expected, in a smaller extent of the cavity. The high intensity turbulence found close to the building rapidly decayed as it was transported downwind. The axisymmetry of the building wake was likely a result of the building design (height equal to one-half the length) and the orientation of the building perpendicular to the wind. Other building designs or orientations may produce a quite different structure of the wake, particularly close to the building.

Dispersion in the simulated atmospheric boundary layer in the absence of the building was found to be well described by Pasquill-Gifford Category C - D dispersion parameters. Since dispersion in the absence of any building influence was characterized, the examination of dispersion under the influence of the building resulted in a straight-forward demonstration of the building effects.

Oscillations in the leeward cavity size and shape were observed to cause unsteadiness in the plume that greatly enhanced the vertical dispersion in the immediate wake of the building. When the plume was emitted into the cavity from the ground, rapid horizontal spreading also occured. A simple mathematical model (a Gaussian plume model with enhanced dispersion parameters) was tested against the wind tunnel concentration mappings. The model was found to perform well when the effective source height was less than two building heights. The building influence was found to be greatly reduced with an increase in the effective source height to 2.5 times the building height. The building also affected the rise of the plume. A lowering of the plume centerline height resulted both from increased entrainment of the plume and a general down-drafting of the plume in the wake of the building. In the region beyond 10 building heights, where dispersion of the plume was controlled by background atmospheric turbulence, the net building wake effects were found to be simply accounted for

by changing the effective source location (virtual source). A convergence of the ground-level concentration in the wake of the building to the value measured ir the absence of the building was found to occur in the far wake region.

This study was conducted to examine the general influence of a squat building upon plume entrainment and to provide data that would be useful to an evaluation of presently available methods used to estimate concentrations from stacks near buildings. Sources placed away from the building should be influenced less than was observed in this study. The results are applicable primarily to neutral or slightly unstable atmospheric conditions. Because of the rather complex effects that buildings can have on plume entrainment and the likely variation with each unique situation, additional study is needed to provide further clarification. Further study and guidance is important because the entrainment of plumes emitted from short stacks into the wakes of buildings can result in maximum ground-level concentrations that are significantly greater than those found for similar sources in the absence of buildings.

SECTION 3

DESIGN OF EXPERIMENT

EXPERIMENTAL EQUIPMENT

The study was conducted in the Meteorological Wind Tunnel of the U.S. Environmental Protection Agency's Fluid Modeling Facility. The wind tunnel has a test section 3.7 x 2.1 x 18.3 m. The flow speed within the wind tunnel can be controlled between 0.3 and 10 m/s. Further details of the wind tunnel may be obtained from Snyder (1979a).

For mean velocity and turbulence intensity measurements, a Thermo-Systems, Inc., Model 1054A anemometer was used in conjunction with their Model 1210-20 cylindrical hot-film probes. Signals were fed to a Thermo-Systems Model 1057 signal conditioner and then to a Digital Equipment Corporation PDP-11/40 minicomputer for A/D conversion and processing. Reported measurements are for one-minute averaging times, which were found to yield reasonably stable values.

For making concentration measurements, methane was mixed with the stack gases as a tracer. The amount of methane in the effluent was 1% by volume for all except those concentration measurements taken beyond 15 building heights downwind, where 4% was needed to increase precision. At selected positions, a sample gas stream was drawn through a 0.16 cm i.d. metal probe that was connected by Teflon tubing to a Beckman Model 400 Hydrocarbon Analyzer, which is a flame ionization detector. The sample flow rate through the probe was 200 cm^3/min, of which a 15 cm^3/min sample was diverted through the analyzer. The 0.5 s response time of the analyzer was too long to permit examination any dispersion microstructure. Instead, concentrations were averaged over a sufficiently long time period (one min.) to represent steady-state values. The output from the hydrocarbon analyzer was also digitized and processed on the minicomputer.

The hydrocarbon analyzer has a linear response for concentrations less than about 4%. The analyzer scale was first zeroed by sampling bottled air, which contained less than 0.5 ppm hydrocarbons. The upper limit of the

scale was set by sampling the stack effluent stream. Pollutant concentrations down to dilution levels of 1:10,000 can be accurately measured. Background concentrations were carefully monitored. The change in background concentration during the period of measurement was generally small (of the order of 1/10,000th of the stack concentration). A linear time dependence was assumed and found to quite adequately account for the change in background; in processing the data, the background was first subtracted out. In the regions of lowest concentration (outer fringe of the plume), where measured concentrations were of the order of the change in the background, measurements cannot be considered to be as accurate.

A smoke generator was used for the visualization of the stack effluent path. The oil-fog generator was connected in-line with the stack air line. Photographs of the side views of the smoke plumes were taken using a 35 mm camera with a 135 mm lens. The camera was mounted 10 m perpendicularly to the plume centerline. A four-second continuous exposure on ASA 400 film was used to provide the photographs shown in this report.

SIMILARITY CRITERIA

In order to insure that the flow in the model simulates that under full-scale atmospheric conditions, it is necessary to meet certain similarity criteria. Various nondimensional parameters must be matched in model and prototype. Discussions of similarity criteria can be found, for example, in Snyder (1972, 1979b), Cermak (1971), and Halitsky (1969). Since this study is concerned only with neutrally stable atmospheric flows and relatively small scales, the Richardson and Rossby numbers may be ignored. In modeling buoyant stack effluents, however, the stack Froude number is important. The parameters of significance are as follows;

$$\frac{L}{H_b}, \frac{B}{H_b}, \frac{\delta}{H_b}, \frac{U}{U_r}, \frac{(\overline{u^2})^{1/2}}{U}, \frac{H_s}{H_b}, \frac{D_s}{H_b}, \frac{W_s}{U_s}, \frac{\rho_s}{\rho_a},$$

$$\frac{W_s}{[gD_s(\rho_a-\rho_s)/\rho_a]^{1/2}}, \frac{W_s D_s}{\nu}, \frac{U_r H_b}{\nu}.$$

The first two of these parameters are easily matched by constructing a scale model. The model building, 25 cm in height, was constructed with a length (perpendicular to the wind) to height ratio, L/H_b, of 2:1 and a width to height ratio, B/H_b, of 1:1.

In performing fluid modeling studies, it is important to simulate the atmospheric boundary layer. A method similar to that of Counihan (1969), which uses a barrier at the test section entrance slightly upstream from vortex generators, was used to produce a thick, simulated atmospheric boundary layer. These experiments used a 0.38 m high castellated barrier placed at the test section entrance followed immediately by four 1.83 m high semi-elliptic wedge-shaped vortex generators. These were followed by 0.019 x 0.051 m roughness slats placed downstream at 0.457 m intervals to maintain the boundary layer in equilibrium. A previous experimental study showed the boundary layer to maintain equilibrium and uniformity beyond 8 m downwind from the vortex generators. The model building was placed 9 m downwind from the vortex generators for all experiments except part of those in Phase III, where the building was moved 2.5 m upwind. A sketch of the experimental arrangement is shown in Figure 2.

Mean velocity and turbulence intensity measurements taken at the building location and at 10 building heights downwind are shown in Figures 3 and 4. All experiments were conducted under these conditions. Previous experimental study showed a free-stream velocity greater than 1.5 m/s was necessary for the development of an equilibrium boundary layer.

The depth of the boundary layer δ was 1.8 m. This fixed the boundary layer thickness to building height ratio δ/H_b equal to 7:1. The velocity profile U/U_r was found to fit a one-sixth power law, which is generally representative of neutral atmospheric flow over moderately smooth terrain (Davenport, 1963). The reference velocity U_r was measured at 1.5 H_b above the surface. The local turbulence intensity was 25 percent near the surface, which is also representative of neutral conditions over moderately smooth terrain (Harris, 1968).

A variety of combinations of ratios of stack height to building height H_s/H_b, stack diameter to building height D_s/H_b, stack effluent speed to wind speed at the top of the stack W_s/U_s, and the stack effluent density to ambient air density ρ_s/ρ_a were modeled.

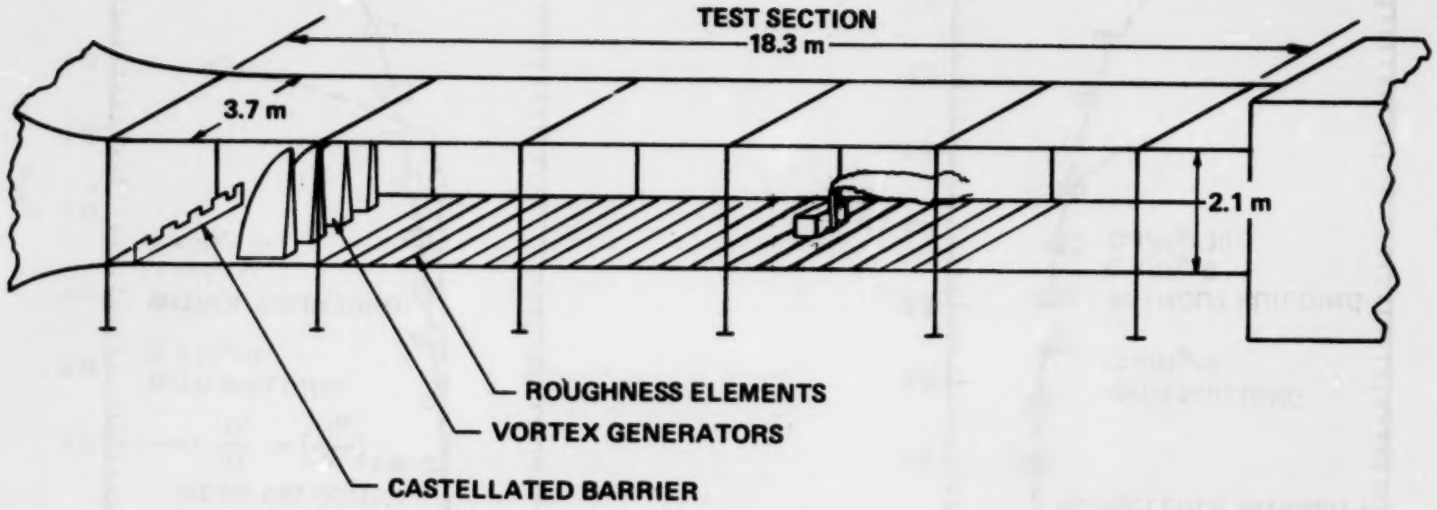

Figure 2. Diagrammatic sketch of the wind tunnel and experimental arrangement.

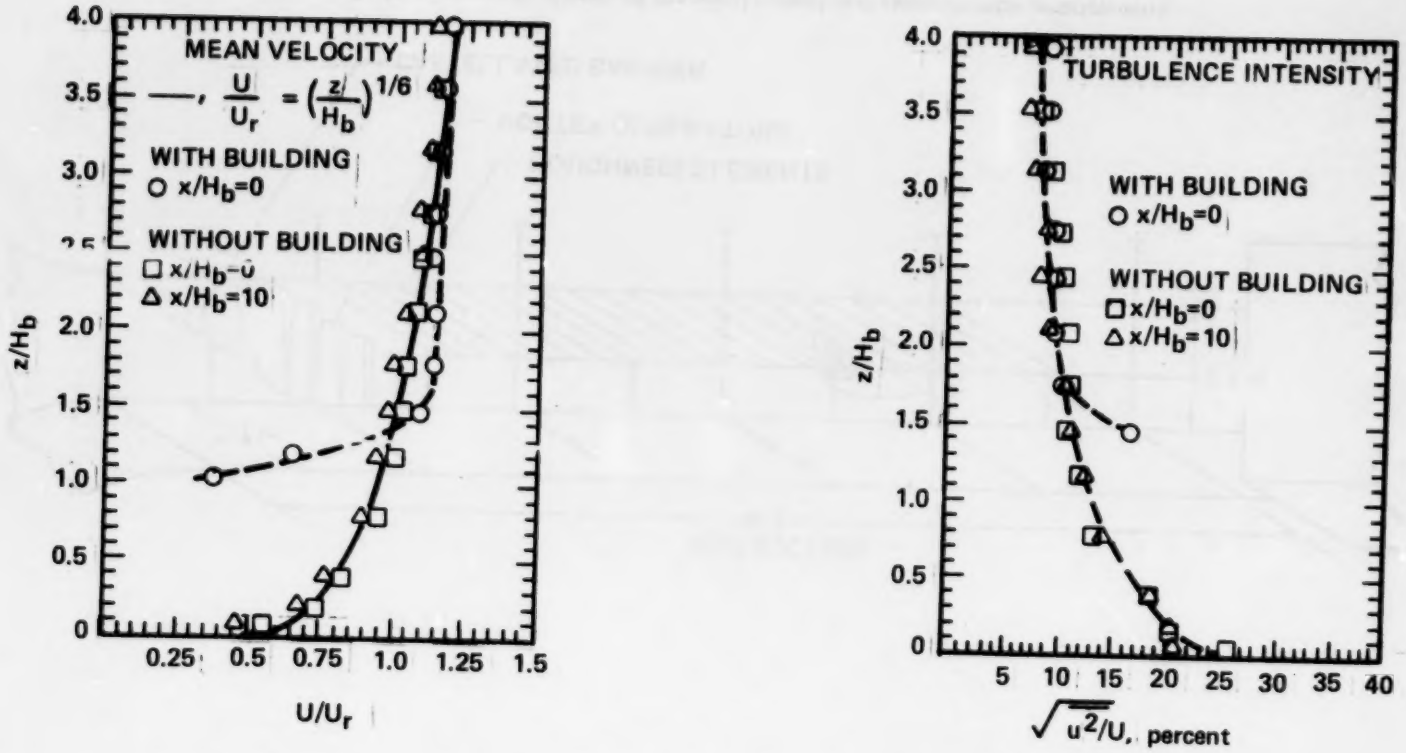

Figure 3. Velocity and local turbulence intensity measurements, U_r = 2.34 m/s (U_r = reference velocity at z/H_b = 1.5).

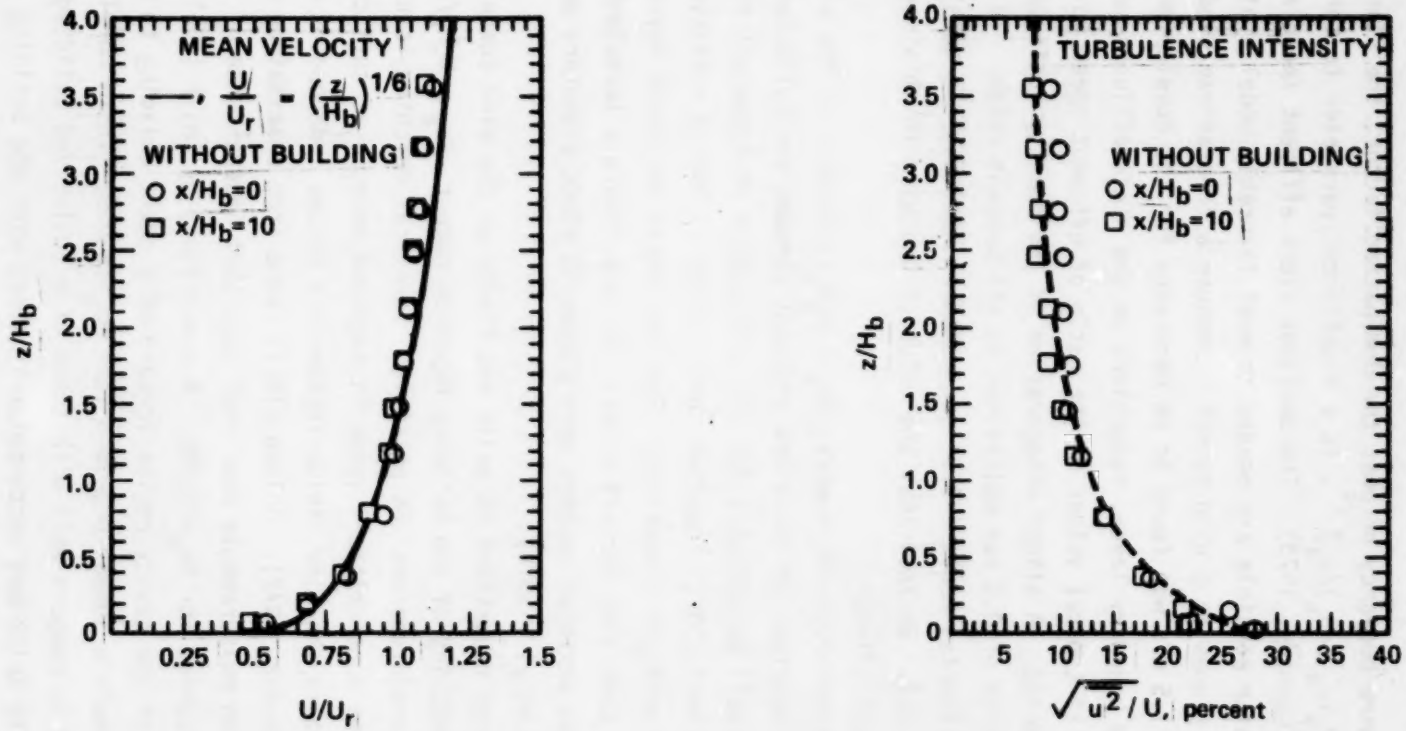

Figure 4. Velocity and local turbulence intensity measurements, U_r = 4.34 m/s (reference velocity at z/H_b = 1.5)

Plume rise near the stack is dominated by the momentum flux of the effluent, so that correct modeling of the ratio $\rho_s W_s^2 / \rho_a U_s^2$ is important. Farther downwind where buoyancy becomes the dominating factor, the stack Froude number, $Fr = W_s/[gD_s(\rho_a - \rho_s)/\rho_a]^{1/2}$, is a significant parameter to consider (Briggs, 1975, and Csanady, 1973). The smallest stack effluent speed and the largest stack diameter possible are needed to most favorably model typical buoyancy-dominated plumes in a wind tunnel. Because a free-stream wind tunnel speed greater than 1.5 m/s was found to be necessary for the development of a uniform equilibrium boundary layer, reductions in the stack effluent velocity are rather limited if typical values of the ratio of effluent speed to wind speed are to be modeled. A slight exaggeration of the density ratio $\Delta\rho/\rho_a$ was possible. A value of 0.5 was maintained in all buoyant cases. To avoid entrainment effects, Hoult (1973) suggested maintaining the density ratio at less than 0.4. We feel that the value of 0.5 used in this study introduced no unusual effects.

Matching the stack Reynolds number, $Re_s = W_s D_s/\nu$ where ν is the kinematic viscosity, is not important if the stack effluent streams are fully turbulent. A value of 2000 is well established for the maintenance of turbulent flow in a pipe. Hoult and Weil (1972) reported that a value of 300 is sufficient for modeling stack gas effluent situations. For this study the stack Reynolds number was greater than 1000 for all cases. To help insure a turbulent effluent stream, two serrated washers were placed 10 stack diameters upstream from the exit (Lin et al., 1974).

Because of large reductions in scale and limits on the wind tunnel air speed, identical matching of the building Reynolds number, $Re_b = U_r H_b/\nu$, between model and prototype was not possible. Identical matching is not required provided that some critical value is exceeded because at sufficiently large Reynolds numbers the flow fields fortunately become independent of Reynolds number (Snyder, 1972). Golden (1961) found from examination of tracer concentration measurements over roof tops that independence of Reynolds number occurred for $Re_b > 11{,}000$. A model study by Smith (1951) showed the extent of the cavity region leeward of a squat building to be independent of Reynold's number provided that $Re_b > 18{,}000$. These model results were found to compare well with those of a full-sized building. The building examined by Smith was rectangular in shape with the building length

(perpendicular to the wind direction) about twice the building height. This is similar in design to the one used in the present study where the building Reynolds number exceeded a value of 36,000 in all cases.

The choice of building height is a compromise. Large scale models permit a more refined network of sampling points and provide higher Reynolds numbers. In modeling situations where buoyant stack emissions are considered, larger scale models additionally permit smaller, more favorable, stack Froude numbers. However, the scale model size is limited by the test section size of the wind tunnel, hence, the simulated boundary layer depth. For this experimental study, a 1:200 scale model of a 50 m high prototype building would be an appropriate example. On this scale, the wind tunnel boundary layer (1.8 m) represents a 360 m deep atmospheric boundary layer.

Concentrations measured in the model are related to those that would be measured in the field over a time period where the background flow remained constant and similar to the model case (of the order of 10 min). For the situations modeled in this study, the stack effluent may be assumed to behave as if it were emitted from a point source. Thus, the field concentration χ_F is linearly related to the model concentration χ_M, to the inverse of the model emission rate Q_M, to the field emission rate Q_F, and to the dilution ratio $(U_r H_b^2)_M / (U_r H_b^2)_F$. The dilution ratio represents a comparison of a unit volume of flow in the model to the similar scaled volume in the full-scale flow. These basic relations result in the expression

$$\left(\frac{\chi U_r H_b^2}{Q}\right)_{\text{Field}} = \left(\frac{\chi U_r H_b^2}{Q}\right)_{\text{Model}} .$$

All concentration data are presented in the above nondimensional form. The reference velocity U_r was taken at an elevation of 1.5 building heights. The velocity at this position was found to be 85 percent of the free-stream value. The velocity at the top of the other stacks examined were within 10 percent of this value (except, of course, the ground level source).

EXPERIMENTAL PLAN

The main objective of this study was to examine the wake effects, from a typical building, upon effluents under a variety of stack exit conditions. This study examined 30 basic cases, whose stack conditions are shown in Table 1. For each case, an examination was made of the plume behavior with the building in position and then similarly repeated with the building removed. This allowed for a simple demonstration of the building wake effects.

The reference velocity was maintained at 2.32 m/s for all cases except those having a velocity ratio W_s/U_s equal to 0.4. For these cases the wind speed was increased to 4.34 m/s. Four different stack diameters were used. On a 1:200 scale, prototype stacks in the range of 1-10 m were thus modeled. The smaller diameters were used for the shorter stacks, and the largest diameter was used solely for the tallest stack. The lower Froude number situations (Case Nos. 3, 14, 16, 22, 24, 28, 30), for example, are representative on a 1:200 scale of a stack effluent with a gas temperature of 600 K and exit velocity of 20 m/s. The experimental study was conducted in three phases, as outlined below.

Phase I: Flow Visualization

For all 30 cases, side view photographs were taken of the smoke plumes within the near building region. Case Nos. 1-20 were found to be representative of the most significant building effects.

As mentioned in the introduction, the conceptual cavity of Halitsky (1968) has been contested by Britter et al. (1976). Reverse flow still occurs downwind of the building, but Britter et al. contend that the streamline that leaves the building at the separation line is not necessarily the same as the streamline that reattaches at the rear stagnation line (see Figure 1). Since the recirculating region of flow is not closed, it is difficult to define a "cavity" in terms of streamlines. Since the concept of a building cavity is a useful one for discussion purposes, it will be redefined here. The bubble (enclosing the cavity) is really a three-dimensional surface, a point not fully addressed by Halitsky or Britter et al. The bubble, as defined here, begins on the vertical plane of the upstream separation line(s) (but not necessarily on the surface of the building itself). To decide whether an arbitrary point (x,y,z) downstream of this plane is within the

TABLE 1. EXPERIMENTAL CASES

Case No.	H_s/H_b	D_s/H_s	W_s/U_s	ρ_s/ρ_a	Fr
1	0.0	∞	---	1.0	∞
2	1.2	0.052	0.7	1.0	∞
3	1.2	0.052	0.7	0.5	5.8
4	1.2	0.052	1.5	1.0	∞
5	1.2	0.052	1.5	0.5	13.0
6	1.2	0.052	2.2	1.0	∞
7	1.2	0.052	4.0	1.0	∞
8	1.2	0.052	4.0	0.5	33.4
9*	1.2	0.021	1.5	1.0	∞
10	1.2	0.021	8.4	1.0	∞
11	1.5	0.017	0.4	1.0	∞
12	1.5	0.017	0.4	0.5	11.0
13	1.5	0.042	0.4	1.0	∞
14	1.5	0.042	0.4	0.5	5.8
15	1.5	0.042	0.7	1.0	∞
16	1.5	0.042	0.7	0.5	5.8
17	1.5	0.042	1.5	1.0	∞
17a	2.5	0.025	1.5	1.0	∞
18	1.5	0.042	1.5	0.5	13.0
19*	1.5	0.042	2.2	1.0	∞
20	1.8	0.035	0.7	1.0	∞
21	1.8	0.059	0.7	1.0	∞
22	1.8	0.059	0.7	0.5	4.5
23	1.8	0.091	0.7	1.0	∞
24	1.8	0.091	0.7	0.5	4.2
25*	1.8	0.091	0.4	1.0	∞
26*	1.8	0.091	0.4	0.5	4.2
27*	2.15	0.076	0.7	1.0	∞
28	2.15	0.076	0.7	0.5	4.2
29	2.5	0.065	0.7	1.0	∞
30	2.5	0.065	0.7	0.5	4.2

*No concentration measurements.

cavity, we place a point source of tracer in the flow at this point and answer the question: does any of the tracer eventually touch the building surface? If it does, then this point is inside the cavity; if not, then it is outside the cavity. This definition leads to a bubble boundary ABCDEA in Figure 1; the outer edge of this cross section of the cavity is coincident with the downstream reattachment line.

Whereas this definition may be untenable mathematically, it is useful conceptually and is experimentally measurable. At various downwind positions in the vertical plane along the building mid section ($y/H_b = 0$), a smoke source was raised in the vertical to a point where no smoke could be seen recirculating back to the base of the building. These vertical positions were used to define the vertical boundary of the leeward cavity region. The building wake envelope was determined from observations of the maximum vertical spread of smoke that was emitted from a source within the cavity region. The lateral cavity region and wake envelope boundaries were similarly determined in the horizontal plane halfway between the base and top of the building ($z/H_b = 0.5$).

Phase II: Concentration Measurements

For all cases except as noted in Table 1, concentration measurements were taken. Ground-level concentration measurements along the plume center-line, downwind to 15 building heights, were taken. Vertical concentration profiles were measured near the point where the maximum ground-level concentration was found. We selected this position for the vertical measurements, hoping that it was far enough downwind to result in a profile representative of the building effects on the vertical plume spread and that it would also permit an easy determination of the plume centerline height. The plume centerline height was defined a the position of maximum concentration in the vertical profile since for all elevated stack cases this position was found to be well above ground level.

The ground-level measurements were taken at a position 0.025 m above the wind tunnel floor. (This was necessary to avoid the roughness slats.) This vertical displacement of the ground-level concentration measurements should have little significance, although some local variability in measurements near the slats was found.

Ground-level measurements were limited to 15 building heights downwind from the building. This region should be adequate for analysis of the building wake effect, since the vigorous turbulence in the building wake should have decayed to near background levels within this distance. Turbulence intensity measurements reported by Peterka and Cermak (1975) in the lee of several different model buildings showed this to be true.

For Case No. 17 (building removed), additional vertical and lateral measurements were taken for the purpose of characterizing the background dispersion in the simulated atmospheric boundary layer. Concentration profiles were measured at distances of 5, 10, and 15 building heights downwind. On a 1:200 scale, these positions represent full-scale distances of 250 m, 500 m, and 750 m downwind from the source.

Phase III: Measurements Farther Downstream

Preliminary analysis of the data gathered in Phase II suggested a need for concentration mappings to allow a more thorough examination of the building wake effects. Case No. 1 ($H_s/H_b = 0$) and Case No. 17 ($H_s/H_b = 1.5$) were selected as representing strong and moderate building wake effects. For these cases, additional vertical and lateral profiles were taken at downwind positions of 5, 10, and 15 buildings heights.

There were definite advantages to including some data in the far wake region. The experimental arrangement (building located at 9.0 m downwind from the vortex generators), however, did not permit measurements beyond 20 building heights. The building was thus moved 2.5 m upwind closer to the vortex generators, to a position where the equilibrium state of the boundary layer was somewhat questionable. However, since the building-induced turbulence was the dominating influence in this region, this arrangement was felt to be acceptable; it extended the examinable region in the lee of the building to 30 building heights. For conditions of Case No. 1, Case No. 17, and an additional Case No. 17a. (similar to Case 17 except with the stack height raised to 2.5 building heights), ground-level measurements to 30 building heights were taken. Vertical and ground-level lateral profiles at downwind distances of 15 and 30 building heights were taken for Case No. 1 ($H_s/H_b = 0$).

SECTION 4

RESULTS

As described in the previous section, 30 cases were examined. For 24 of the cases, concentration profiles were measured at ground level under the plume centerline, and vertical profiles were measured near the position of maximum ground-level concentration. Photographs of the smoke plumes were taken for all cases. Complete results for Phase I and Phase II are presented for each individual case in the Appendix. Discussion and analysis of these results and presentation of all additional results follow in this section. To aid the reader and to eliminate continuous referral to Table 1, the pertinent stack parameters are listed in parenthesis after mention of each case number, i.e., (H_s/H_b, D_s/H_s, W_s/U_s, ρ_s/ρ_a).

PHASE I: OBSERVATIONS OF SMOKE PLUMES

Figures 5 and 6 present the cavity boundary and wake envelope measurements in both the vertical and horizontal planes of the building. The cavity size in both planes was approximately 3.0 building heights in extent downwind from the leeward edge of the building. The maximum vertical and lateral extent of the cavity region was approximately 1.5 building heights and was found to occur midway between the leading edge of the building and the leeward end of the cavity. The envelope is slightly larger in the lateral plane. A summary of the observations from the smoke visualization follows below. Photographs of the vertical plume spread are presented in the Appendix.

For the ground-level source, Case No. 1 (0, ∞, --, 1), an instantaneous spreading of the effluent to fill the wake in both the vertical and horizontal planes was observed. This resulted from the strong vertical and horizontal recirculation within the cavity region. For the low stacks ($H_s/H_b < 1.5$) with insufficient effluent momentum to escape the cavity (Case Nos. 2 through 6, 9, and 11 through 14), at least partial vertical mixing of the plumes into the wake cavity was observed. Spreading in the horizontal plane, however, was much less rapid than was observed for the ground source. Case Nos. 7, 8, and 10 also had stack heights less than 1.5 H_b, but, in these cases, the effluent speed was sufficient for the plume to escape the cavity. The major enhancement of the vertical spread of the plume was due primarily to the unsteadiness of the flow within the recirculating cavity region.

For the cases where the effective stack height was above the cavity, there was no entrainment into the cavity, but enhanced vertical dispersion was still observed. Enhancement of dispersion in the horizontal plane was again observed to be minimal. The amount of enhanced vertical plume spread was observed to decrease with increasing effective stack height. The plumes

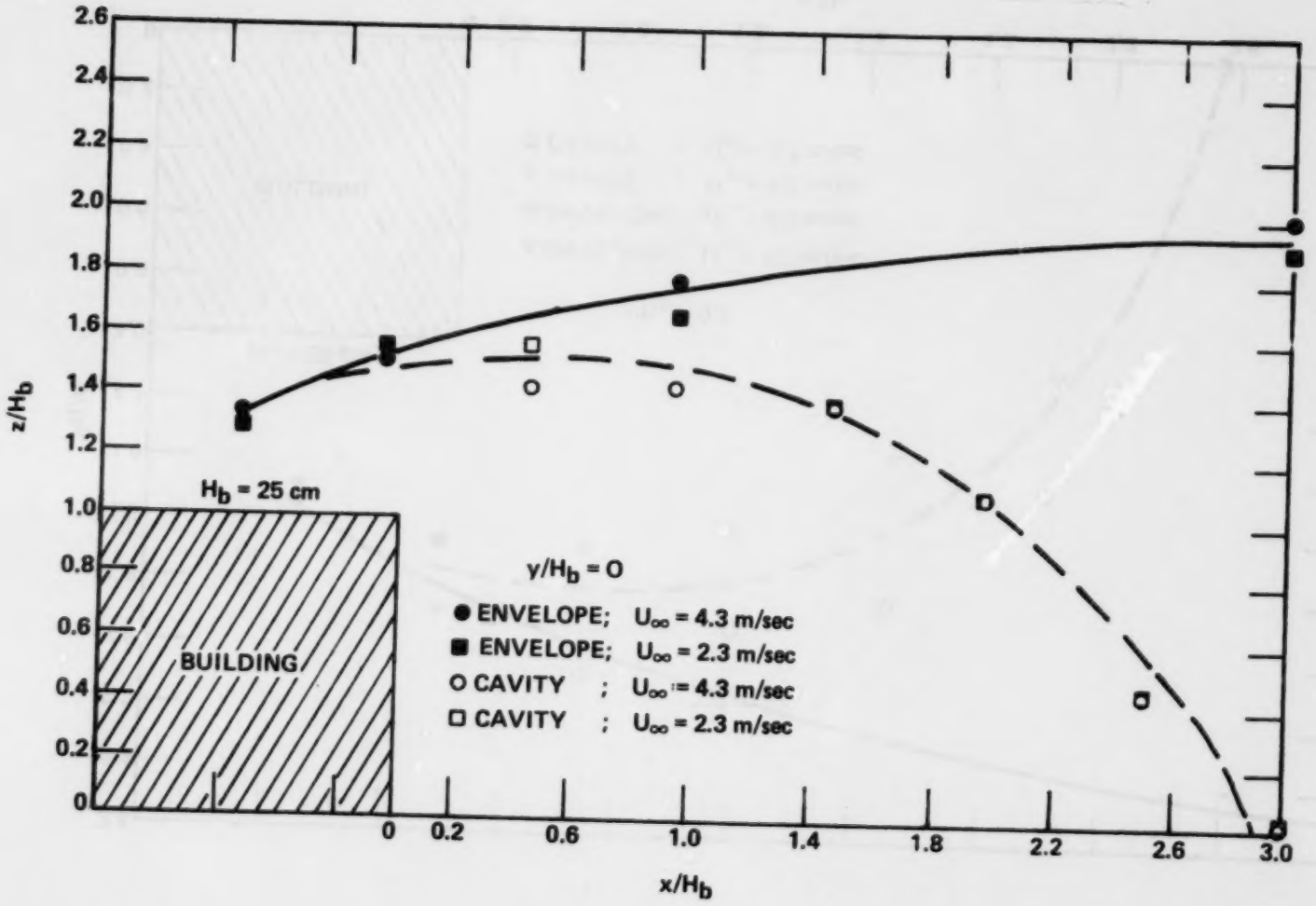

Figure 5. Vertical wake cavity and envelope measurements.

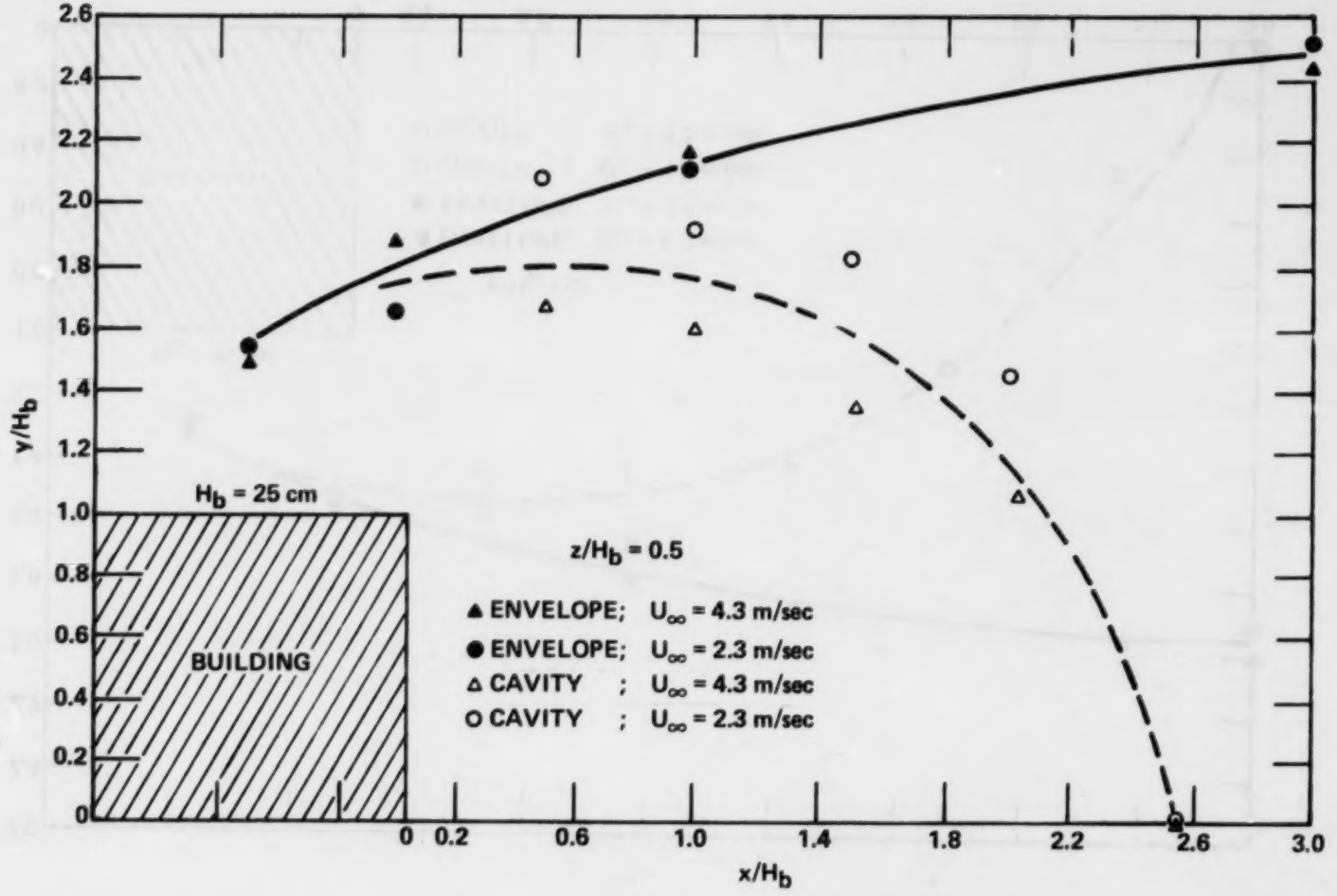

Figure 6. Lateral wake cavity and envelope measurements.

from the most elevated sources (H_s/H_b = 2.15, 2.5) were not affected by the building until the plume naturally spread downward into the wake region. At these downwind distances, the turbulence had significantly decayed from that observed in the cavity of the building. Thus, the overall effects of the wake interactions on the vertical spread of these plumes were smaller.

For all cases, an increase in the effluent speed resulted in an increased plume rise. The effluent speed for Case No. 7 (1.2, 0.05, 4, 1) was selected by varying the effluent speed to determine the critical value for which the plume avoided immediate entrainment into the cavity region. A similar determination was conducted with a smaller diameter stack for Case No. 10 (1.2, 0.02, 8.4, 1). The necessary increase in stack effluent velocity to provide sufficient plume rise resulted in nearly equivalent momentum fluxes, $\rho_s W_s^2 \cdot \pi D_s^2/4$.

Maintaining a ratio of effluent speed to wind speed at stack top of 3:2 was found to avoid aerodynamic downwash of the plumes behind the stacks. For the cases with lower speed ratios (W_s/U_s = 0.7, 0.4), stack downwash was clearly observed. It was even greater if the effluent density was decreased. A decrease in density resulted in a smaller momentum flux, thus, a smaller immediate plume rise. No effects from changing only the stack diameter could be clearly observed. Apparently, any change in momentum flux was offset by a change in the stack wake influence.

PHASE II: CONCENTRATION FIELDS

The ground-level concentration profiles show the overall effects of the building upon plume dispersion for a variety of source characteristics. Vertical concentration profiles provided data to define the plume centerline height and the vertical plume spread. Comparisons between the measurements made with the building in place and those for the isolated stack (building removed) are used to define the building wake effect.

Plume Rise

Table 2 summarizes the evaluation of the plume rise estimates from isolated stacks based on the following equations. Plume rise is composed of a momentum term Δh_m, and a buoyancy term Δh_b, such that the total rise is (Briggs, 1975)

$$\Delta h = [(\Delta h_m)^3 + (\Delta h_b)^3]^{1/3},$$

where

$$\Delta h_m = \left[\frac{3}{4\beta^2}\frac{\rho_s}{\rho_a}\right]^{1/3} \left[\frac{W_s D_s}{U}\right]^{2/3} x^{1/3},$$

$$\Delta h_b = (1.6F^{1/3} x^{2/3})/U,$$

$$\beta = 1/3 + U_s/W_s = \text{entrainment coefficient,}$$

and $$F = gW_s \frac{D_s^2}{4}\left(\frac{\rho_a - \rho_s}{\rho_a}\right) = \text{buoyancy flux.}$$

The downwind distance to final rise x_f was estimated by the equation of Briggs (1971):

$$x_f = 3.5x^*,$$

where

$x^* = 14\ F^{5/8}$, for F less than 55 (m^4s^{-3}), and

$x^* = 34\ F^{2/5}$, for F greater than or equal to 55 (m^4s^{-3}).

TABLE 2. PLUME RISE FROM THE ISOLATED STACKS

Case No.	$\left(\frac{H_s}{H_b}, \frac{D_s}{H_b}, \frac{W_s}{U_s}, \frac{\rho_s}{\rho_a}\right)$	$\frac{x}{H_b}$	$\frac{x_f}{H_b}$	$\frac{3D_s}{H_b}\frac{W_s}{U_s}$	$\frac{\Delta h_m}{H_b}$	$\frac{\Delta h_b}{H_b}$	$\frac{\Delta h}{H_b}$ (est.)	$\frac{\Delta h}{H_b}$ (obs.)
4	(1.2,0.052,1.5,1.0)	3	___	0.28	0.21	___	0.21	0.1-0.3
17	(1.5,0.042,1.5,1.0)	6	___	0.28	0.27	___	0.27	0.0-0.2
5	(1.2,0.052,1.5,0.5)	3	2.7	0.28	0.17	0.16	0.21	0.0-0.2
18	(1.5,0.042,1.5.0.5)	6	2.7	0.28	0.21	0.16	0.23	0.0-0.2
7	(1.2,0.052,4.0,1.0)	10	___	0.75	1.1	___	1.1	0.8-1.0
8	(1.2,0.052,4.0,0.5)	10	5.0	0.75	0.87	0.45	0.9	0.8-1.0
10	(1.2,0.017,0.4,1.0)	10	___	0.63	1.2	___	1.2	0.8-1.0

The estimated plume rise was in genera' agreement with that observed in all cases. Case Nos. 7 and 10 demonstrate that a cutoff position (final rise) for estimating plume rise due to the initial momentum of the source is needed. It does appear, however, that the maximum plume rise for these nonbuoyant sources can be roughly estimated by the generally applied rule of thumb, $3\ D_s W_s/U_s$ (Briggs, 1969).

The effect of the building upon plume rise was evaluated from the vertical concentration profiles (see Appendix). The analysis was limited because only one vertical profile was taken in most cases. Table 3 summarizes the effect of the building wake upon the plume centerline height (vertical position of maximum concentration). For most cases the plume centerline determined by maximum concentration was found to be clearly defined because the profiles were taken close to the source where the maximum was pronounced.

Only Case Nos. 7 (1.2, 0.05, 4, 1), 8 (1.2, 0.05, 4, 0.5), and 10 (1.2, 0.02, 8, 1) afforded the opportunity to clearly evaluate plume rise, because for all other cases the plume rise was minimal. At a position of 10 building heights downwind, the plume rise in the wake of the building was found to be less than two-thirds that found for the isolated stack. This reduction was, of course, a result of increased entrainment of the plume by the building wake. A change of the plume entrainment constants used in the plume rise model could conceivably account for the reduction, but further studies are needed. The lowering of the plume centerline height may also be the result of a general down-drafting of the plume in the immediate wake of the building. The other cases, although not having significant plume rise, did indicate a slight reduction of the plume centerline height in the wake of the building. In those isolated stack cases where the velocity ratio W_s/U_s was less than 1.5, the plume centerline height was found to be lower than the source height as a result of stack downwash.

Characterization Of Wind Tunnel Dispersion

Vertical concentration profiles for the isolated stack of Case No. 17 (1.5, 0.04, 1.5, 1) were measured at 5, 10, and 15 building heights downwind, and were used in characterizing dispersion in the simulated atmospheric boundary layer. Lateral concentration profiles at the height of the plume centerline were also made at these downwind positions. Case No. 17 was selected because its plume height was average for all the cases examined and no stack downwash effects were observed. Figures 7 and 8 present the horizontal and vertical concentration profiles and their estimated Gaussian distributions, expressed as,

$$\frac{\chi U_r H_b^2}{Q} = \frac{\left(\exp\left(-\frac{1}{2}\frac{y^2}{\sigma_y^2}\right)\right)\left(\exp\left(-\frac{1}{2}\left(\frac{z-H_s}{\sigma_z}\right)^2\right) + \exp\left(-\frac{1}{2}\left(\frac{z+H_s}{\sigma_z}\right)^2\right)\right)}{2\pi\sigma_y\sigma_z/H_b^2}.$$

TABLE 3. SUMMARY OF EFFEC~ OF BUILDING ON PLUME RISE

Case No.	$\left(\frac{H_s}{H_b}, \frac{D_s}{H_b}, \frac{W_s}{U_s}, \frac{\rho_s}{\rho_a}\right)$	Longitudinal position of vertical profile	Vertical position of maximum concentration	
		(x/H_b)	Isolated Stack (z/H_b)	Building (z/H_b)
1	(0.0,∞,---,1.0)	3	0.0	0.0
2	(1.2,0.052,0.7,1.0)	3	1.0 - 1.2	1.2 - 1.4
3	(1.2,0.052,0.7,0.5)	3	1.0 - 1.2	1.1 - 1.3
4	(1.2,0.052,1.5,1.0)	3	1.3 - 1.5	1.1 - 1.3
5	(1.2,0.052,1.5,0.5)	3	1.2 - 1.4	1.1 - 1.3
7	(1.2,0.052,4.0,1.0)	10	2.0 - 2.2	1.6 - 1.8
8	(1.2,0.052,4.0,0.5)	10	2.0 - 2.2	1.4 - 1.6
10	(1.2,0.021,8.4,1.0)	10	2.0 - 2.2	1.4 - 1.6
11	(1.5,0.017,0.4,1.0)	3	1.1 - 1.3	1.1 - 1.3
12	(1.5,0.017,0.4,0.5)	3	1.1 - 1.3	0.8 - 1.0
13	(1.5,0.042,0.4,1.0)	3	1.1 - 1.3	1.1 - 1.3
14	(1.5,0.042,0.4,0.5)	3	1.0 - 1.2	1.1 - 1.3
15	(1.5,0.042,0.7,1.0)	3	1.3 - 1.5	1.1 - 1.3
16	(1.5,0.042,0.7,0.5)	3	1.3 - 1.5	1.1 - 1.3
17	(1.5,0.042,1.5,1.0)	6	1.5 - 1.7	1.3 - 1.5
18	(1.5,0.042,1.5,0.5)	6	1.5 - 1.7	1.3 - 1.5
20	(1.8,0.035,0.7,1.0)	8	1.5 - 1.7	1.2 - 1.6
21	(1.8,0.059,0.7,1.0)	8	1.9 - 2.1	1.5 - 1.7
22	(1.8,0.059,0.7,0.5)	8	1.7 - 1.9	1.5 - 1.7
23	(1.8,0.091,0.7,1.0)	8	1.7 - 1.9	1.6 - 1.8
24	(1.8,0.091,0.7,0.5)	10	1.4 - 1.6	1.5 - 1.7
28	(2.15,0.076,0.7,0.5)	10	1.9 - 2.1	1.8 - 2.0
29	(2.5,0.065,0.7,1.0)	10	2.3 - 2.5	2.3 - 2.5
30	(2.5,0.065,0.7,0.5)	10	2.3 - 2.5	2.3 - 2.5

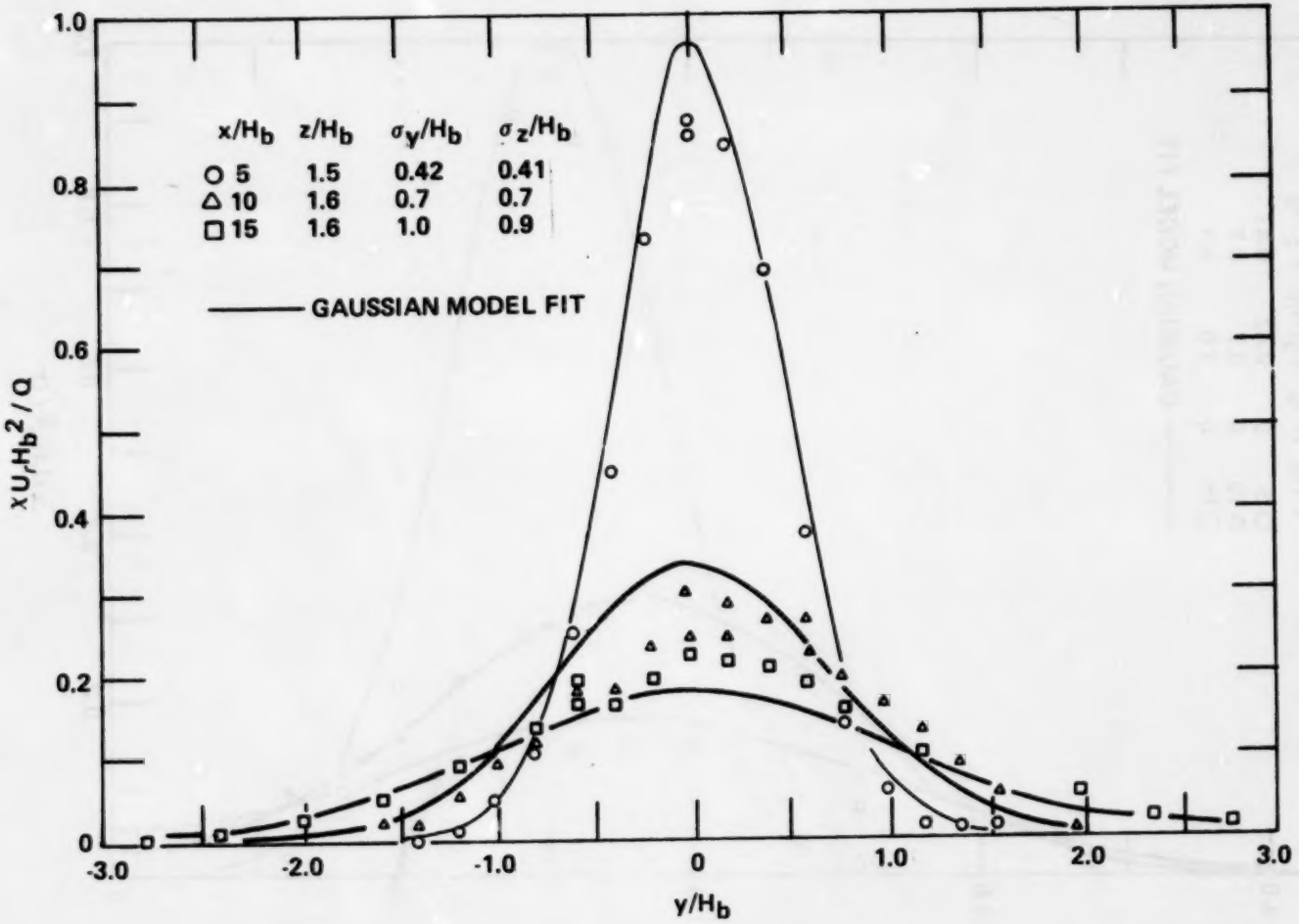

Figure 7. Lateral concentration profiles taken through the plume centerline; Case No. 17 (1.5, 0.042, 1.5, 1.0), isolated stack.

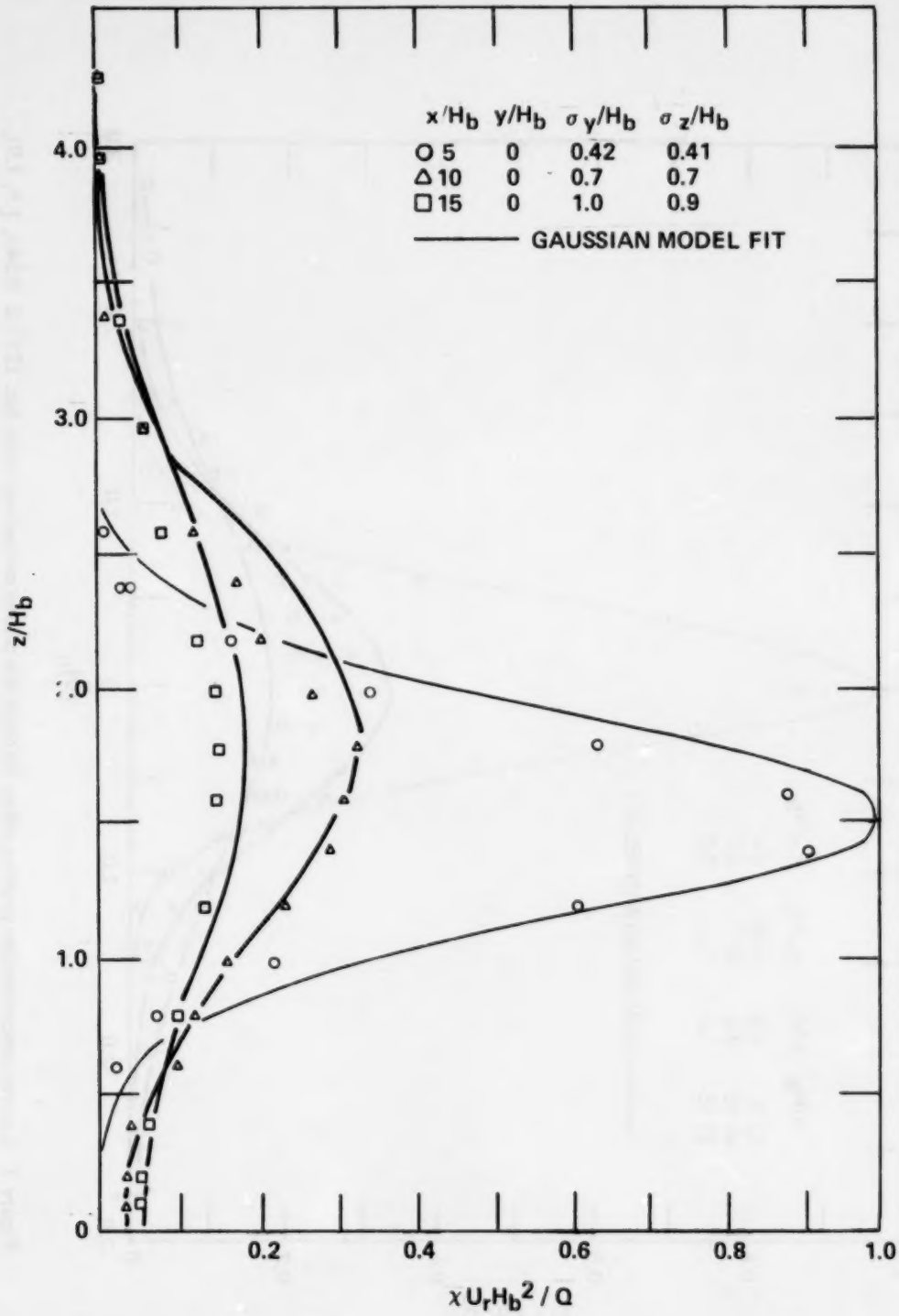

Figure 8. Vertical concentration profiles taken through the plume centerline; Case No. 17 (1.5, 0.042, 1.5, 1.0), isolated stack.

Standard deviations σ_y and σ_z were computed from the concentration distributions plotted on log-probability paper and then slightly adjusted to provide a better fit to the lower half of the vertical profiles, since this was the region of greatest interest.

The wind tunnel dispersion parameters are plotted along with the Pasquill-Gifford curves for stabilities B, C, D, and E (Turner, 1970) in Figure 9. Vertical dispersion within the wind tunnel boundary layer is closest to stability C, slightly unstable conditions. Horizontal dispersion is closer to stability D. However, the boundary layer flow within the wind tunnel is not truly thermally unstable. A better description of the boundary layer would be urban, neutral. Dispersion curves based on a diffusion experiment in St. Louis by McElroy and Pooler (1968) (presented by Briggs, 1973) provide a better comparison. The wind tunnel horizontal dispersion is closely related to the reported experimental results under neutrally stable atmospheric conditions. Note that consideration of the model scale is necessary since the rate of dispersion is not a linear function of downwind distance. The growth in plume spread was found to be well described by

$$\sigma_z/H_b = \sigma_y/H_b = 0.115\ (x/H_b)^{0.8}.$$

Isolated Stack Data Compared With Gaussian Plume Model

The dispersion parameters (σ's) were determined, as discussed above, from Case 17 (1.5, 0.04, 1.5, 1). These same dispersion parameters were then used in the Gaussian plume model to estimate the concentration profiles for the other cases. These comparisons are shown in Figure 10. It can be seen that the fits are exceptionally good, even for the highest stack (Case No. 29 (2.5, 0.065, 0.7, 1)).

Figures 11a and b present some of the longitudinal ground-level profiles measured downwind of the isolated stacks. No profiles from the tallest stacks were included here because the ground-level concentrations were too close to the laboratory background. For all the isolated stacks, the plume was visually observed to reach the ground only intermittently ($x/H_b = 15$). A longer averaging time would have resulted in more significant values for these situations, and, perhaps, better agreement with the Gaussian model. Poorer representations by the model were found as the source height was increased; this may be due partly to the insufficient averaging time and the increasing significance of the background level.

A much better evaluation could have been made in the region farther downwind, where ground-level concentrations would have been higher. The measured concentrations for these longitudinal profiles, in contrast with those for the vertical profiles, are at levels where the fluctuations in the background concentration are significant. Considering the above difficulties and the good comparisons of the Gaussian model estimates to the measurements of the

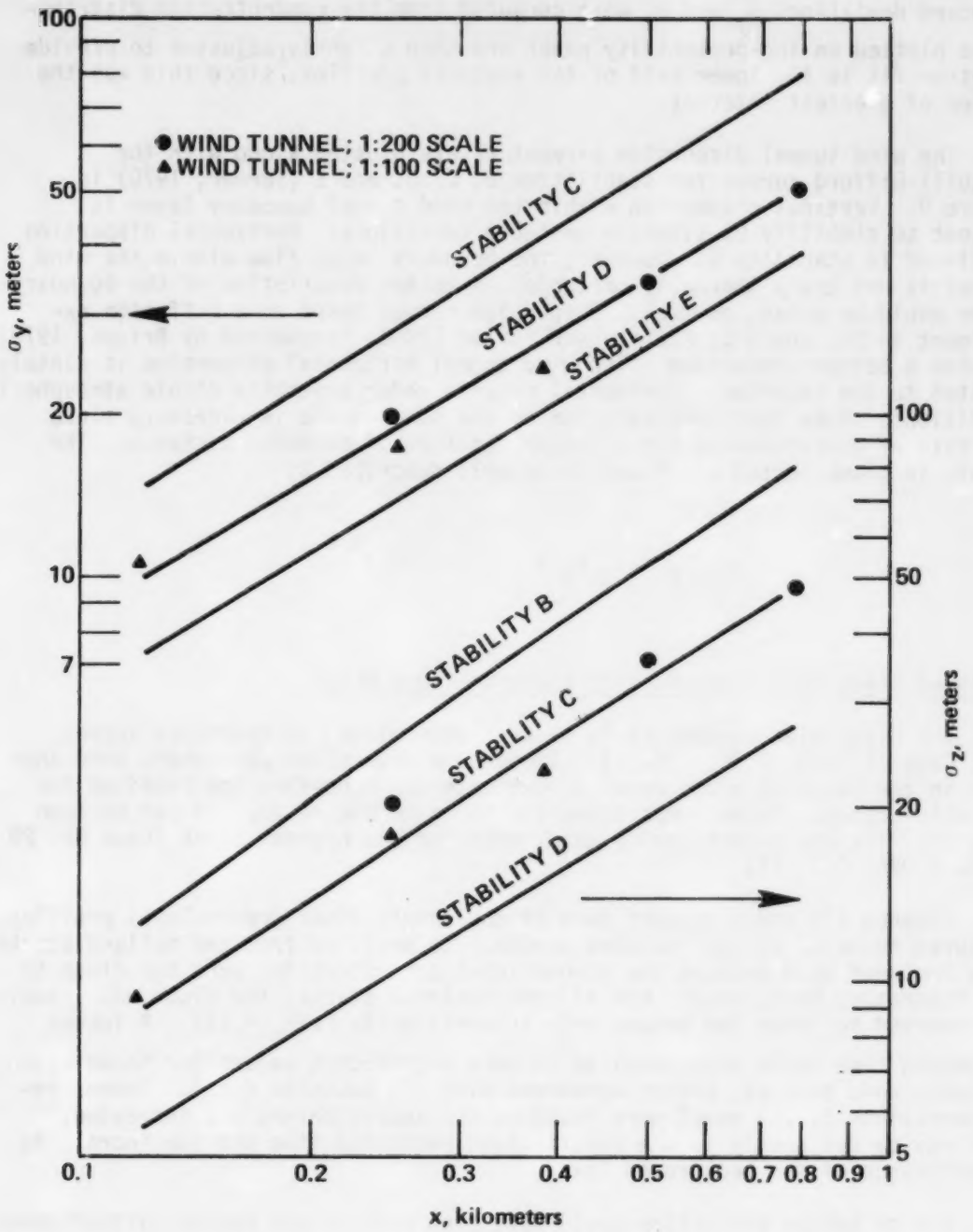

Figure 9. Estimated wind tunnel dispersion parameters compared with Pasquill - Gifford values (Turner, 1970).

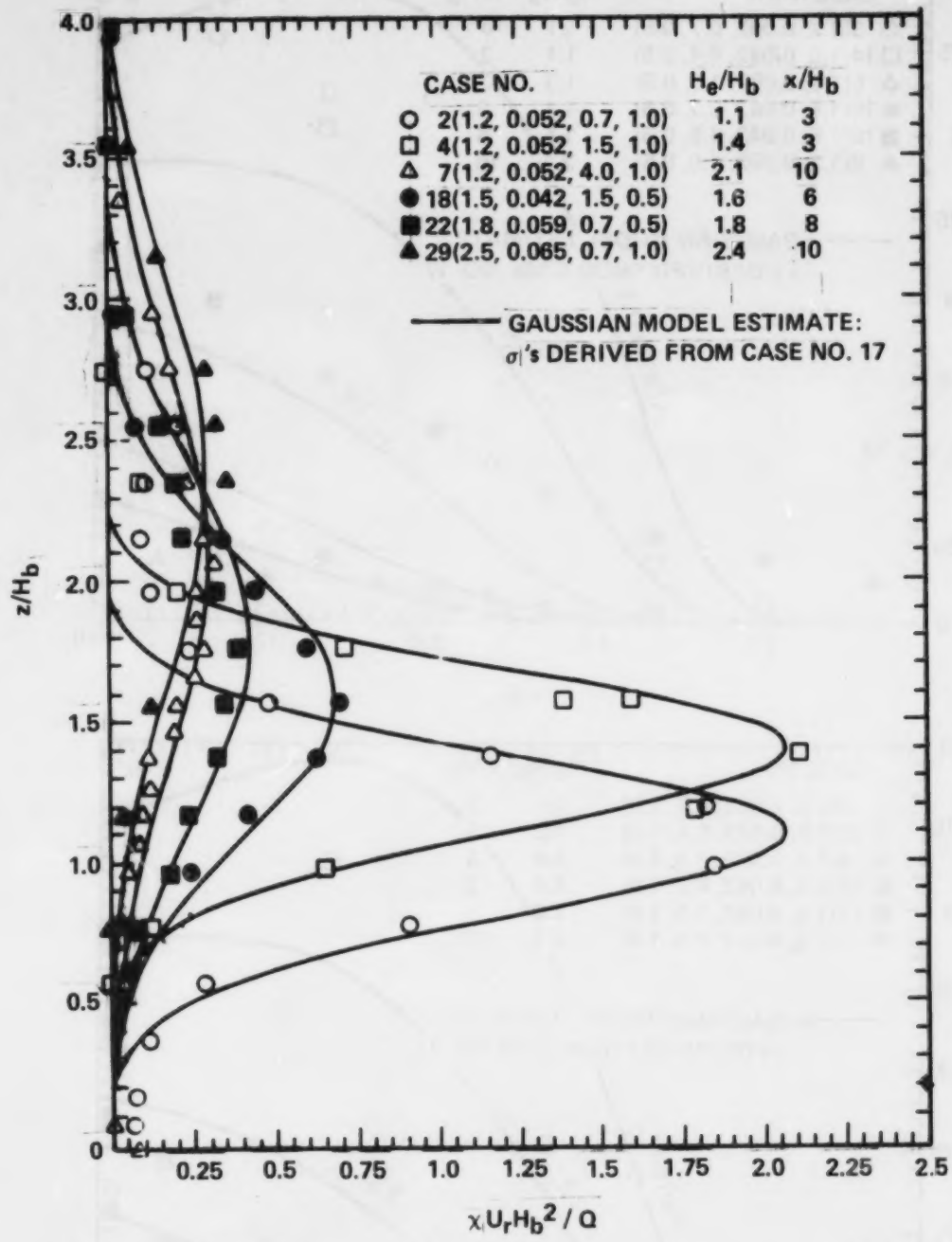

Figure 10. Vertical concentration profiles for isolated stack. In this and following legends, H_e/H_b identifies the presumed effective stack height as determined from analysis of vertical concentration profiles at position, x/H_b (see table 3).

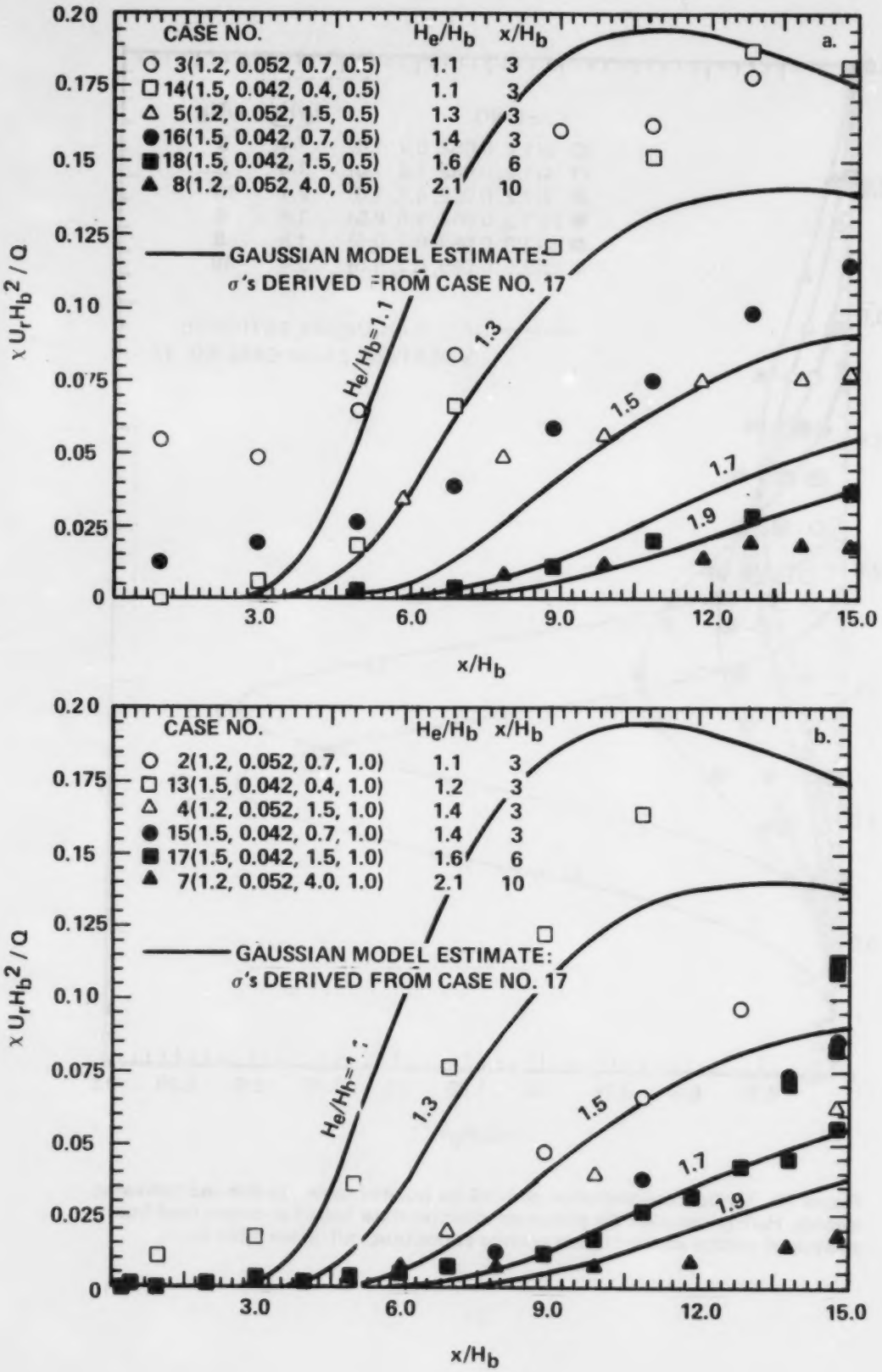

Figure 11. Longitudinal ground-level concentration measurements downwind from isolated stacks.

vertical profiles, dispersion downwind from the isolated stack is considered to be well represented by the estimated dispersion parameters.

The Effects of The Building

Figures 12 through 14 present all the longitudinal ground-level concentrational profiles taken in the lee of the building. The longitudinal profiles are grouped and presented here to allow for a simple comparison to be made between the situations influenced by the building wake. For a case-by-case comparison between the situation with the isolated stack and the situation with the building in place, see the Appendix.

Note that for the ground source, Case No. 1 (0, ∞, -, 1), a point is reached where ground-level concentrations were lower than those from the elevated stacks (See Figure 12). This is distinctly different from what occurs from sources in the absence of any building wake or terrain influences. For the ground source, greater enhanced dispersion occurs in both the vertical and lateral direction, which results in the lower concentrations downwind. This is in good agreement with the observations of the smoke plumes as reported in Phase I. In Figures 12 through 14 the effective plume height H_e is the position of maximum plume concentration as determined from the vertical profiles taken at distance x as reported in the caption.

For all the elevated stack cases (Figures 12 through 14), the positions of maximum concentration are much closer to the source than were found downwind from the corresponding isolated stacks (Figures 11a and b). Also, ground-level concentrations are significantly higher in the wake of the building. These results are also in agreement with the observations made in Phase I. The building wake has significantly enhanced the vertical plume spread. A quantification of the enhancement is described below.

Modified Gaussian Model

A simple model (Huber and Snyder, 1976) was developed to account for the enhanced dispersion found in the wake of this building. The dispersion parameters are of the form:

$$\sigma'(x) = 0.7H_b + 0.067(x-3H_b), \text{ for } 3 \leq x/H_b \leq 10, \text{ and}$$

$$\sigma'(x) = \sigma(x+S) \text{ for } x/H_b > 10,$$

where $\sigma(x)$ = dispersion parameter in absence of building effects at downwind distance x,

$\sigma'(x)$ = enhanced dispersion parameter (with building effects),

and S = virtual source location.

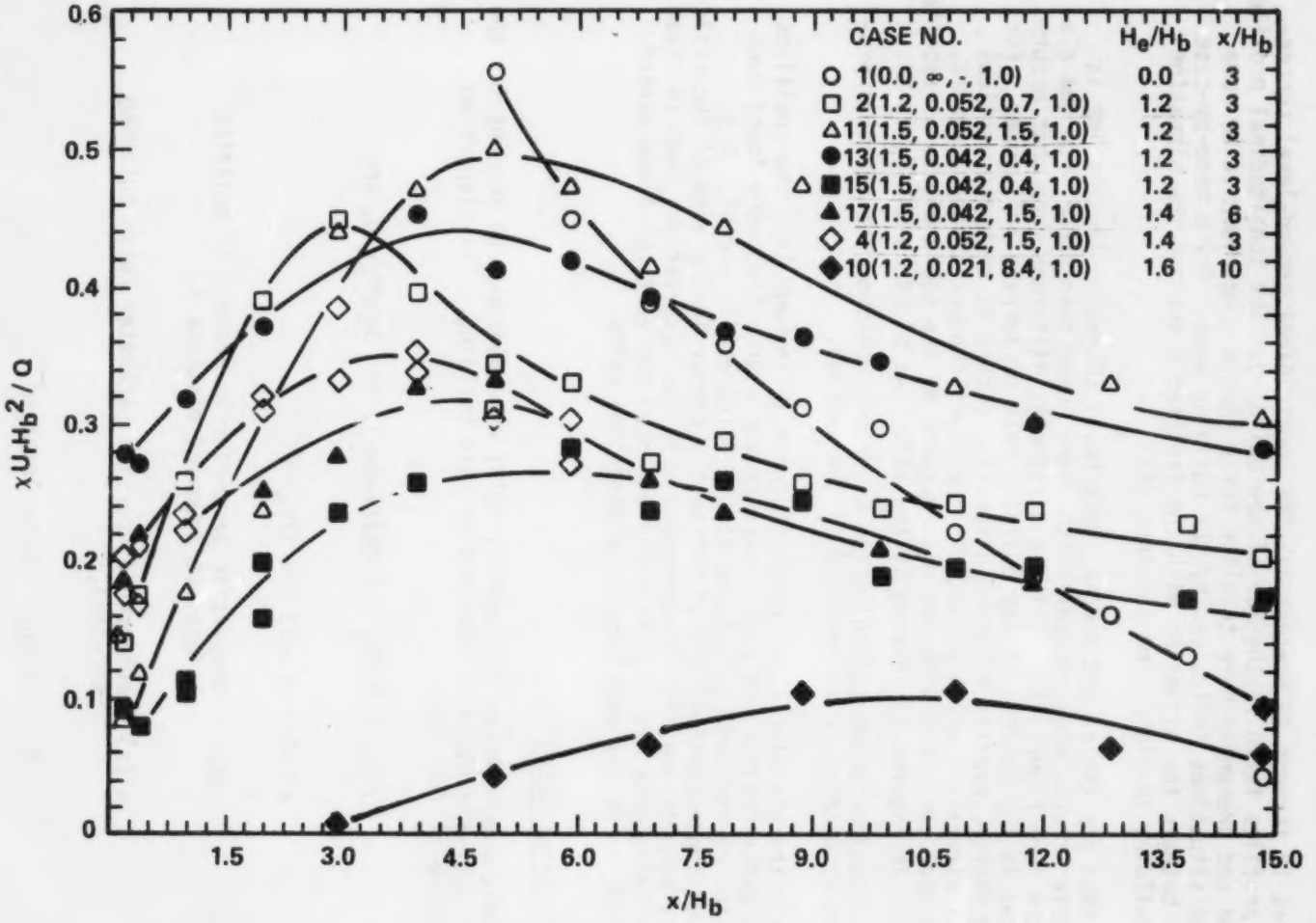

Figure 12. Longitudinal ground-level concentration measurements in the lee of the building; neutrally buoyant sources with $H_s/H_b \leq 1.5$.

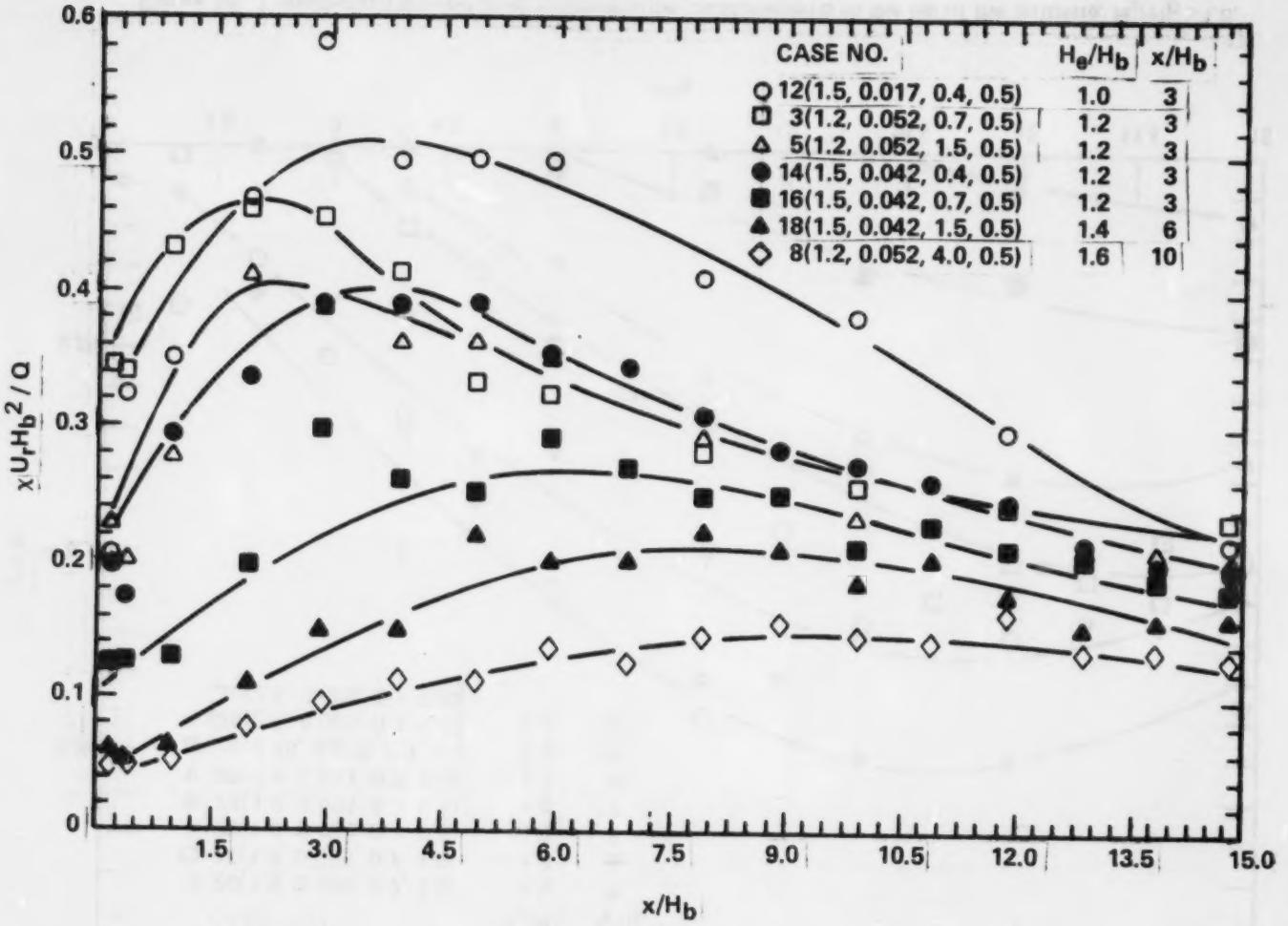

Figure 13. Longitudinal ground-level concentration measurements in the lee of the building; slightly buoyant sources with $H_s/H_b \leq 1.5$.

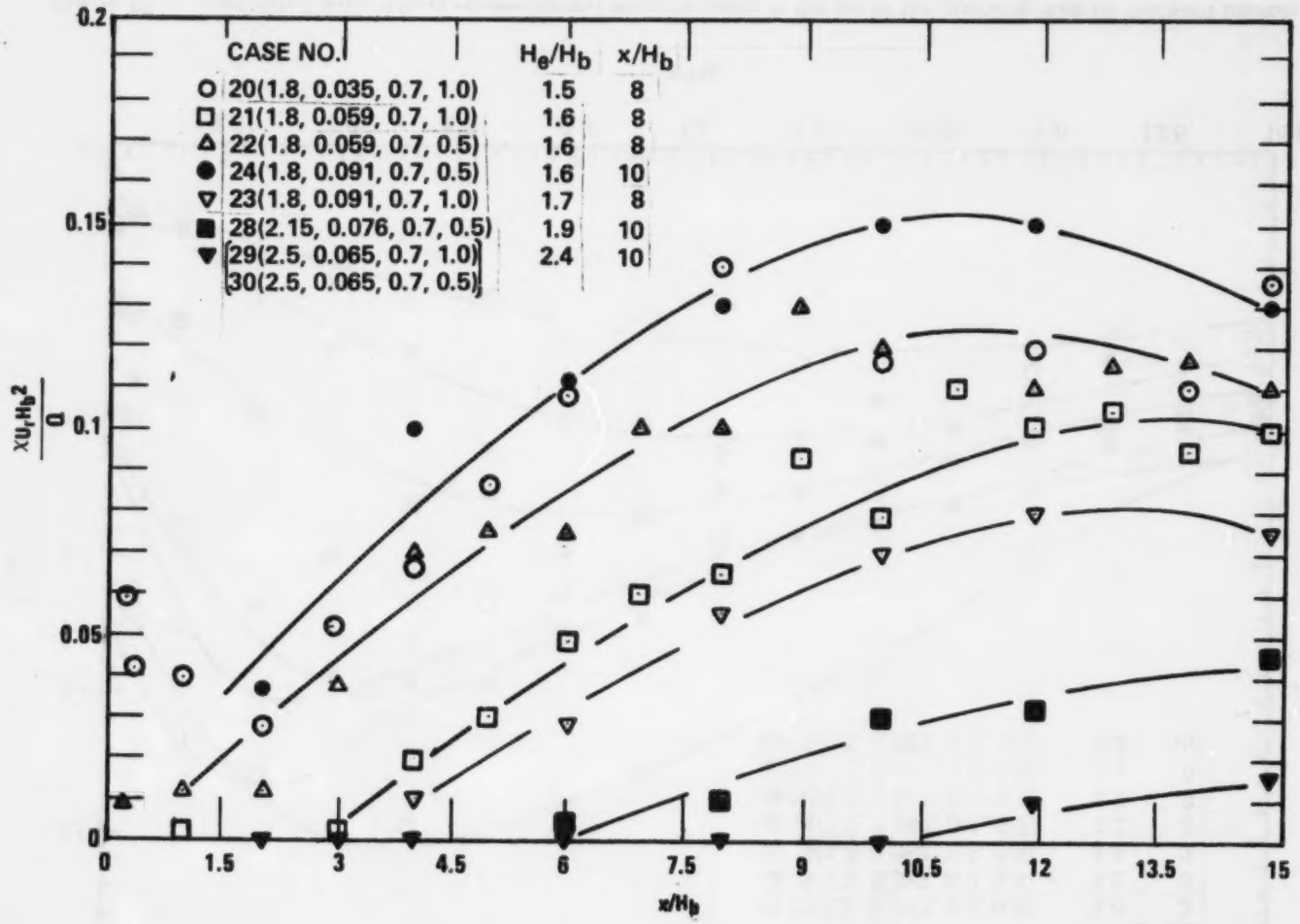

Figure 14. Longitudinal ground-level concentration measurements in the lee of the building; $H_s/H_b > 1.5$.

The above equations were derived to provide best agreement with the longitudinal ground-level profiles for the ground source (Figure 15), with enhancement of both the vertical and lateral dispersion parameters assumed. The virtual source location was determined by matching the above equations at 10 building heights downwind where the enhanced rate of dispersion has likely ceased, leaving only a residual wider plume. For the conditions of this study, the virtual source location was found to equal eight building heights; $S = 8H_b$.

Figures 16 and 17 present the vertical and lateral concentration profiles for the ground source. Estimates using the modified Gaussian model for the ground source data were found to be good, with slightly higher centerline values estimated near the surface at $x/H_b = 5$.

For elevated sources, concentration estimates are based on modifying only the vertical dispersion parameter because a significant increase in lateral spread appeared to be absent. This results from the vertical oscillations in the disturbed flow over the building sweeping above the building as expected while the lateral oscillations sweep laterally only near the building. Longitudinal ground-level concentration profiles based on the modified Gaussian model are presented in Figure 18 for various effective source heights, H_e/H_b. These profiles were compared with the measurements found in Figures 12-14. Agreement was very good for all except the most elevated cases where ground-level concentrations were over-estimated. There was less building influence, as expected, for the more elevated sources.

Vertical and lateral concentration profiles for elevated source, Case No. 17 (1.5, 0.042, 1.5, 1.0), are compared with the modified Gaussian model in Figures 19 and 20. Profiles for this stack in the absence of the building have already been presented in Figures 7 and 8. The vertical profiles (Figure 19) at the lower levels are found to be in agreement with the model estimates, but the vertical spread at $x/H_b = 5$ is overestimated; the data show that the plume was contained below about two building heights, whereas the model predicts that the plume will reach three. The lateral profiles (Figure 20) taken at the elevated levels are in very good agreement with the model estimates. At ground level, the maximum concentrations are predicted quite well by the model, but the horizontal widths of the plume are considerably underestimated. Perhaps near the ground, influences upon the horizontal spread must be additionally considered.

PHASE III: MEASUREMENTS TO 30 BUILDING HEIGHTS DOWNSTREAM

The longitudinal concentration profiles that were taken to examine the region downwind to 30 building heights are presented in Figure 21. Model concentration estimates both in the wake of the building and in the absence of the building are also included in the figure. For the two elevated stacks, only enhancement of the vertical plume spread was considered. Very good agreement with the model was found for the ground source, Case 1, and Case 17 (1.5, 0.042, 1.5, 1.0). The use of an area-source model (Gifford, 1960),

$$\frac{xU_r H_b^2}{Q} = \frac{1}{K\left[\frac{\text{Area}}{H_b^2}\right] + \pi\left[\frac{\sigma_y}{H_b}\right]\left[\frac{\sigma_z}{H_b}\right]},$$

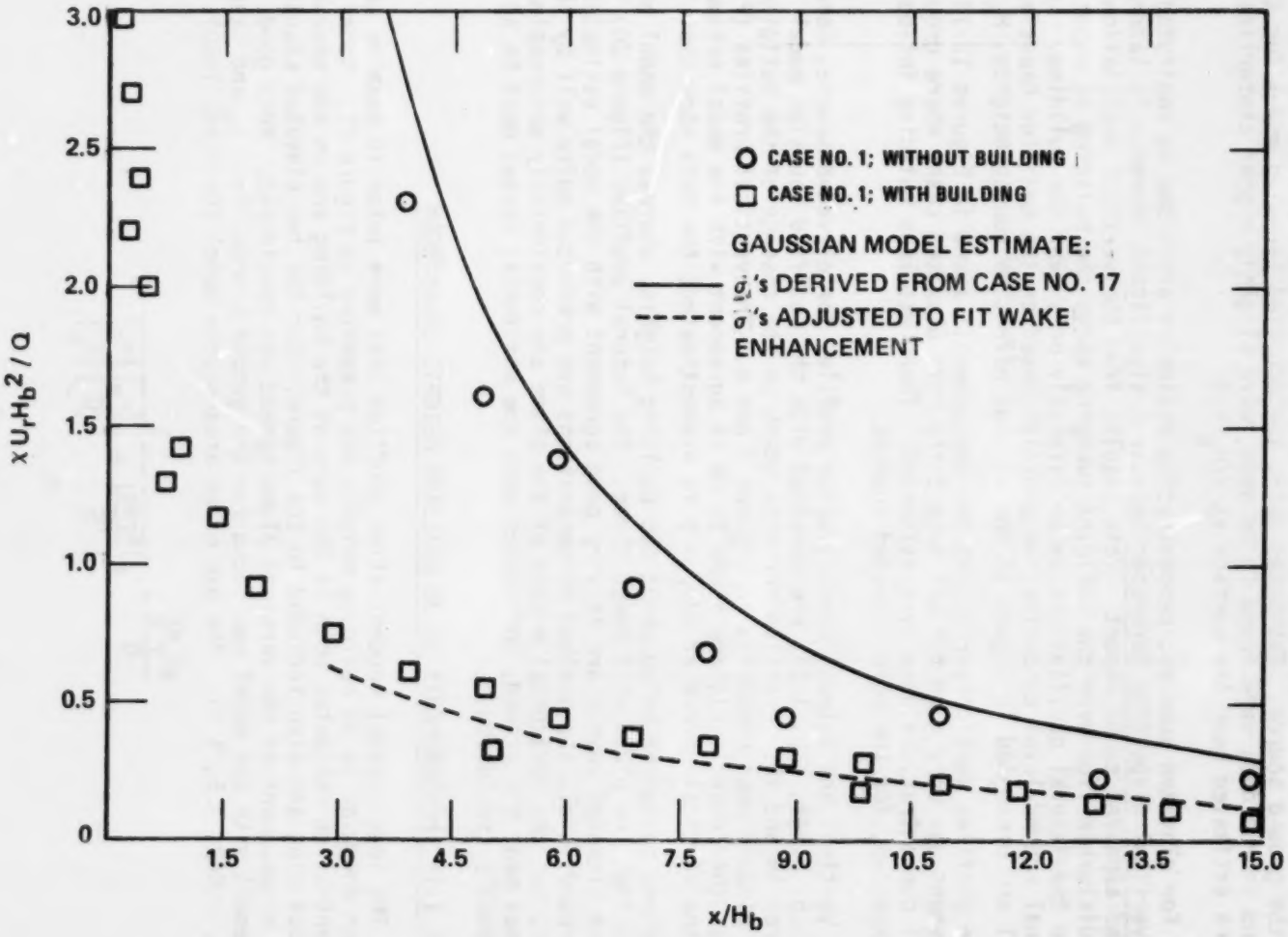

Figure 15. Longitudinal ground-level concentration measurements for ground source; Case No. 1.

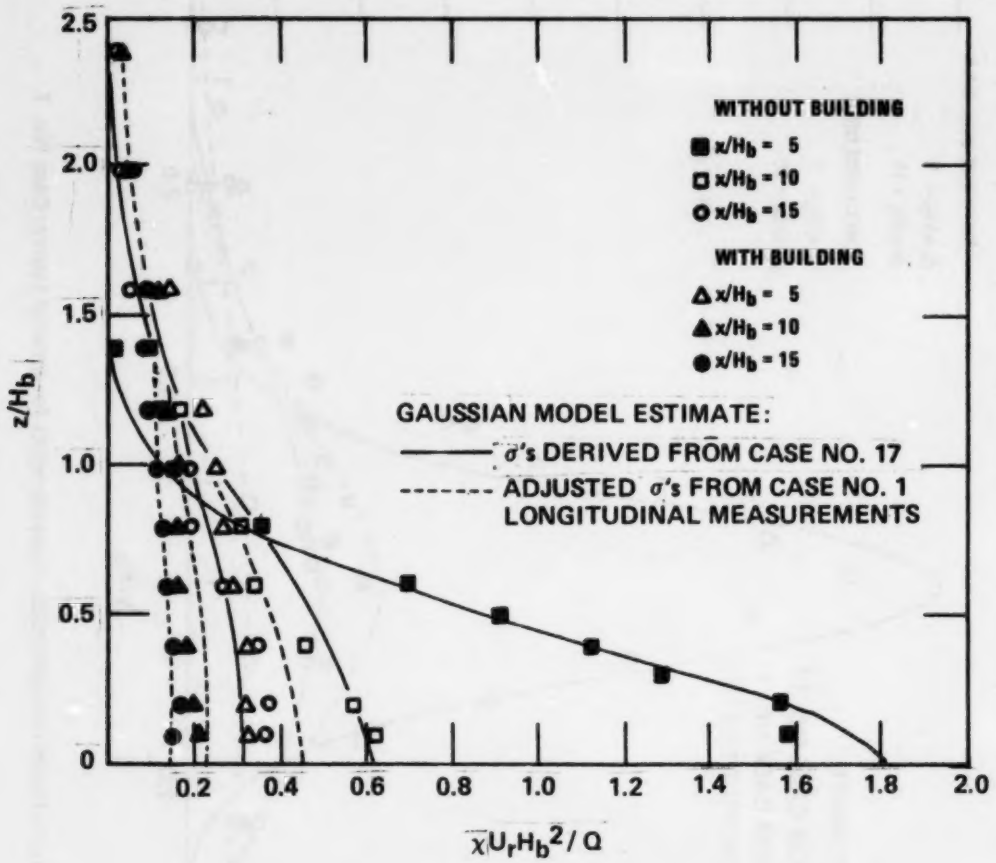

Figure 16. Vertical concentration measurements for ground source; Case No. 1.

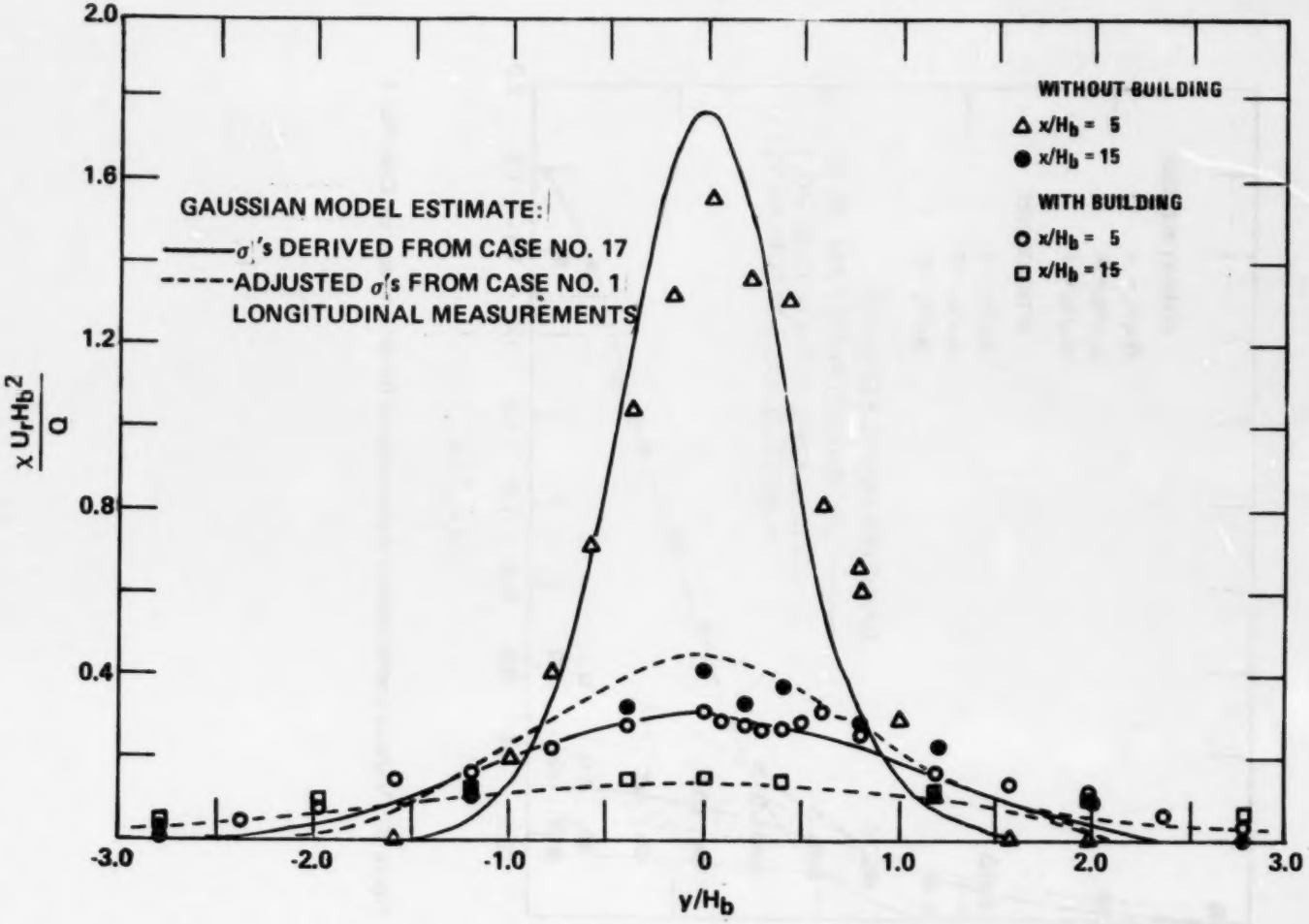

Figure 17. Lateral ground-level concentration measurements for ground source; Case No. 1.

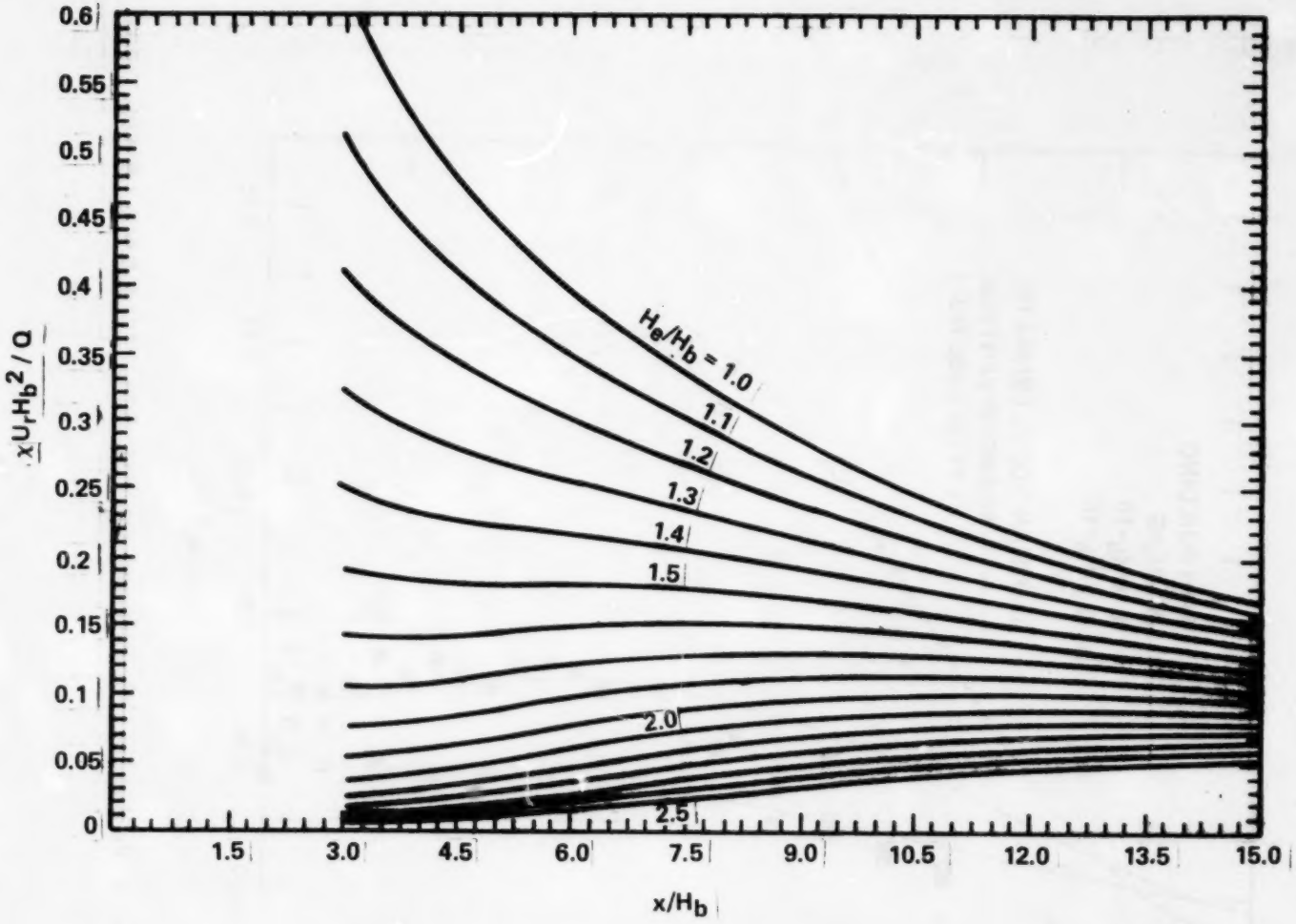

Figure 18. Longitudinal ground-level concentration profiles for elevated sources based on the Gaussian model using an adjusted vertical σ from Case No. 1.

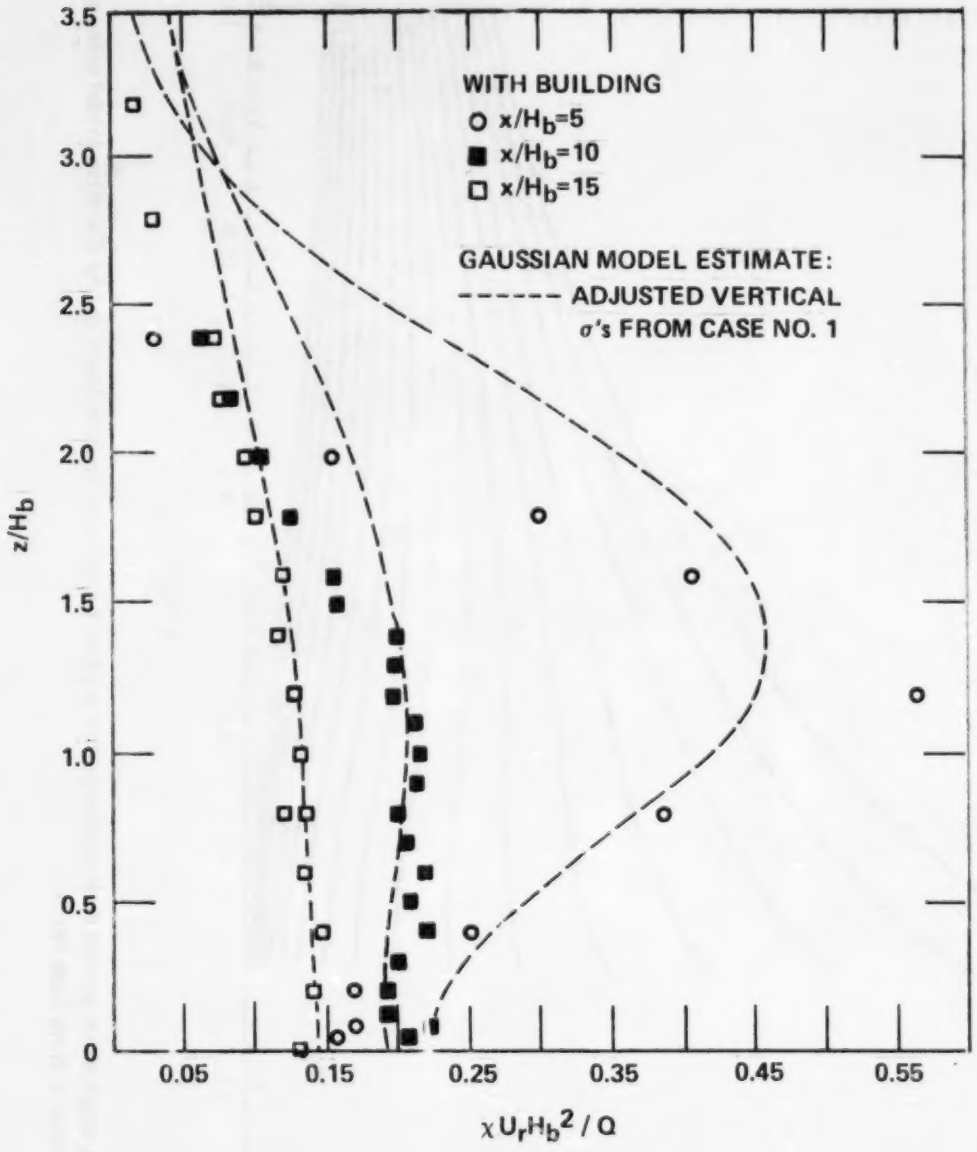

Figure 19. Vertical concentration measurements; Case No. 17 (1.5, 0.042, 1.5, 1.0).

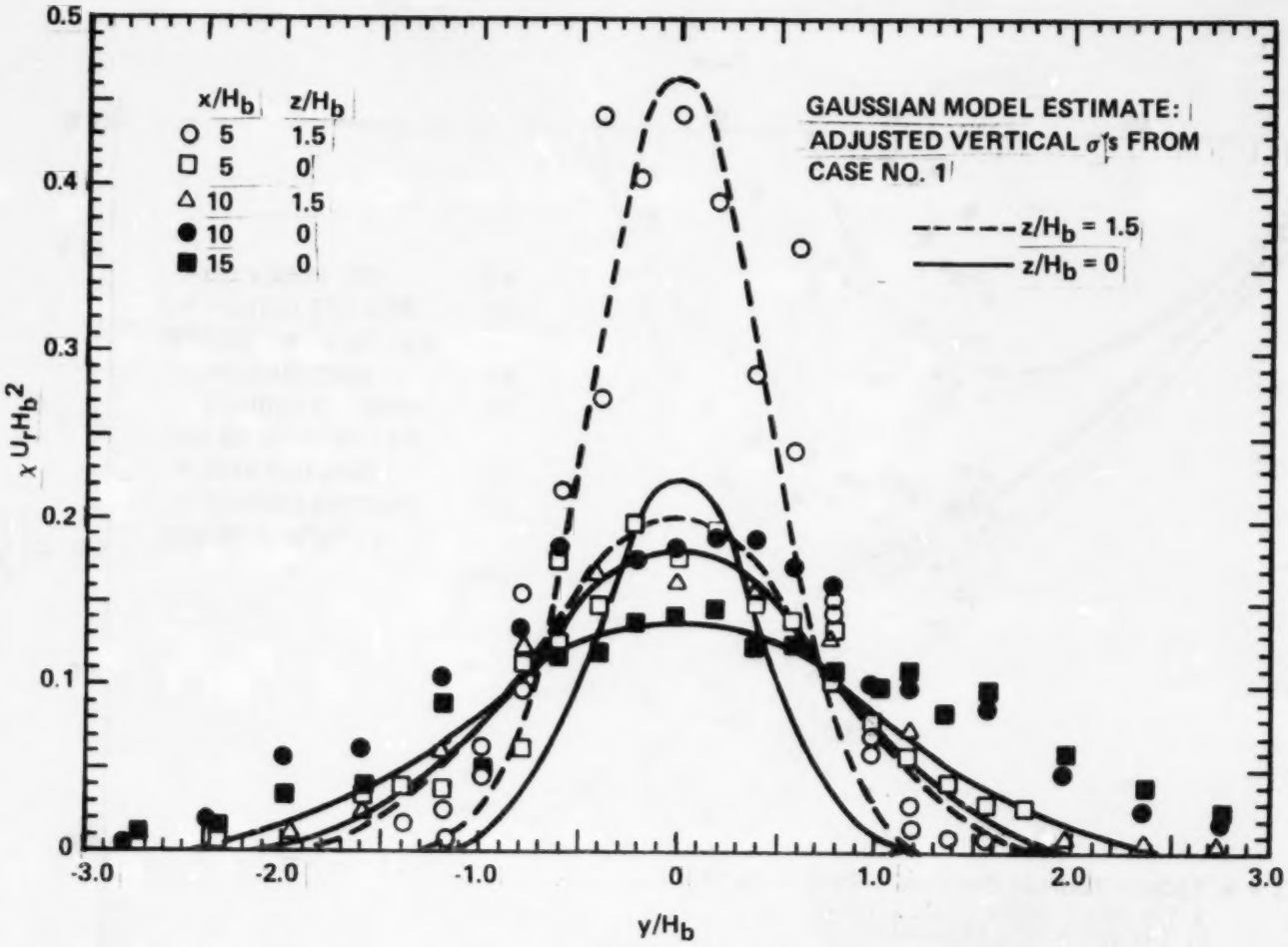

Figure 20. Lateral concentration profiles; Case No. 17 (1.5, 0.042, 1.5, 1.0).

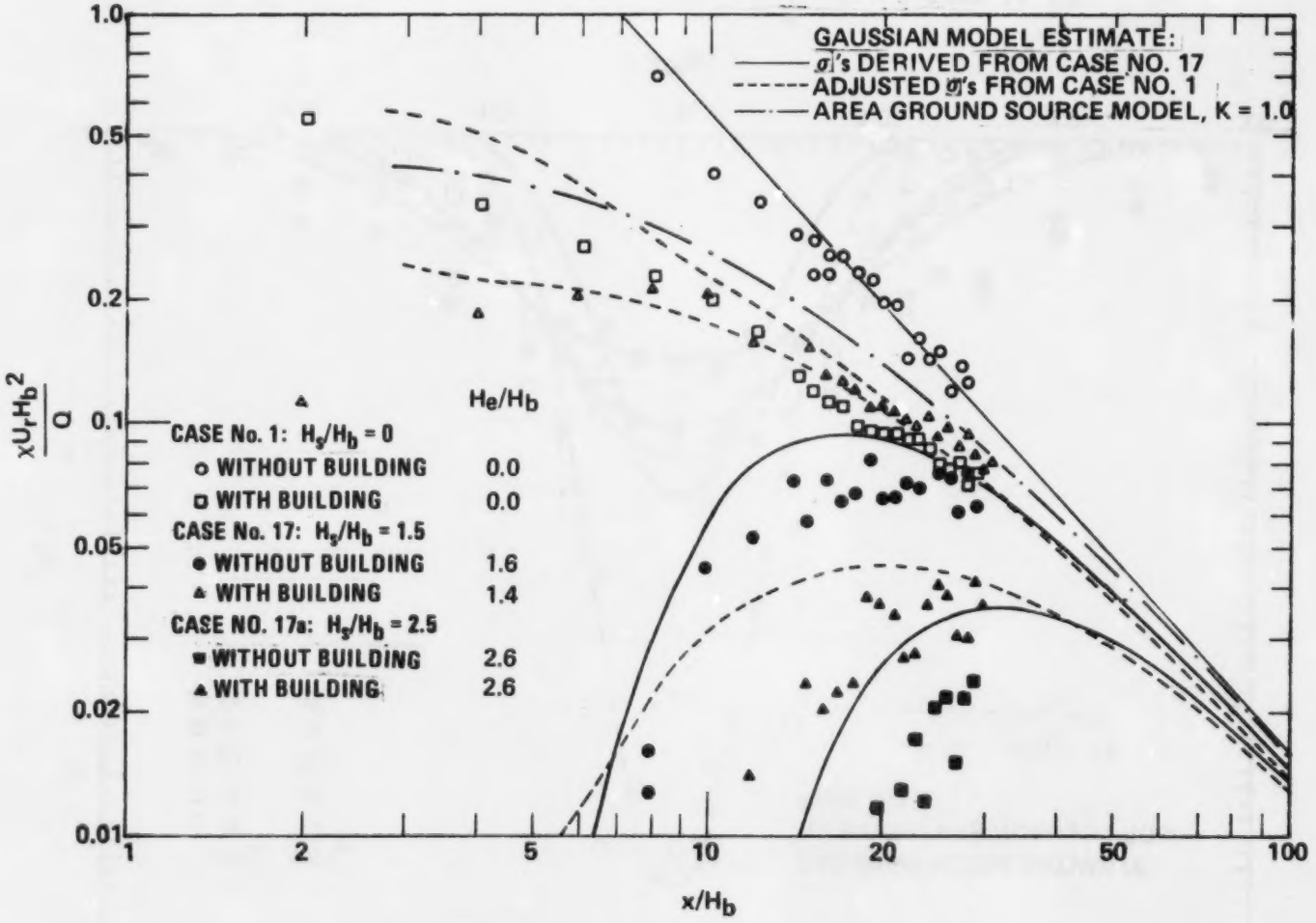

Figure 21. Longitudinal ground-level concentration measurements, Phase III.

was found to provide a good estimate of the ground-level concentrations when K=1. For Case 17a with H_s/H_b = 2.5, an overestimation of concentration was found both in the wake of the building and in the absence of the building. The background dispersion parameters were estimated from data for a lower stack (H_s/H_b = 1.5), which may be the cause of the difference. The overestimate of concentration in the wake of the building is an indication, as expected, that the building wake has less effect as the stack height is increased.

Figure 21 provides a good overview of the building wake effects on short stack effluents. For the ground-level source, the building wake greatly increased the plume spread (horizontal and vertical) in the immediate lee of the building, thus resulting in decreased ground-level concentrations from those that occurred in the absence of the building. Farther downwind, the plume dispersion was controlled by the background turbulence. Therefore, the measured concentrations slowly converge to values that occured in the absence of the building. For the elevated sources, the major building wake effect was that of an increased vertical plume spread, which caused the point of maximum ground-level concentration to shift upwind. For H_s/H_b = 1.5, this effect caused the absolute maximum concentration to increase by a factor of three over that which occurred in the absence of the building. A similar, somewhat decreased effect was found for the situation with H_s/H_b = 2.5. A convergence of the ground-level concentration, for the elevated stacks, to the value measured in the absence of the building was also found to occur in the far wake region. However, the downwind position of convergence appears to be somewhat farther downstream.

For the ground source (Case No. 1), vertical and lateral concentration profiles were taken at 15 and 30 building heights downwind. These data and model estimates are presented in Figures 22 and 23. Near the ground and close to the plume centerline, the model concentration estimates at 15 building heights downwind of the building were found to be slightly overestimated, but at 30 building heights downwind from the isolated stack, the model slightly underestimated concentrations. The lateral profiles demonstrate that for all situations the model overestimates the lateral plume spread even though concentration estimates near the plume centerline are well estimated. The reasons for this are not apparent since, for the earlier profiles, the lateral plume spread was well modeled. Perhaps the profiles taken in Phase III were influenced differently by a lateral inhomogeneity in the turbulent boundary layer since the profiles were measured at a position farther from the sources and the building was closer to the vortex generators.

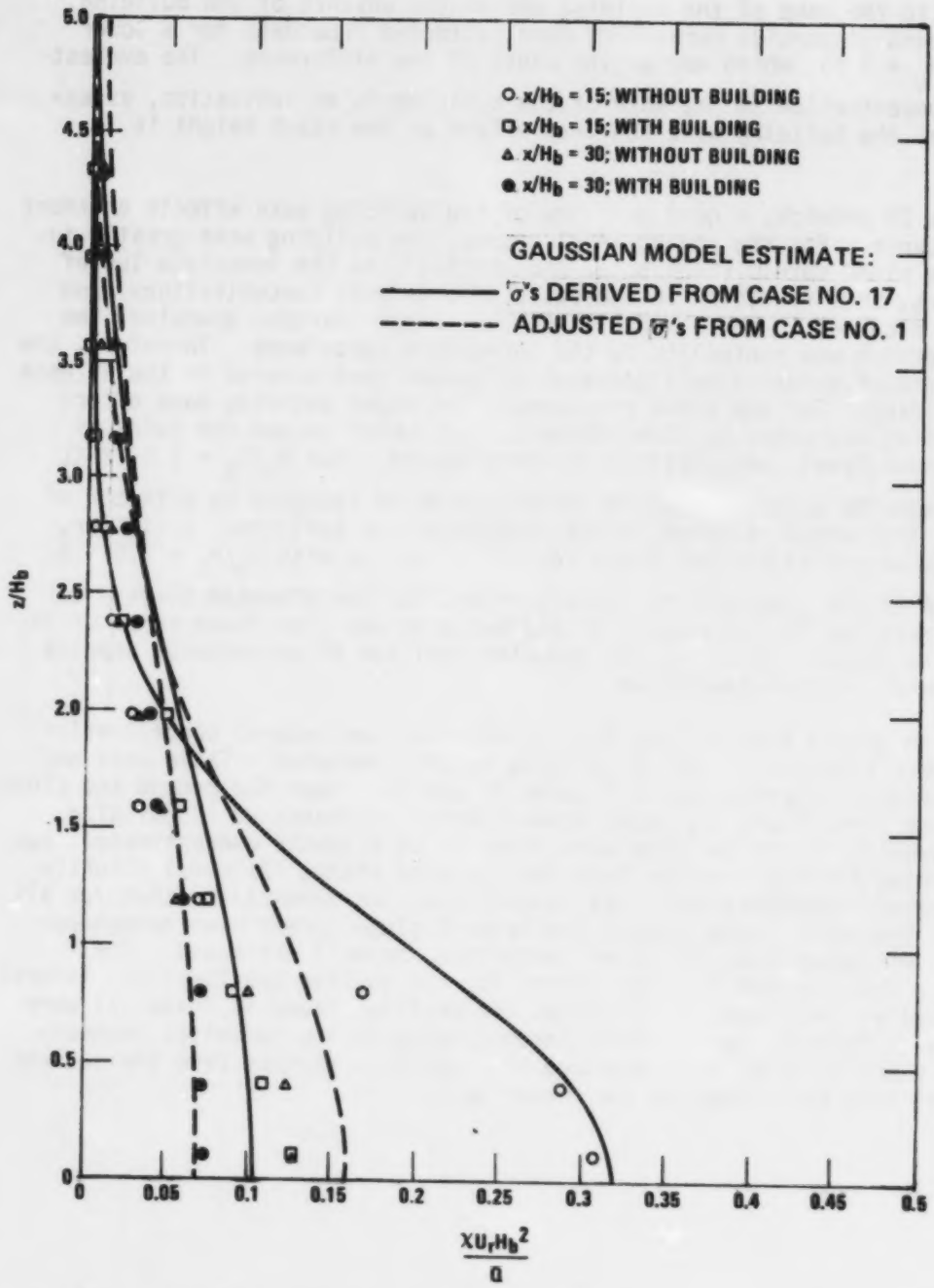

Figure 22. Vertical concentration measurements for ground source; Case No. 1, Phase III.

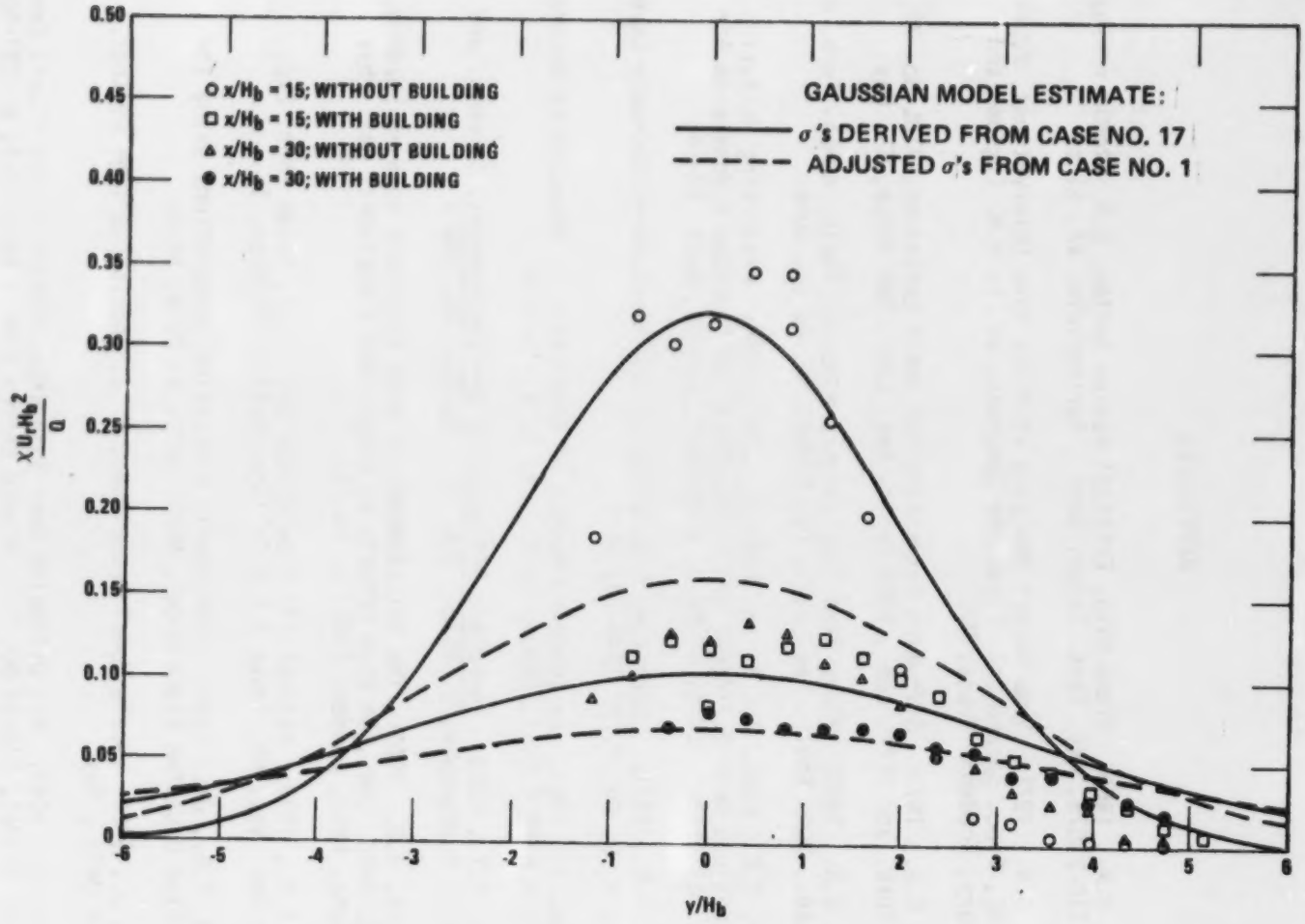

Figure 23. Lateral ground-level concentration profiles for ground source; Case No. 1., Phase III.

REFERENCES

Briggs, G.A., 1969: Plume Rise, Critical Review Series, U.S. Atomic Energy Comm., TID-25075, Nat. Tech. Infor. Serv., Springfield, VA, 81 p.

Briggs, G.A., 1971: Some Recent Analyses of Plume Rise Observations, Paper No. ME 8E, Proc. Second Int. Clean Air Congress, ed. by H.M. Englund and W.T. Beery, Academic Press, NY.

Briggs, G.A., 1973: Diffusion Estimation for Small Emissions, ATDL No. 79, Atmos. Turb. and Diff. Lab., NOAA Envir. Res. Lab., Oak Ridge, TN, May.

Briggs, G.A., 1975: Plume Rise Predictions, ATDL No. 75/15, Atmos. Turb. and Diff. Lab., NOAA Envir. Res. Lab., Oak Ridge, TN, 46 p., June.

Britter, R.E., Hunt, J.C.R. and Puttock, J.S., 1976: Predicting Pollution Concentrations Near Buildings and Hills, Conf. on "Systems & Models in Air & Water Pollution", Inst. of Meas. & Control, London, Sept. 22-24.

Cermak, J.E., 1971: Laboratory Simulation of the Atmospheric Boundary Layer, AIAA J., v. 9, no. 9, p. 1746-54, Sept.

Counihan, J., 1969: An Improved Method of Simulating an Atmospheric Boundary Layer in a Wind Tunnel, Atmos. Envir., v. 3, p. 197-214.

Csanady, G.T., 1973: Turbulent Diffusion in the Environment, Geophys. and Astrophys. Monographs, D. Reidel Pub. Co., Boston, MA, 248 p.

Davenport, A.G., 1963: The Relationship of Wind Structure to Wind Loading, Paper 2, Proc. Conf. on Wind Effects on Bldgs. and Structures, Nat. Phys. Lab., June, HMSO, London, 1965, p. 54-102.

Evans, B.H., 1957: Natural Air Flow around Buildings, Texas Engr. Exp. Station Res. Rpt. 59, Texas A & M College, College Station, TX.

Gifford, F.A., Jr., 1960: Atmospheric Dispersion Calculations using the Generalized Gaussian Plume Model, Nucl. Saf., v. 2, p. 56-9.

Golden, J., 1961: Scale Model Techniques, M. S. Thesis, College of Engr., New York Univ., May.

Halitsky, J., 1968: Gas Diffusion Near Buildings, Meteorol. and Atomic Energy, (ed. D.H. Slade), TID-24190, U.S. Atomic Energy Comm., Sect. 5-5, p. 221-55.

Halitsky, J., 1969: Validation of Scaling Procedures for Wind Tunnel Model Testing of Diffusion Near Buildings, Ph.D. Diss., Rpt. No. TR-69-8, New York Univ., NY, NY.

Harris, R.I., 1968: Measurement of Wind Structure at Heights up to 598 feet above Ground Level, Symp. Wind Effects on Buildings and Structures, Loughborough Univ. Tech. (Dept. of Transport Technology), England.

Hoult, D.P., 1973: Simulation of Buoyant Pollutants in the Atmospheric Boundary Layer, Flow Studies in Air and Water Pollution, Am. Soc. Mech. Engrg., NY, NY.

Hoult, D.P. and Weil, J.C., 1972: Turbulent Plume in a Laminar Cross Flow, Atmos. Envir., v. 6, no. 8, p. 513-32, Aug.

Huber, A.H. and Snyder, W.H., 1976: Building Wake Effects on Short Stack Effluents, Proc. 3rd Symp. on Atmos. Turb., Diff. and Air Quality, Oct. 26-29, Raleigh, NC, Am. Meteorol. Soc., Boston, MA.

Huber, A.H., Snyder, W.H., Thompson, R.S., and Lawson, R.E., Jr., 1976: Stack Placement in the Lee of a Mountain Ridge: A Wind Tunnel Study, Envir. Prot. Agcy. Rept. No. EPA-600/4-76-047, Res. Tri. Pk., NC, Sept., 45 p.

Lin, J.T., Liu, H.T., Pao, Y.H., Lilly, D.K., Israeli, M. and Orszag, S.A., 1974: Laboratory and Numerical Simulation of Plume Dispersion in Stably Stratified Flow over Complex Terrain, Envir. Prot. Agcy. Rpt. No. EPA-650/4-74-044, 70 p., Nov.

McElroy, J.L. and Pooler, F., Jr., 1968: St. Louis Dispersion Study, Vol. II-Analysis, Nat. Air Poll. Control Admin. Pub. No. AP-53, Cincinnati, OH.

Meroney, R.N., 1971: Gaseous Plume Diffusion about Isolated Structures of Simple Geometry, Rpt. No. CER71-72RNM19, Colo. State Univ., Ft. Collins, CO, 13 p., Dec.

Meroney, R.N. and Yang, B.T., 1971: Wind Tunnel Study on Gaseous Mixing Due to Various Stack Heights and Injection Rates Above an Isolated Structure, Rpt. No. CER71-72RNM-BTY16, Colo. State Univ., Ft. Collins, CO., (also AEC Rpt. No. COO-2053-6).

Peterka, J.A. and Cermak, J.E., 1975: Turbulence in Building Wakes, 4th Intl. Conf. on Wind Effects on Buildings and Structures, Sept. 8-12, London, England (also Rpt. No. CER74-75JAP-JEC34, Colo. State Univ., Ft. Collins, CO).

Robins, A.G. and Castro, I.P., 1977a: A Wind Tunnel Investigation of Plume Dispersion in the Vicinity of a Surface Mounted Cube, I. The Flow Field, Atmos. Envir., v. 11, no. 4, p. 291-7.

Robins, A.G. and Castro, I.P., 1977b: A Wind Tunnel Investigation of Plume Dispersion in the Vicinity of a Surface Mounted Cube, II. The Concentration Field, Atmos. Envir., v. 11, no. 4, p. 299-311.

Smith, E.G., 1951: The Feasibility of using Models for Predetermining Natural Ventilation, Res. Rep. No. 26, Tex. Engng. Exp. Stn., Texas A & M College, College Station, TX.

Snyder, W.H., 1972: Similarity Criteria for the Application of Fluid Models to the Study of Air Pollution Meteorology, Bound. Layer Meteorol., v. 3, no. 2, p. 113-34.

Snyder, W.H., 1979a: The EPA Meteorological Wind Tunnel: Its Design, Construction, and Operating Characteristics, Envir. Prot. Agcy. Rpt. No. EPA-600/4-79-051, Res. Tri. Pk., NC, 78 p., Sept.

Snyder, W.H., 1979b: Guideline for Fluid Modeling of Atmospheric Diffusion, Draft for Public Comment, Envir. Prot. Agcy. Rpt. No. EPA-450/4-79-016, Res. Tri. Pk., NC, June, 172 p.

Snyder, W.H. and Lawson, R.E., Jr., 1976: Determination of a Necessary Height for a Stack Close to a Building - A Wind Tunnel Study, Atmos. Envir., v. 10, no. 9, p. 683-91.

Turner, D.B., 1970: Workbook of Atmospheric Dispersion Estimates, Office of Air Programs, Pub. No. AP-26, U.S. Envir. Prot. Agcy., Res. Tri. Pk., NC, Jan.

APPENDIX

The complete set of data from Phases I and II are presented for each case. Smoke was visually observed for 30 cases, while concentration measurements consisting of longitudinal and vertical profiles were taken for 24 of the cases. The effect of the building can be easily seen here since visual observations and concentration measurements were made both in the wake of the building and in the absence of the building. Comparisons of the longitudinal profiles for the cases with the tallest stack heights show rather large differences in maximum concentration. These results are due to very slight influences of the building, causing the point of initial ground-level impact to be moved closer to the source. Measurements farther downwind, at the point of maximum concentration, would not show such large differences. Thus, data for these cases cannot be used to quantify the significance of the building influence as can be done for the shorter stacks.

In all cases, the top and bottom photographs of the smoke are with and without the building, respectively. The exposure time for all photographs was 4 seconds. To aid the reader, five parameters have been added in parenthesis following each case number, i.e., (H_s/H_b, D_s/H_s, W_s/U_s, ρ_s/ρ_a, Fr_s).

The concentrations denoted as □ and + represent measurements with and without the building, respectively. In some cases, measured concentrations are negative and lie outside of the boundary of the graph. These situations are a result of the background concentration being over-estimated, as could have been caused by a drifting background during the measurement period.

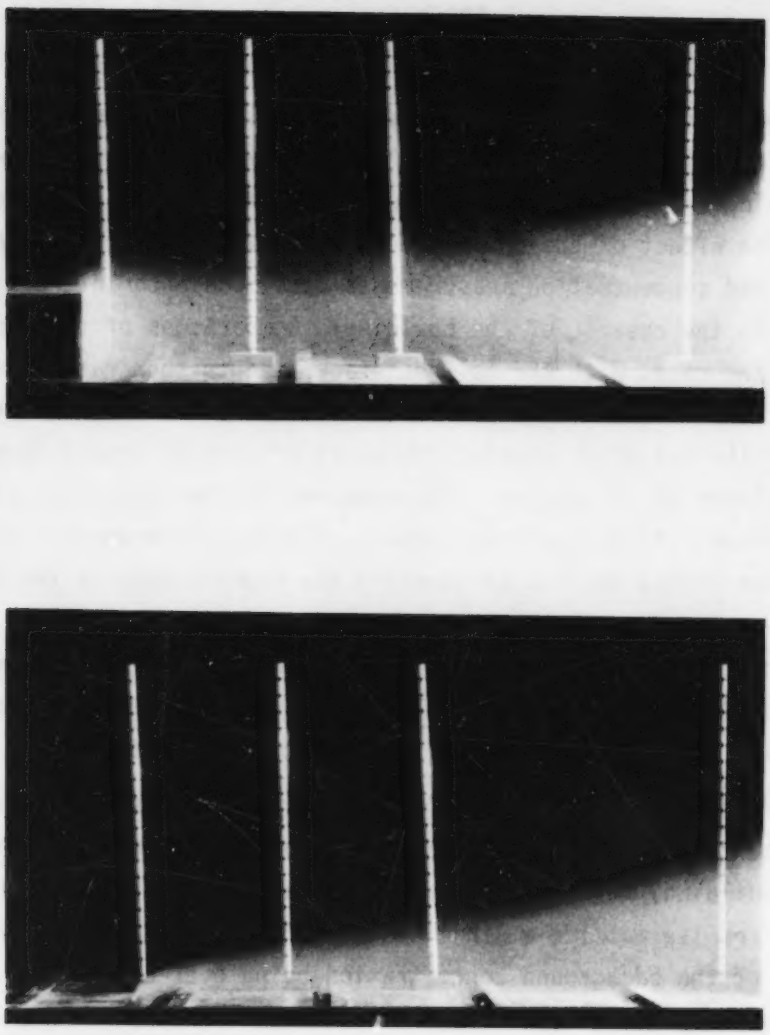

Figure A-1. Case No. 1 Smoke visualization (0, ∞, --, 1.0, ∞).

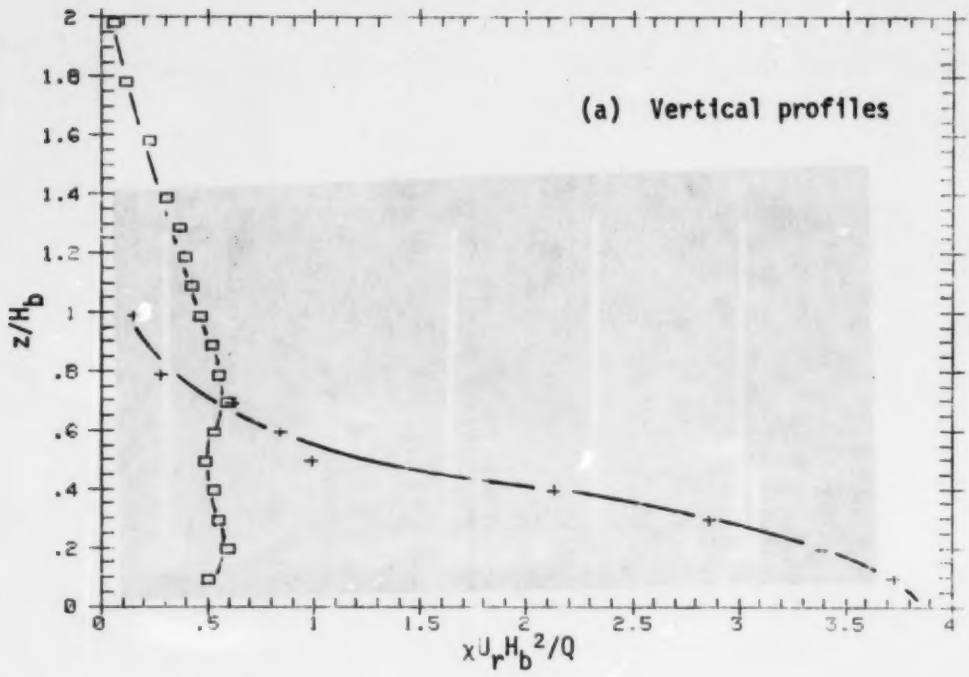

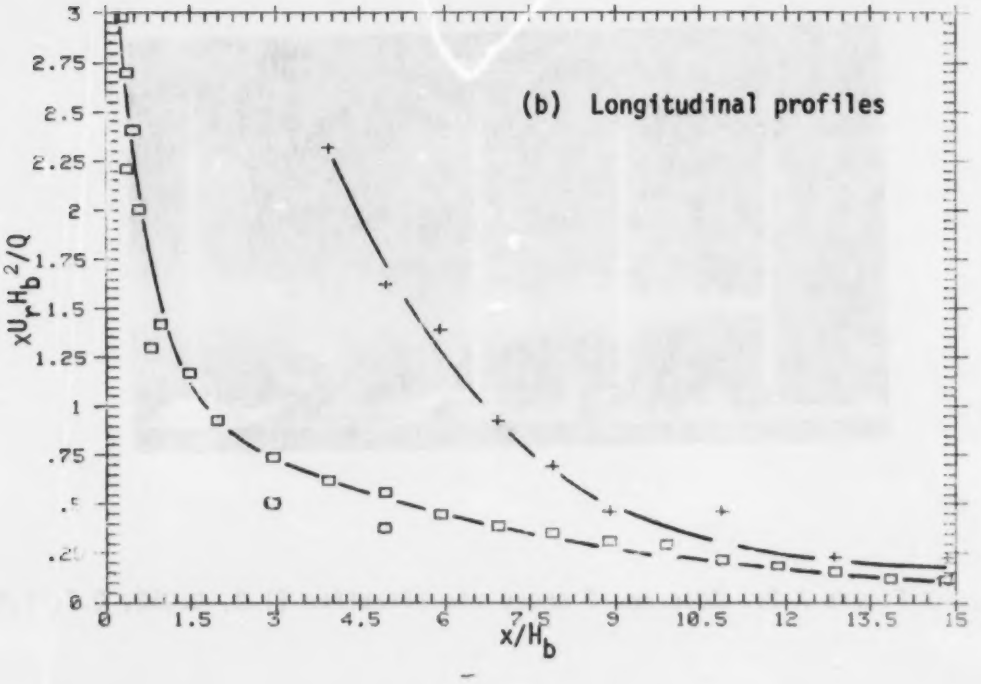

F gure A-2. Case No. 1 concentration measurements.

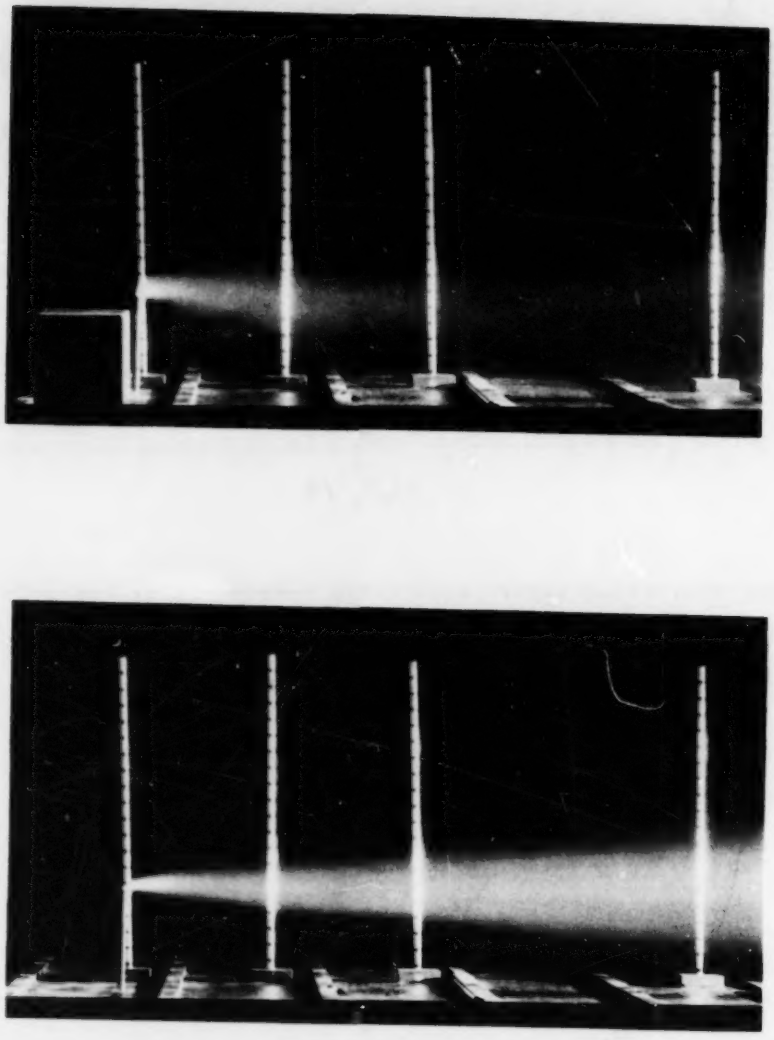

Figure A-3. Case No. 2 smoke visualization (1.2, 0.052, 0.7, 1.0, ∞).

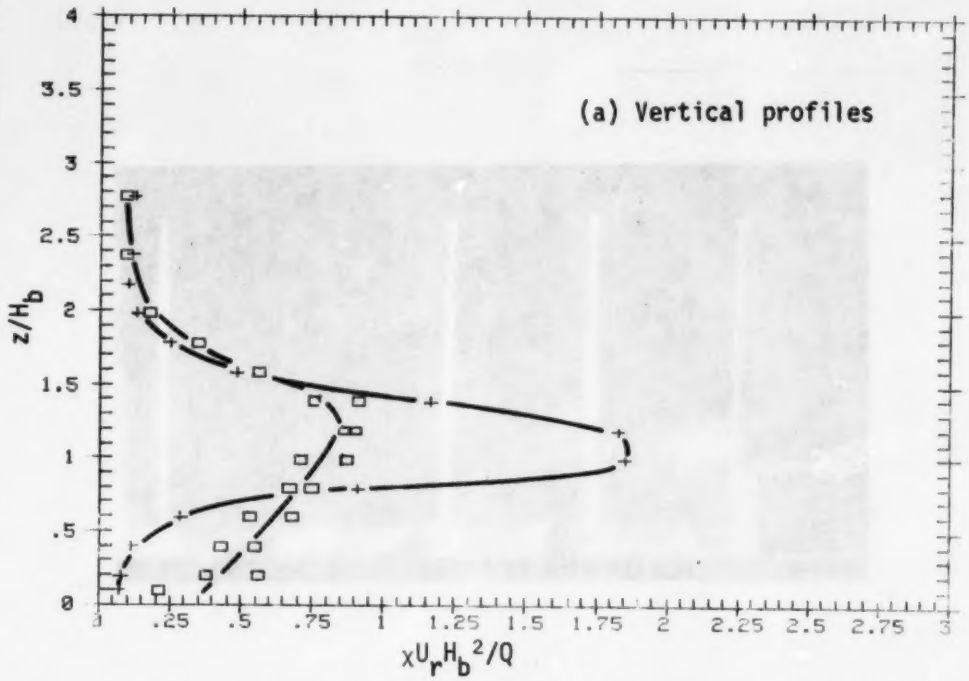

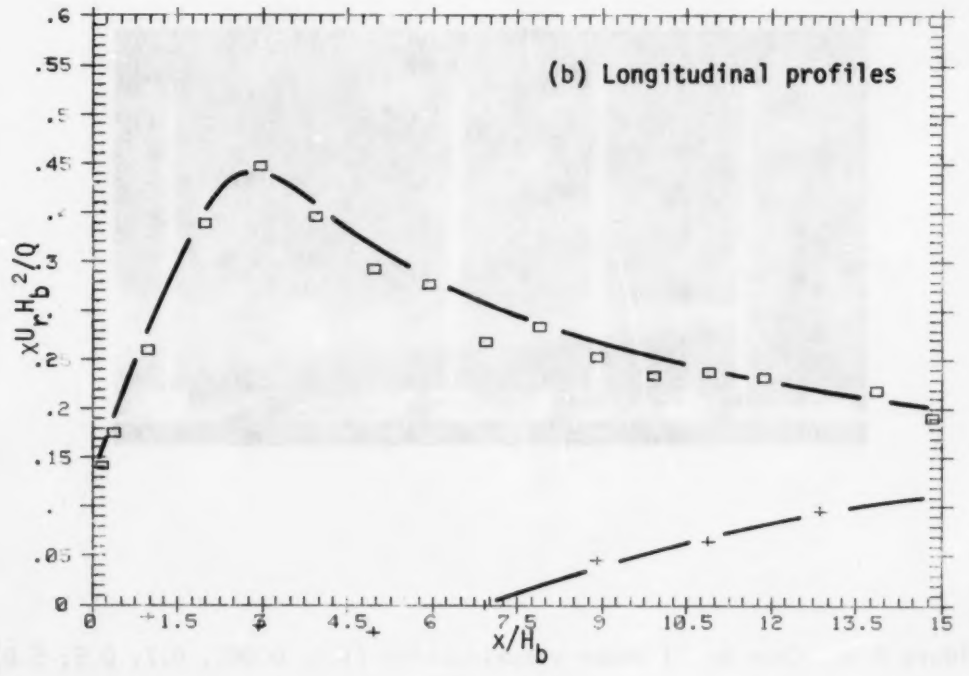

Figure A-4. Case No. 2 concentration measurements.

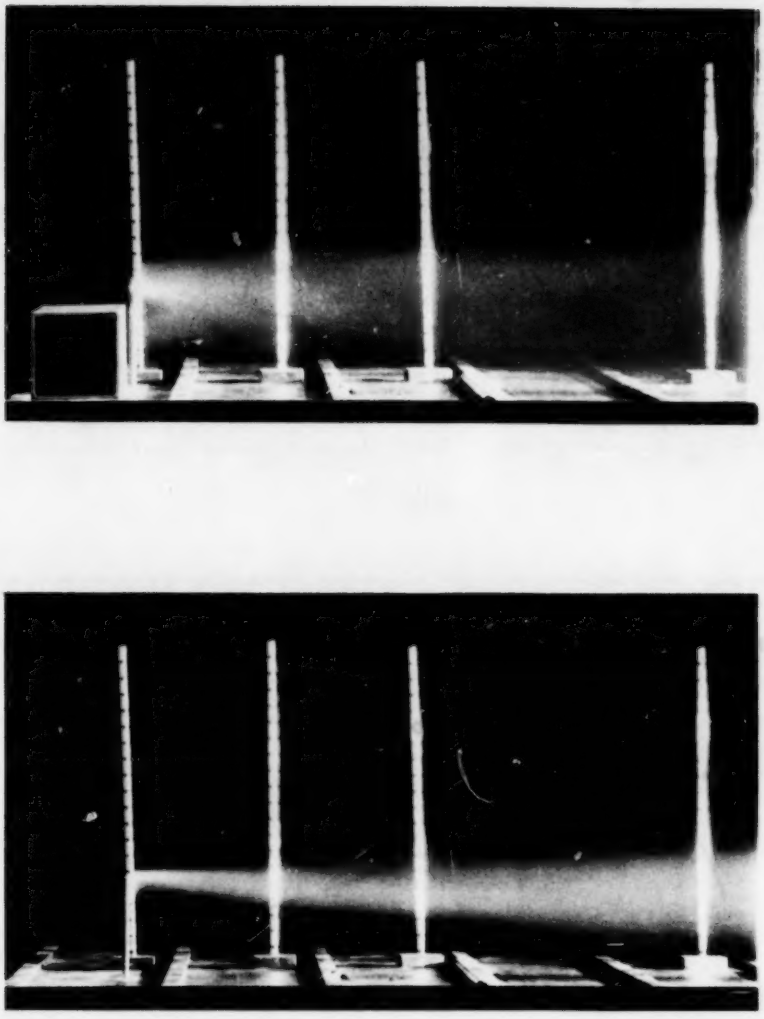

Figure A-5. Case No. 3 smoke visualization (1.2, 0.052, 0.7, 0.5, 5.8).

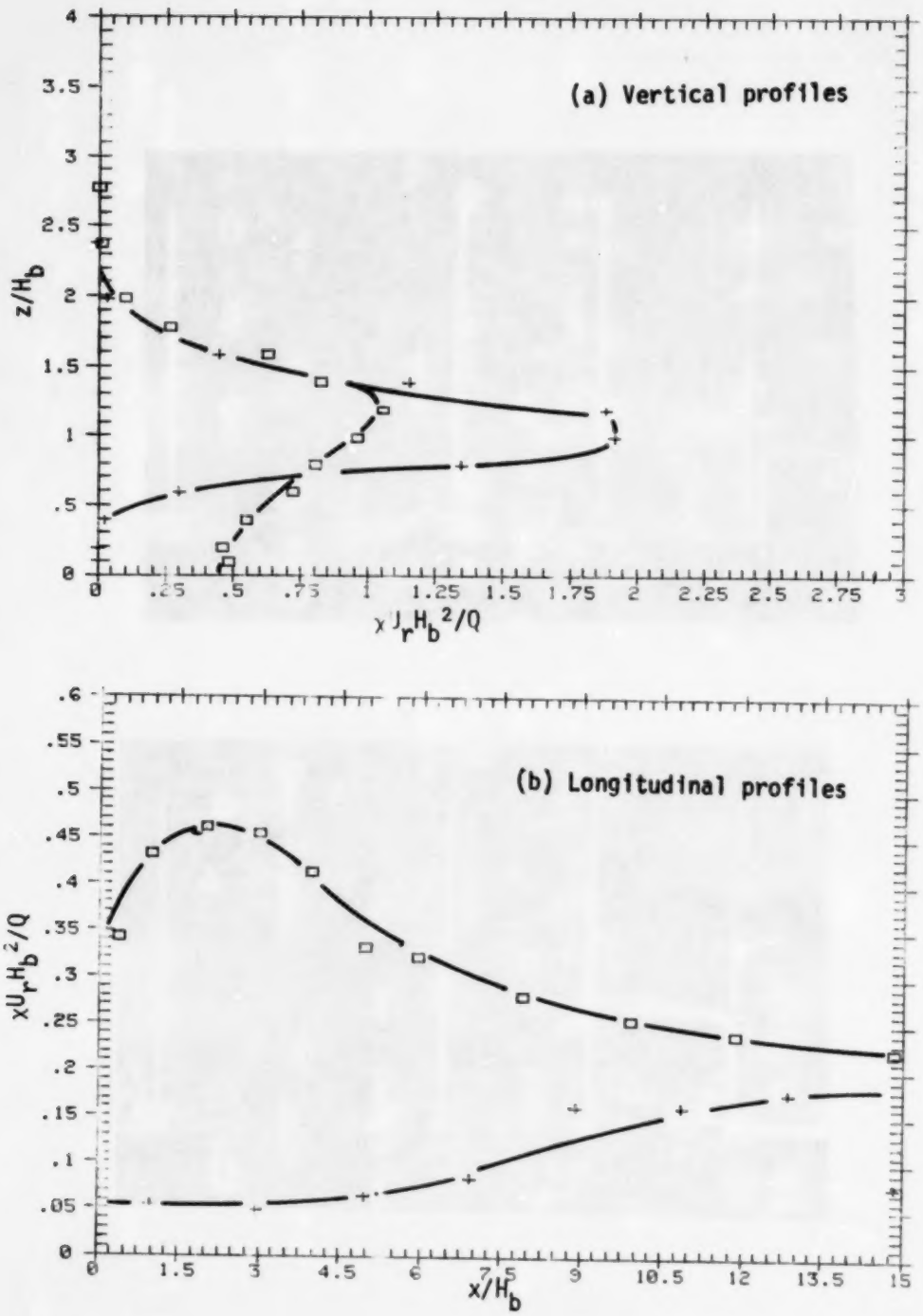

Figure A-6. Case No. 3 concentration measurements.

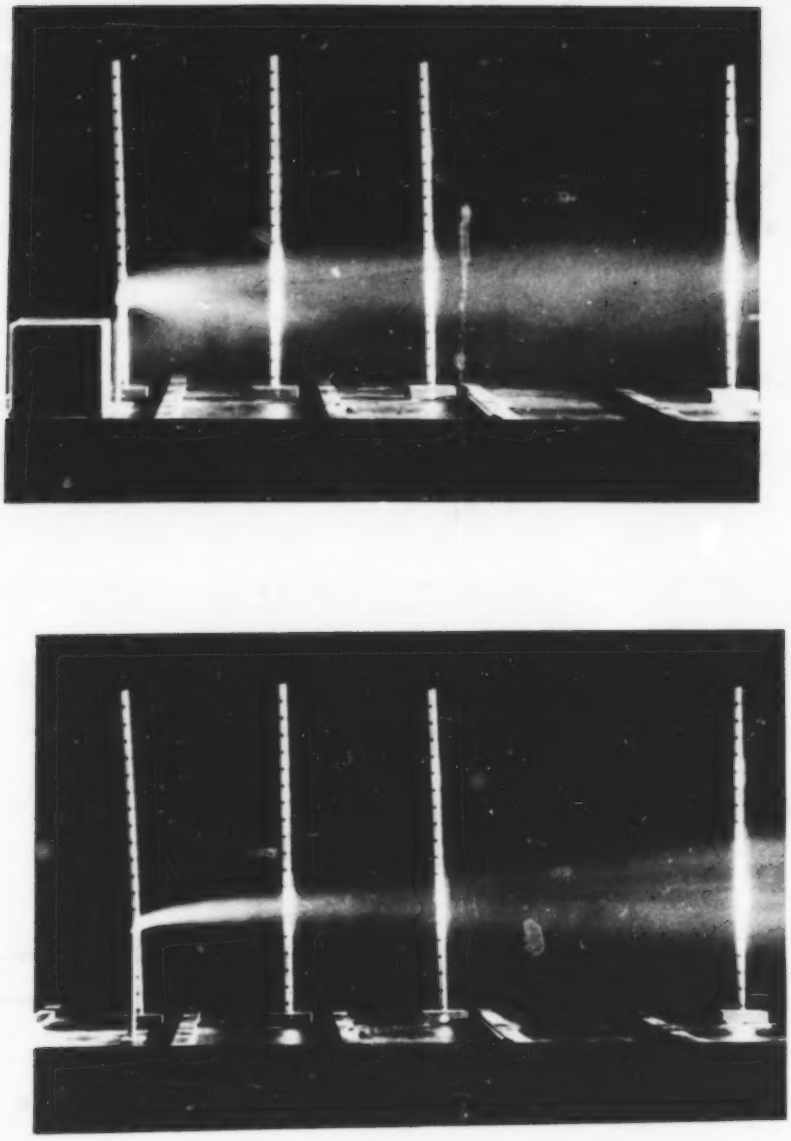

Figure A-7. Case No. 4 smoke visualization (1.2, 0.052, 1.5, 1.0, ∞).

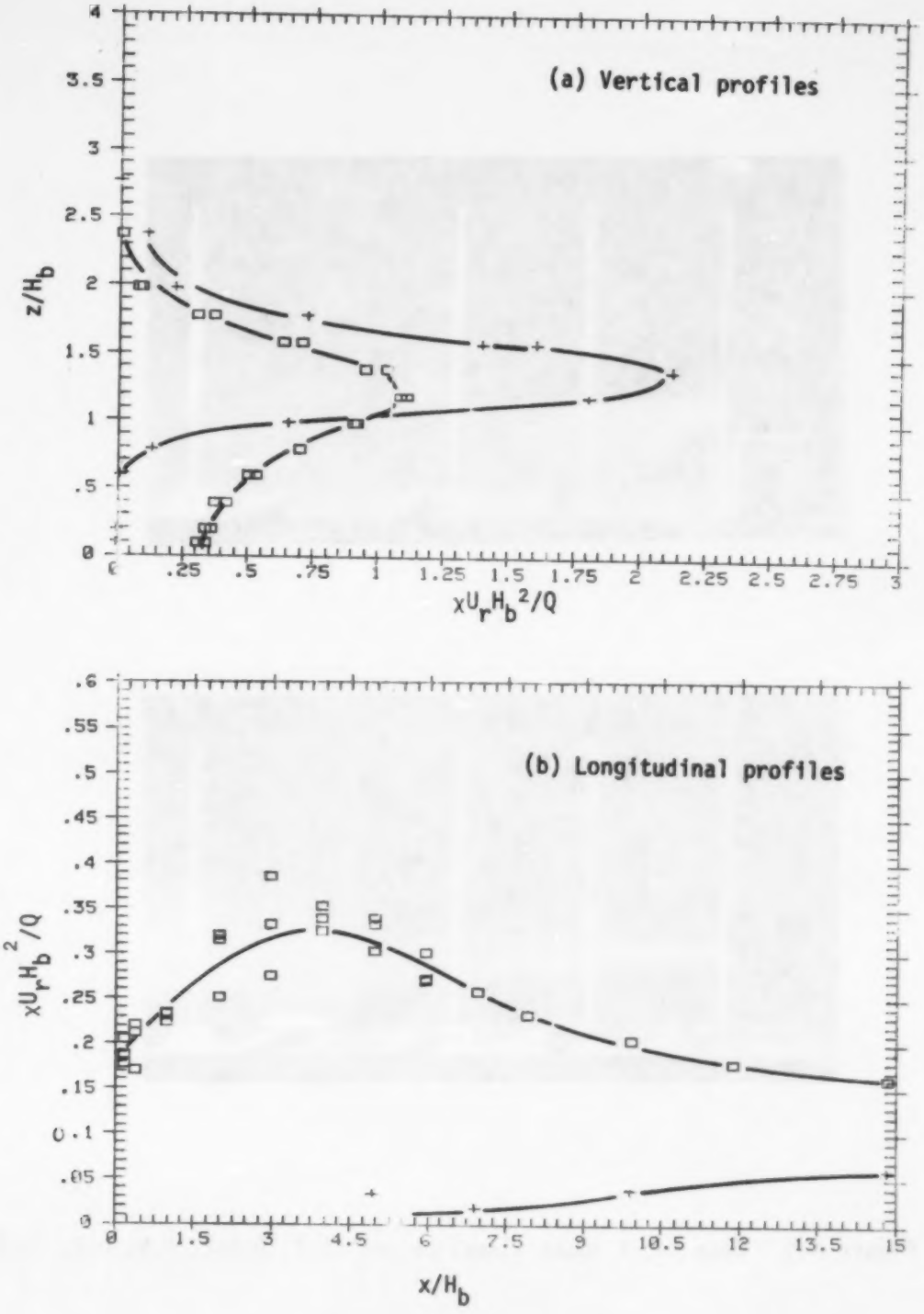

Figure A-8. Case No. 4 concentration measurements.

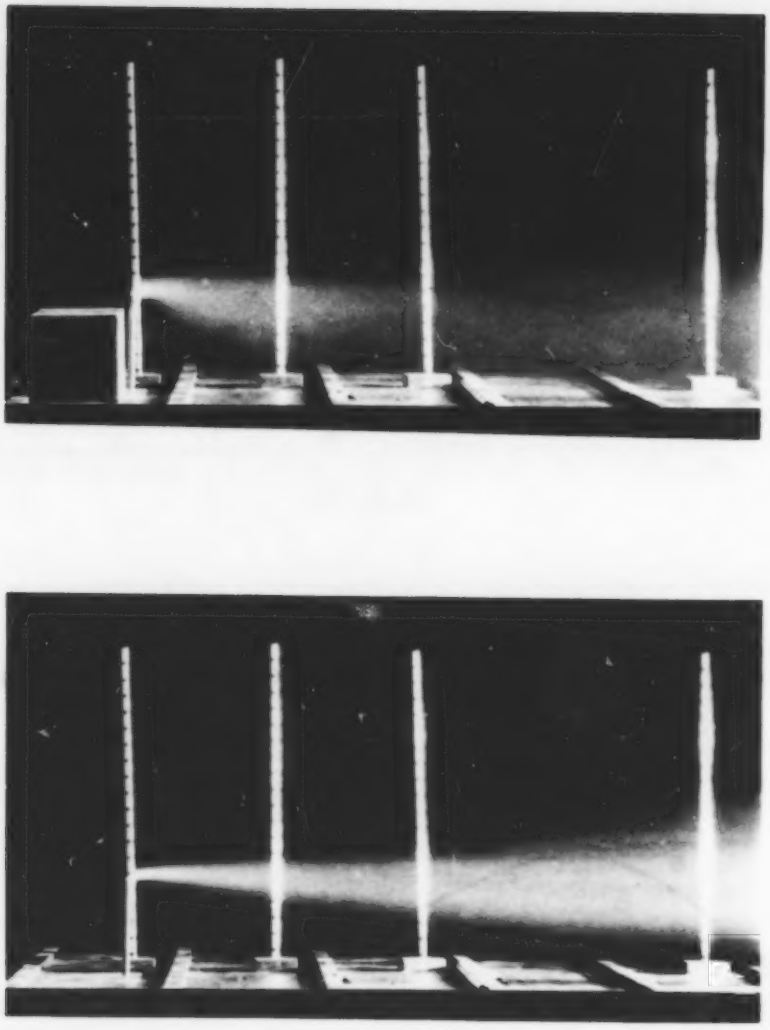

Figure A-9. Case No. 5 smoke visualization (1.2, 0.052, 1.5, 0.5, 13.0).

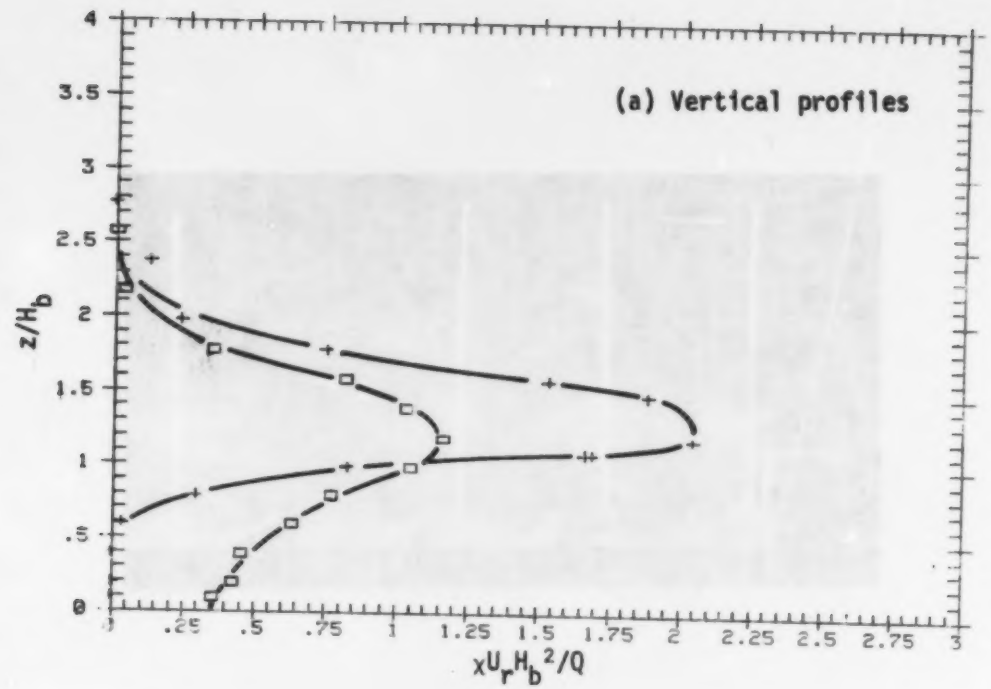

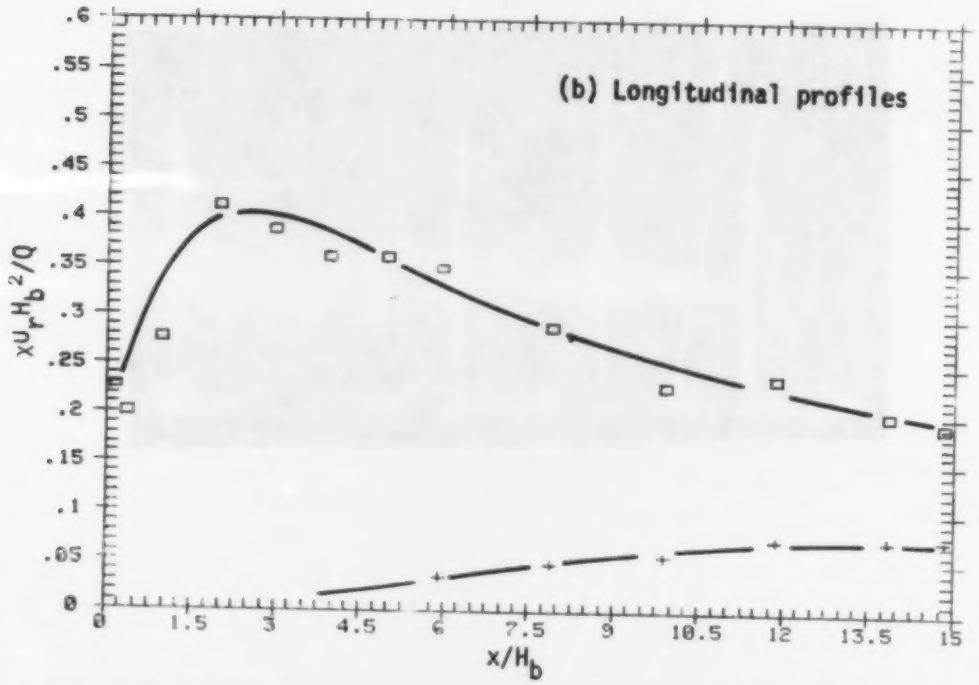

Figure A-10. Case No. 5 concentration measurements.

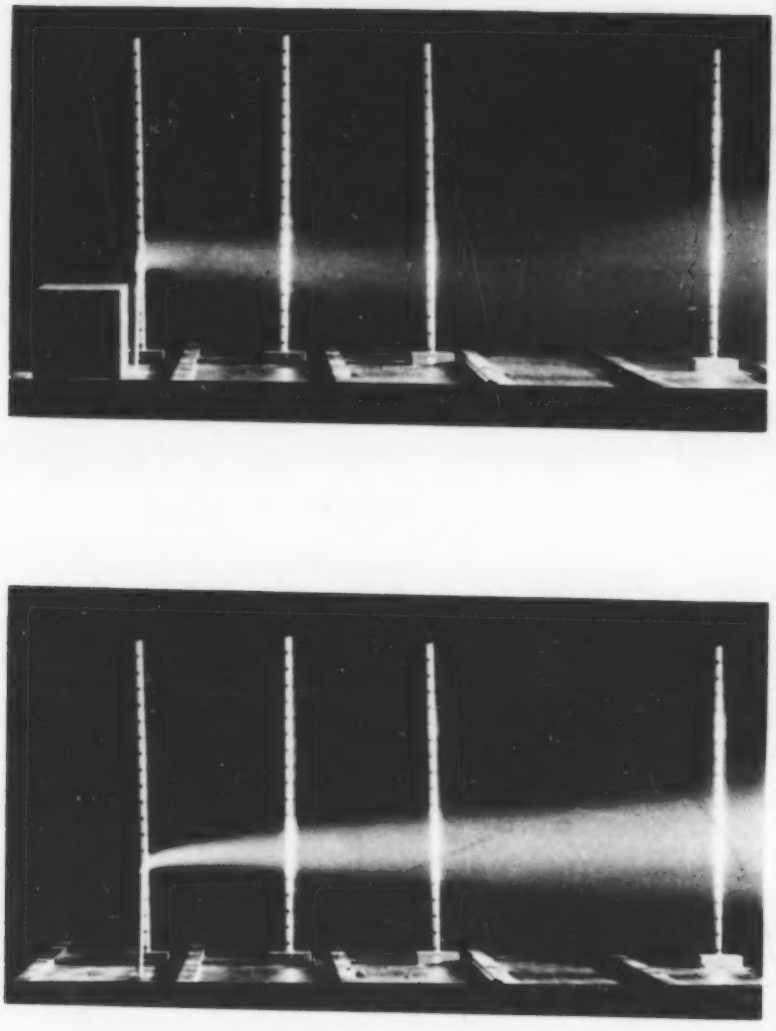

Figure A-11. Case No. 6 smoke visualization (1.2, 0.052, 2.2, 1.0, ∞).

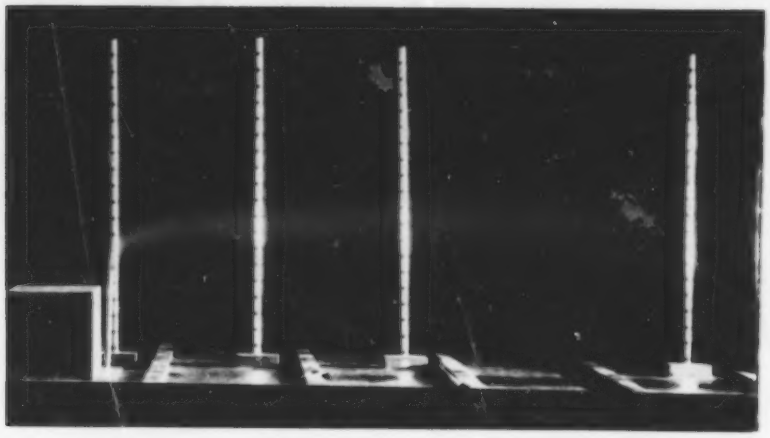

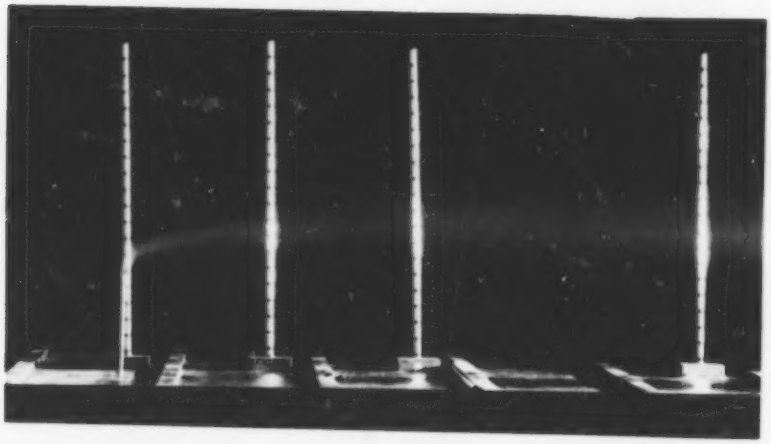

Figure A-12. Case No. 7 smoke visualization (1.2, 0.052, 4.0, 1.0, ∞).

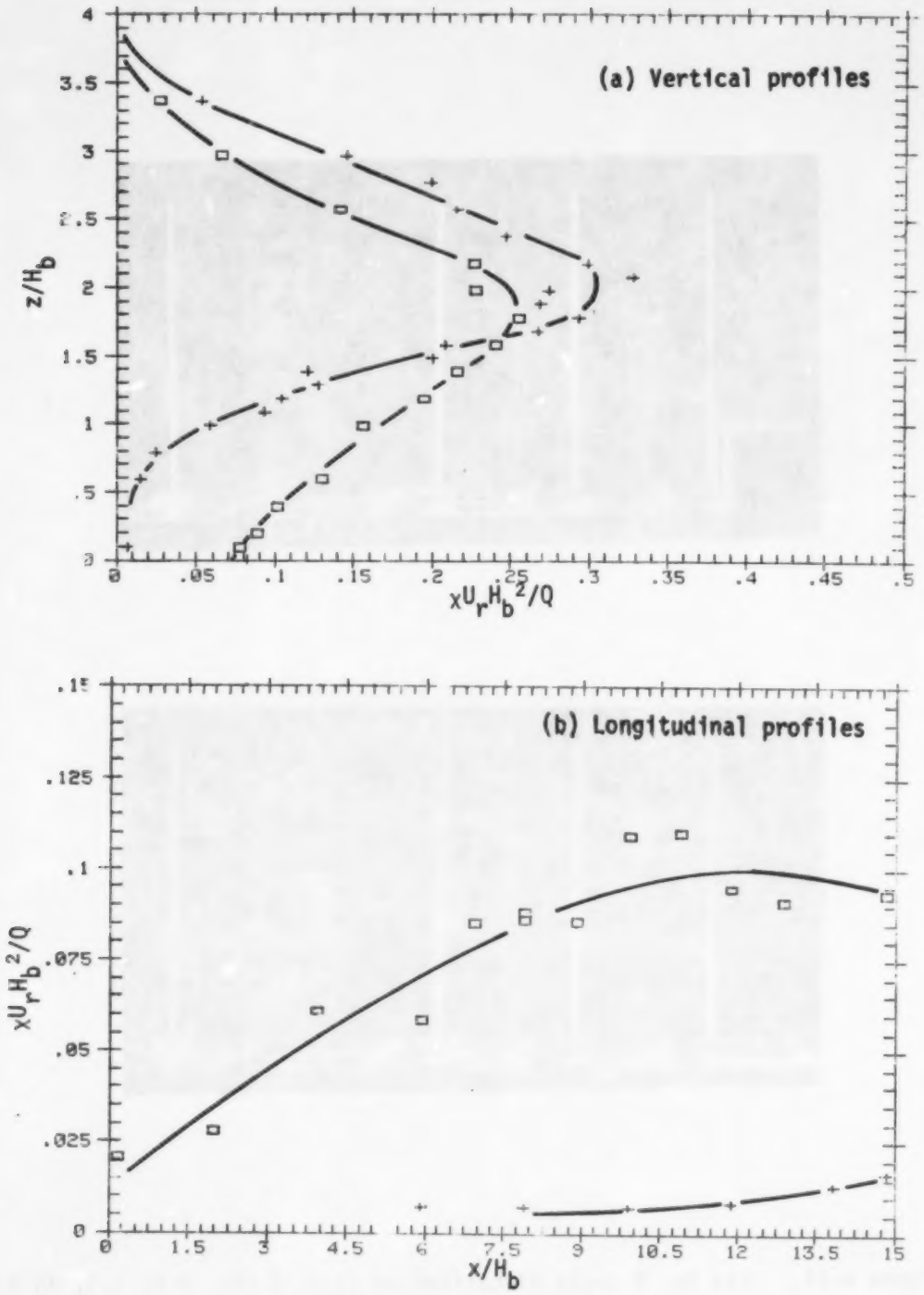

Figure A-13. Case No. 7 concentration measurements.

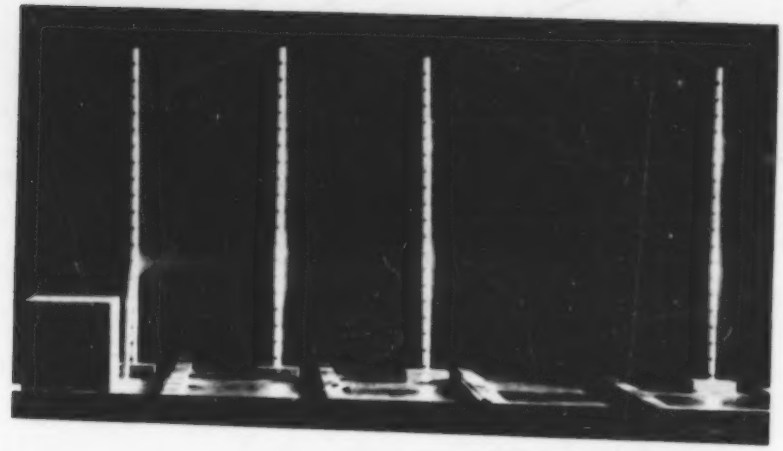

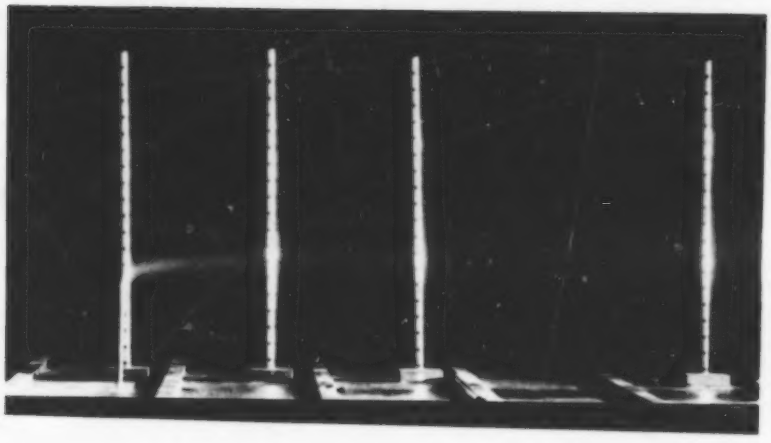

Figure A-14. Case No. 8 smoke visualization (1.2, 0.052, 4.0, 0.5, 33.4).

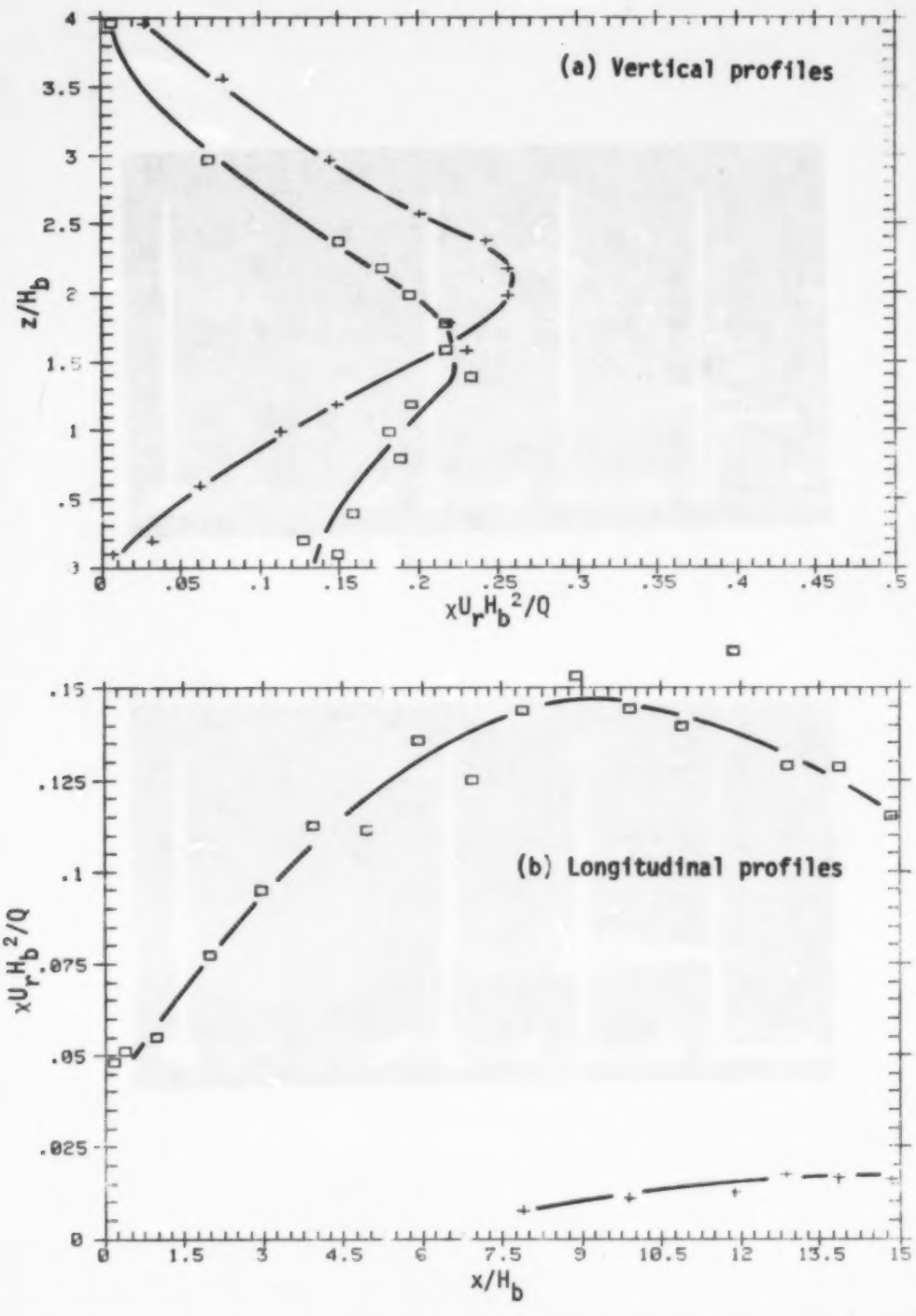

Figure A-15. Case No. 8 concentration measurements.

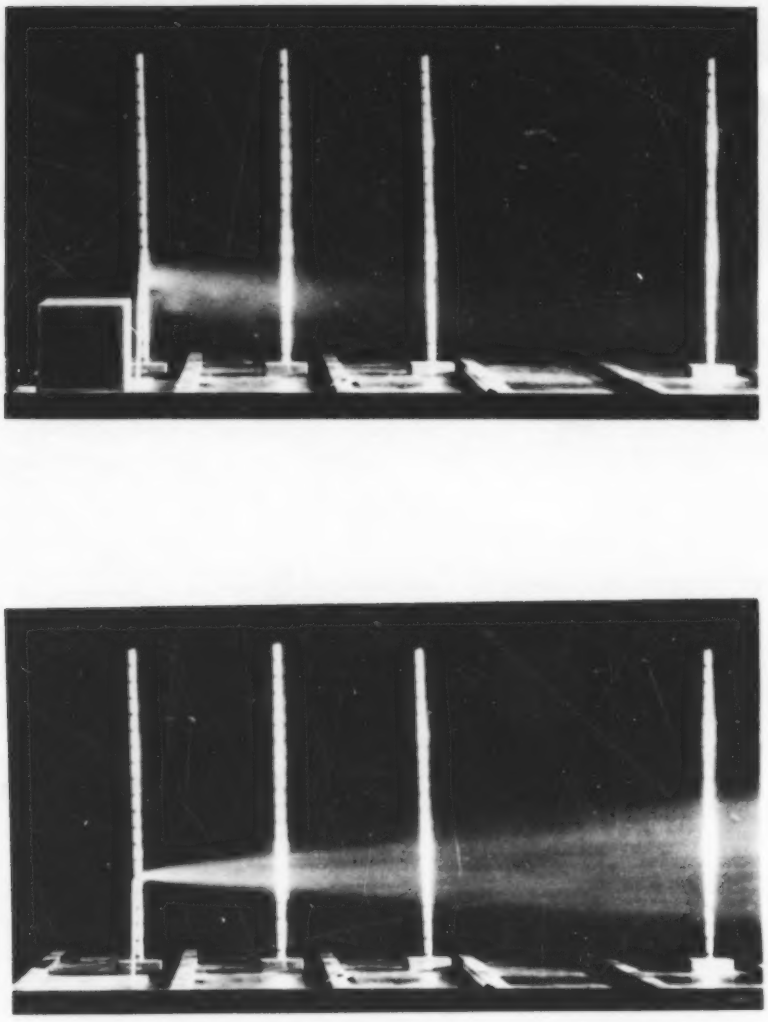

Figure A-16. Case No. 9 smoke visualization (1.2, 0.021, 1.5, 1.0, ∞).

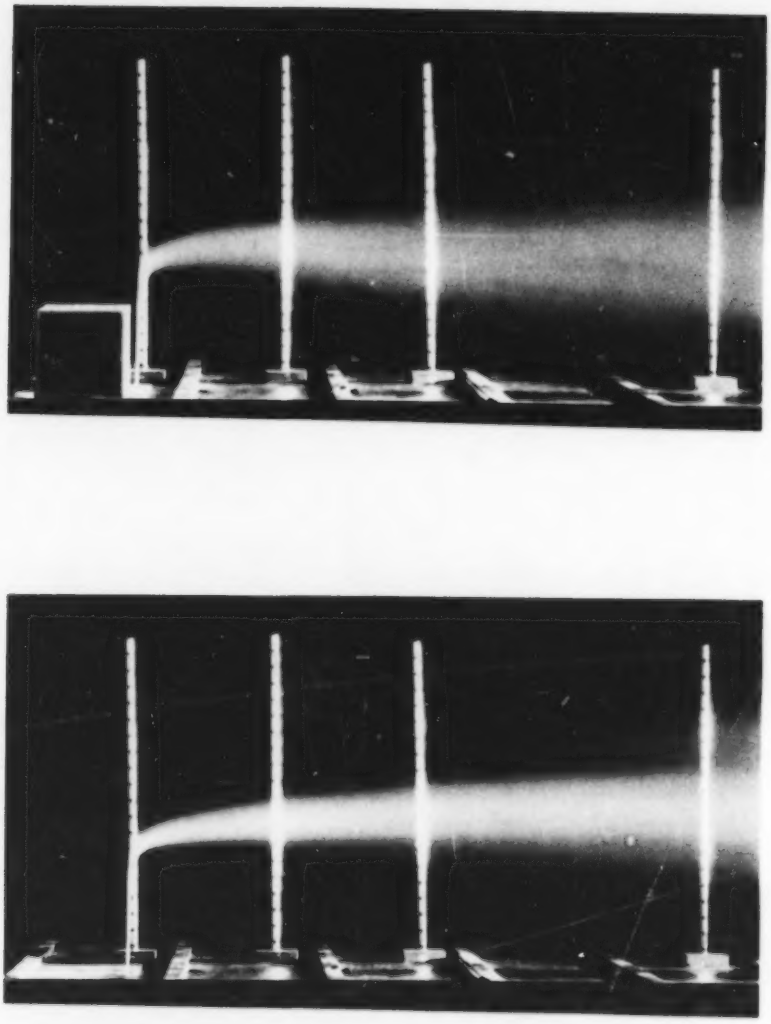

Figure A-17. Case No. 10 smoke visualization (1.2, 0.021, 8.4, 1.0, ∞).

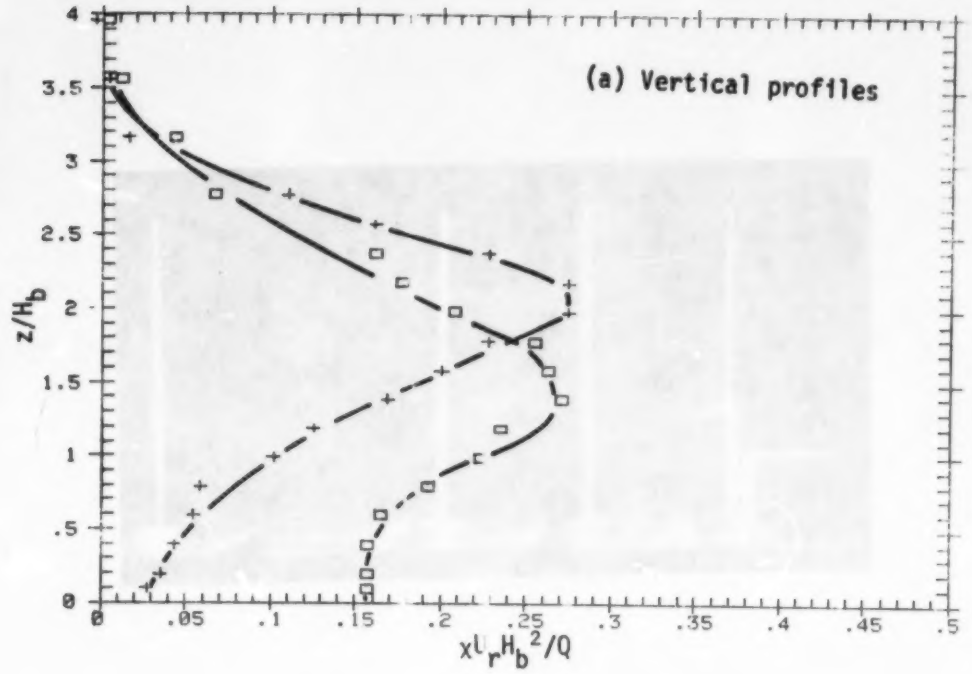

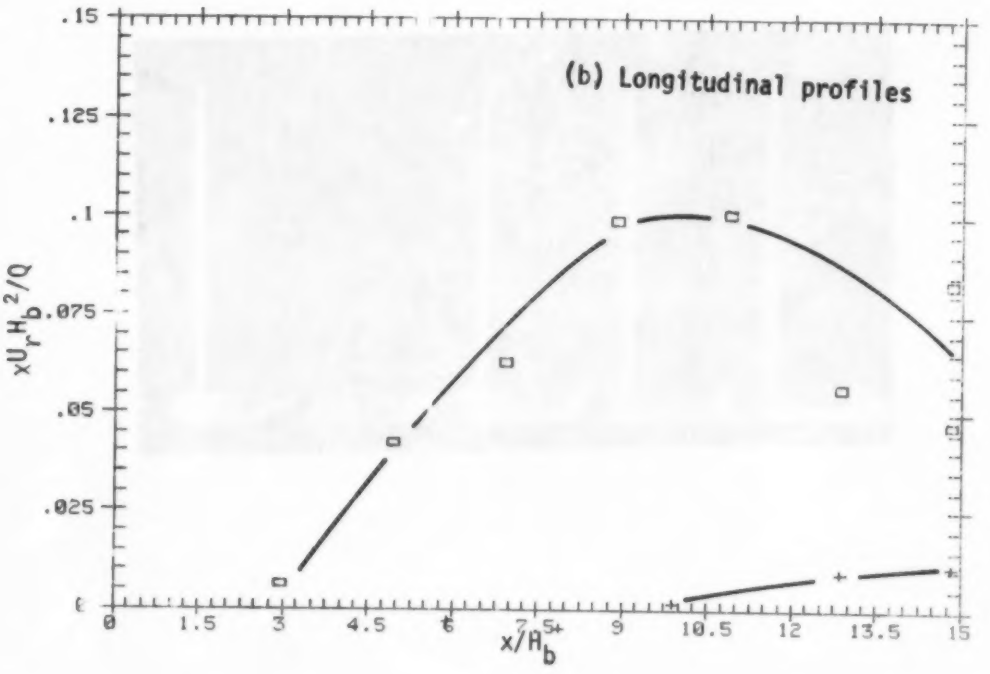

Figure A-18. Case No. 10 concentration measurements.

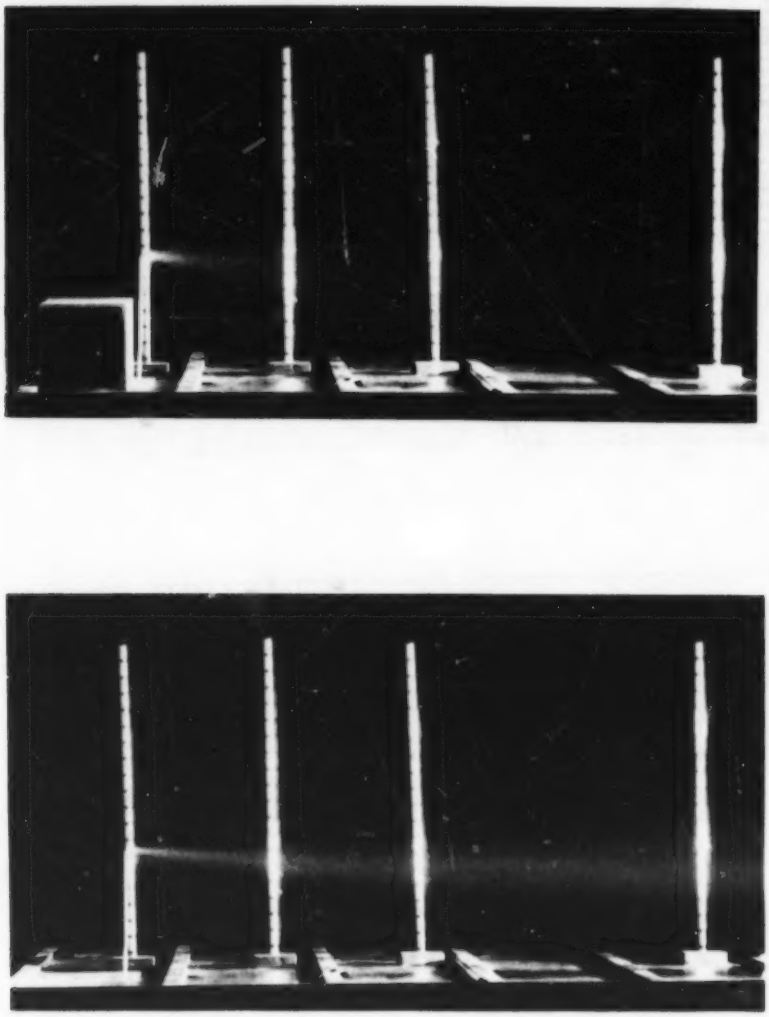

Figure A-19. Case No. 11 smoke visualization (1.5, 0.017, 0.4, 1.0, ∞).

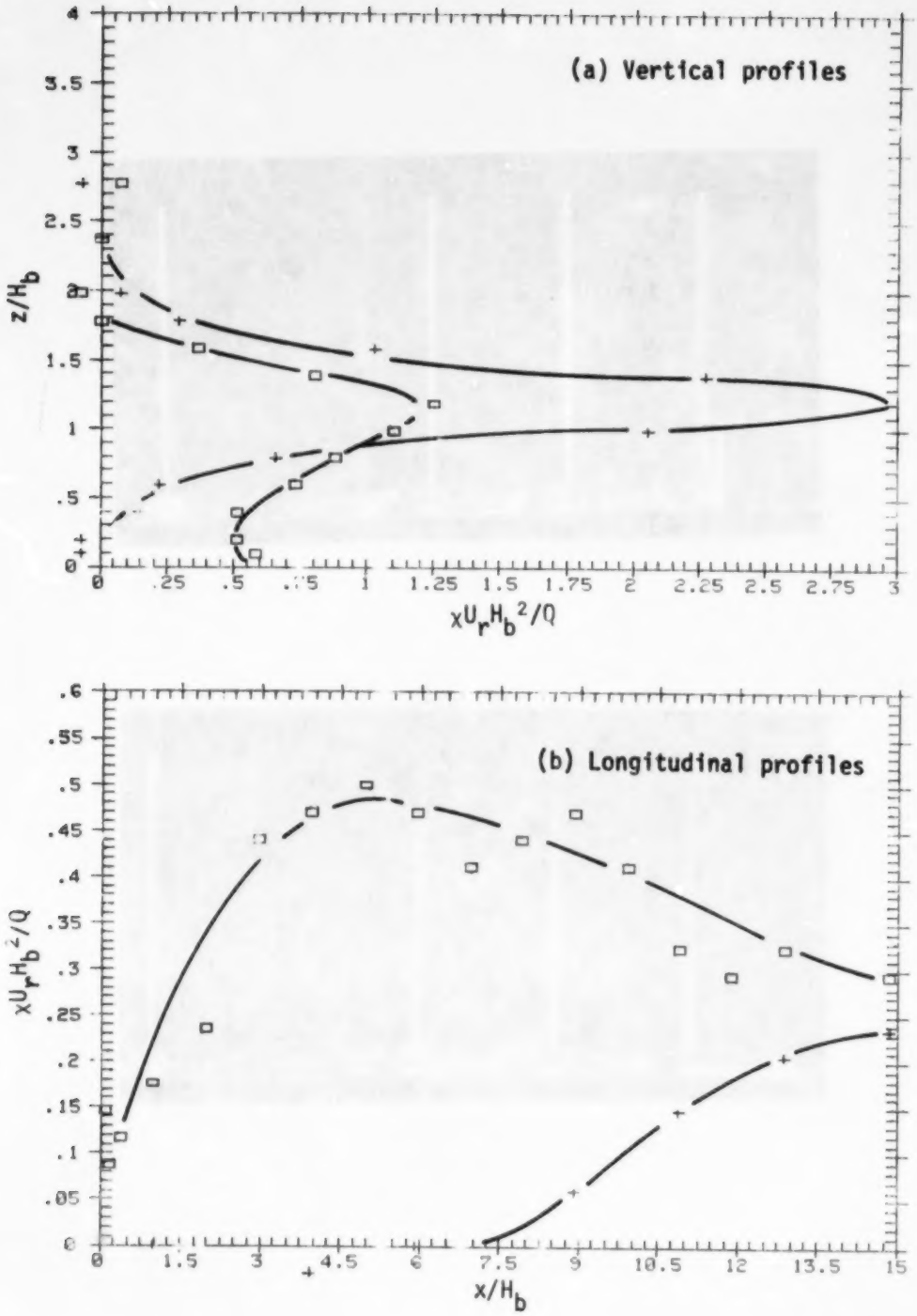

Figure A-20. Case No. 11 concentration measurements.

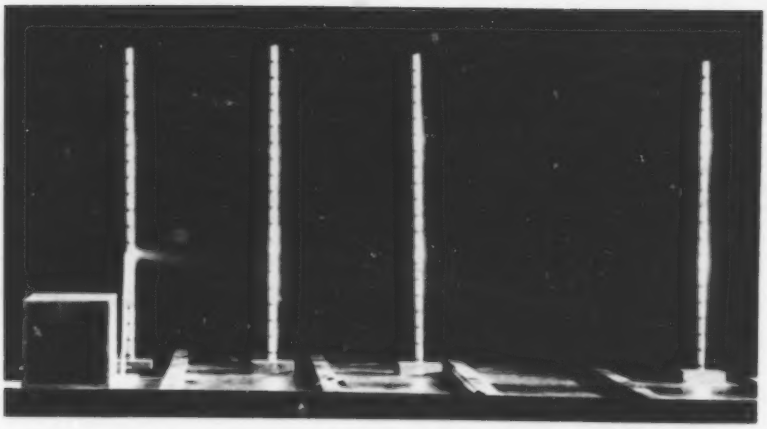

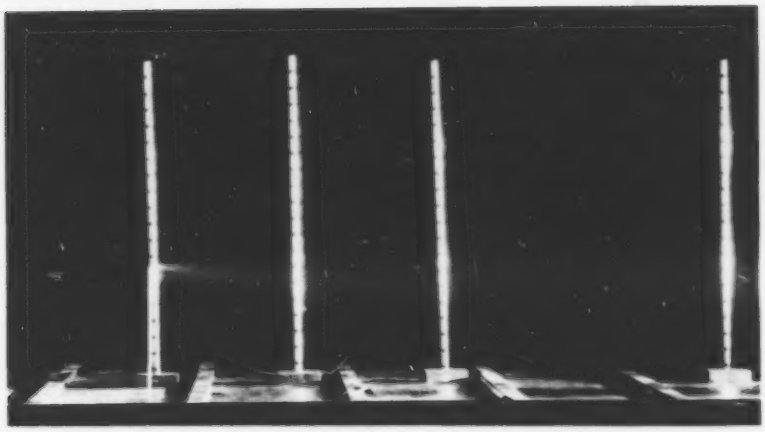

Figure A-21. Case No. 12 smoke visualization (1.5, 0.017, 0.4, 0.5, 11.0).

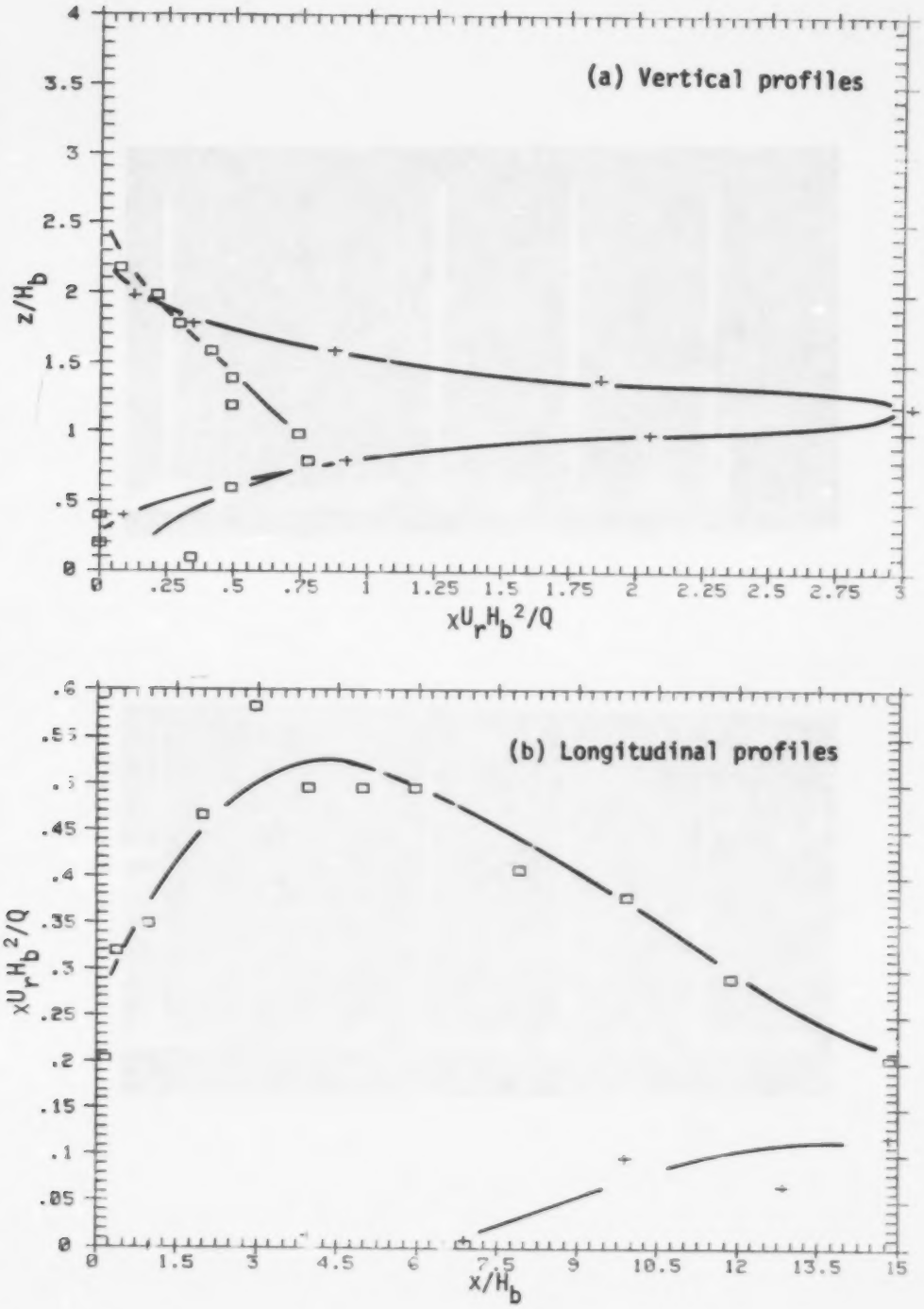

Figure A-22. Case No. 12 concentration measurements.

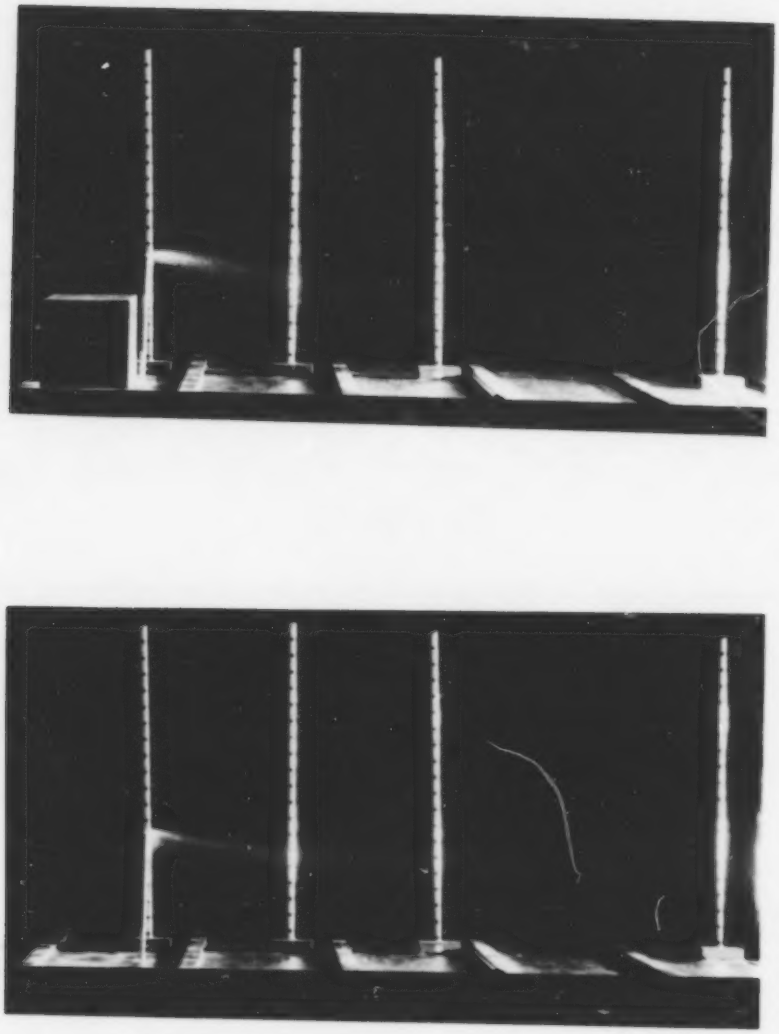

Figure A-23. Case No. 13 smoke visualization (1.5, 0.042, 0.4, 1.0, ∞).

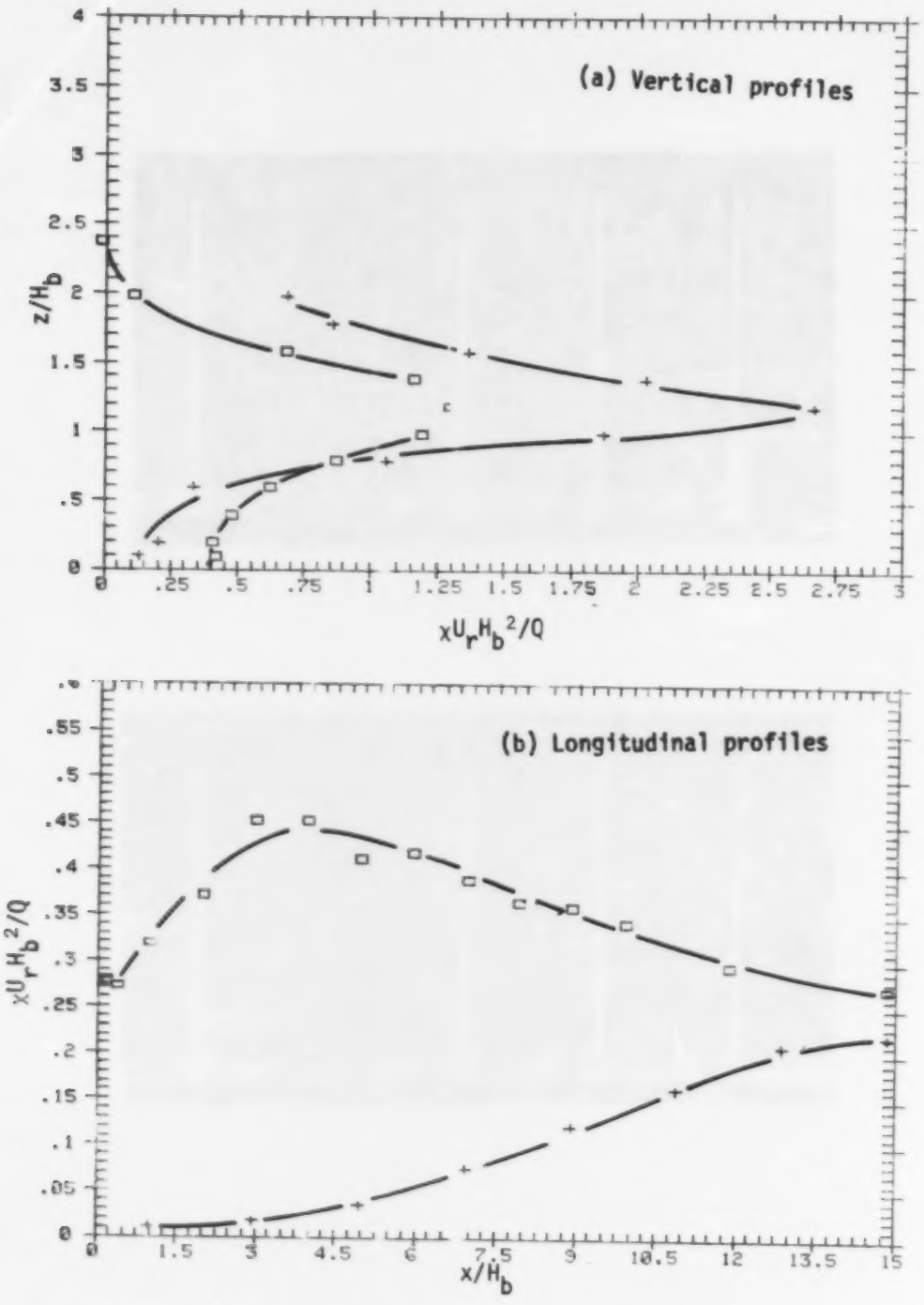

Figure A-24. Case No. 13 concentration measurements.

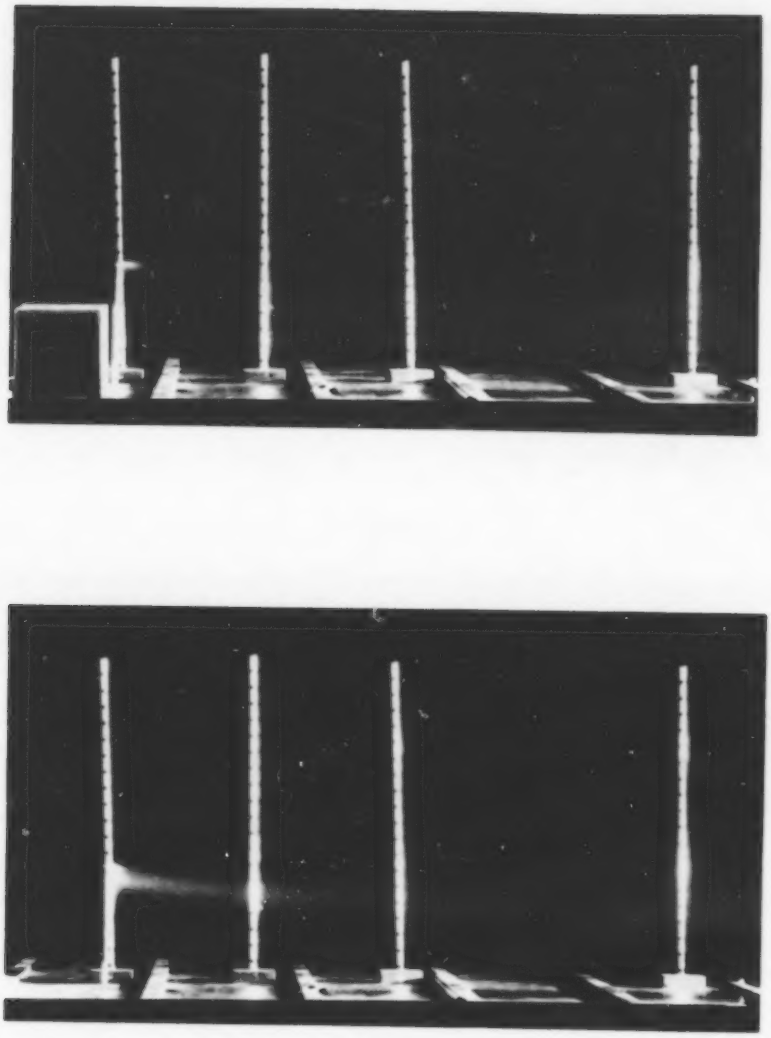

Figure A-25. Case No. 14 smoke visualization (1.5, 0.042, 0.4, 0.5, 5.8).

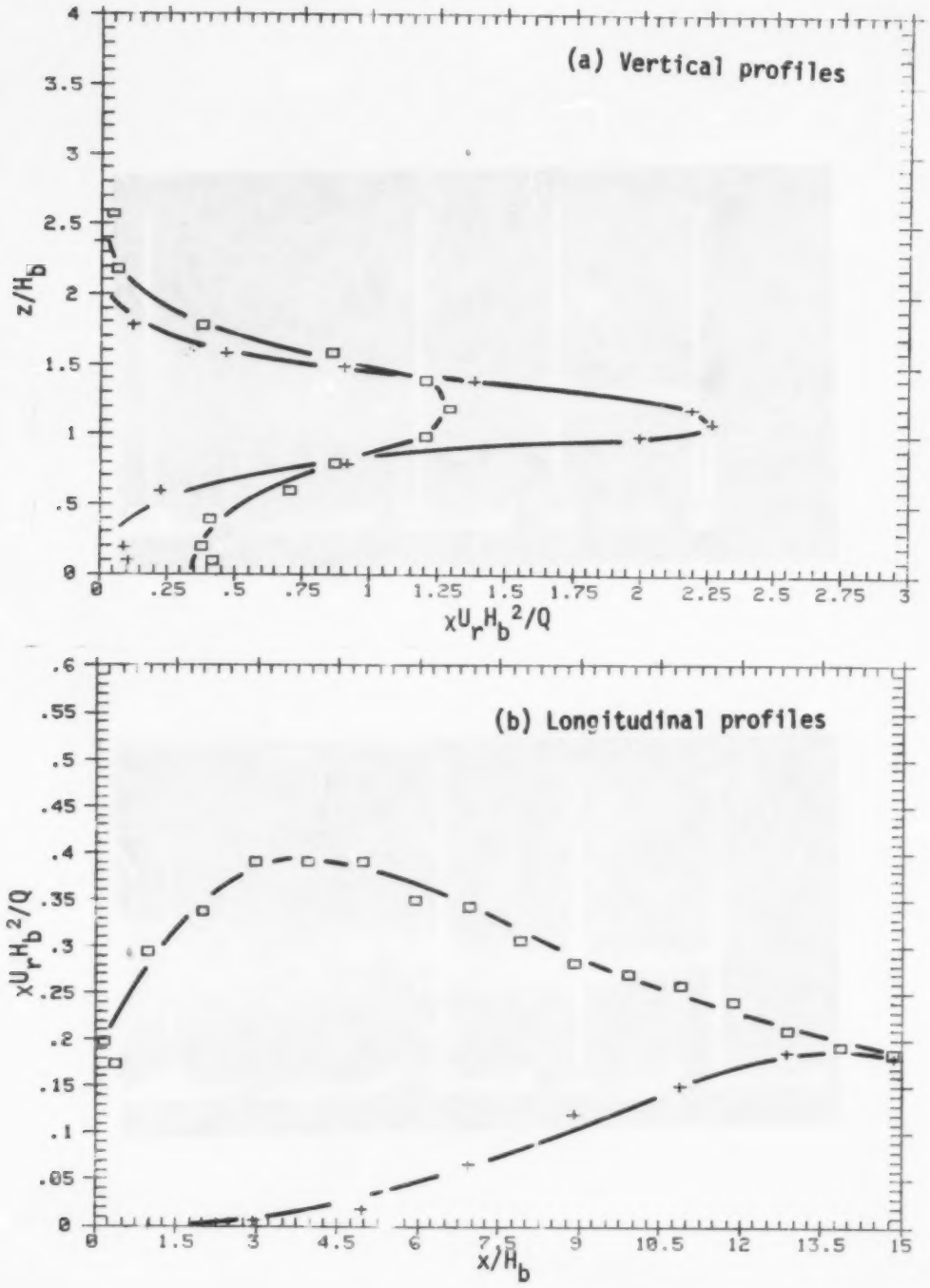

Figure A-26. Case No. 14 concentration measurements.

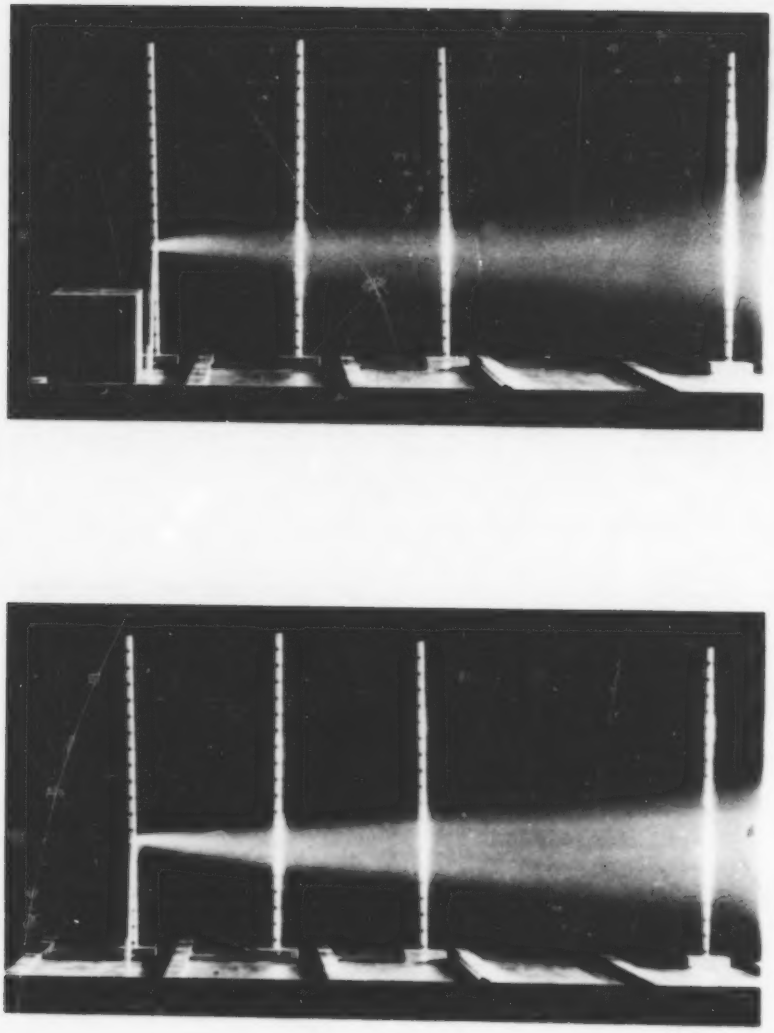

Figure A-27. Case No. 15 smoke visualization (1.5, 0.042, 0.7, 1.0, ∞).

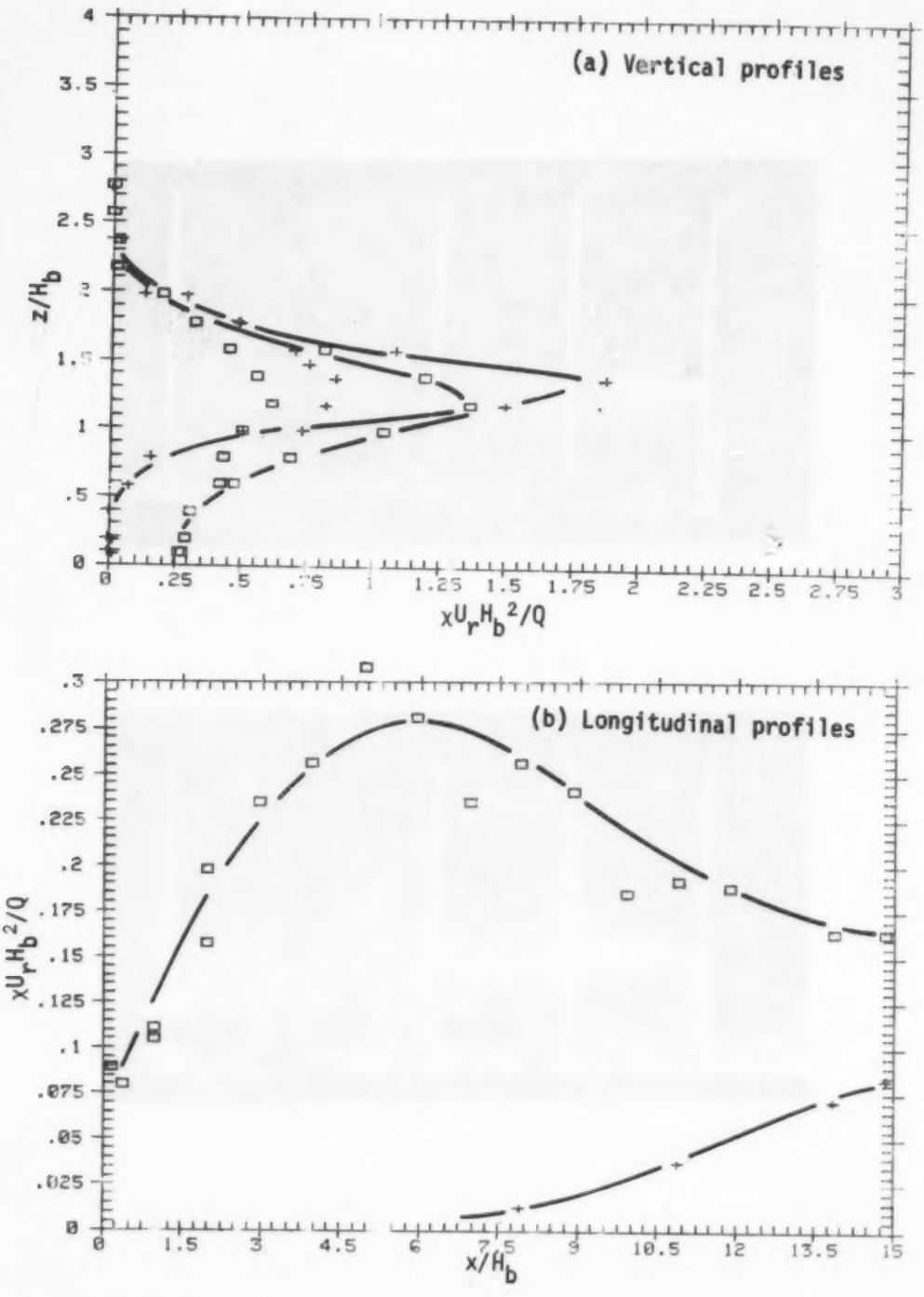

Figure A-28. Case No. 15 concentration measurements.

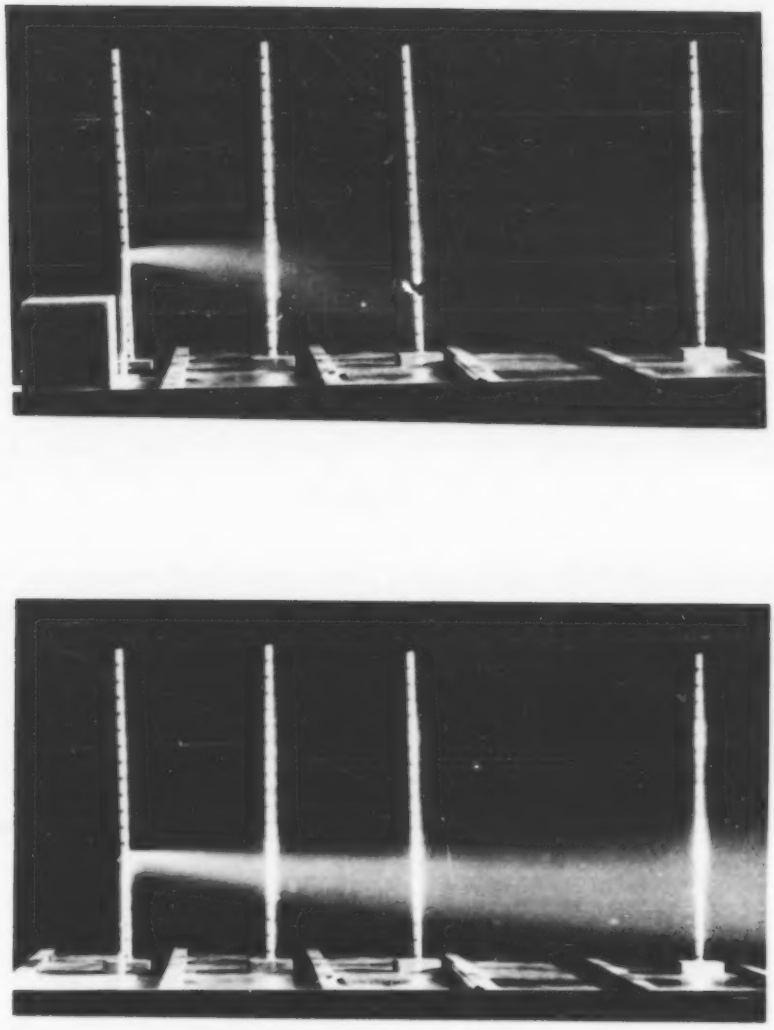

Figure A-29. Case No. 16 smoke visualization (1.5, 0.042, 0.7, 0.5, 5.8).

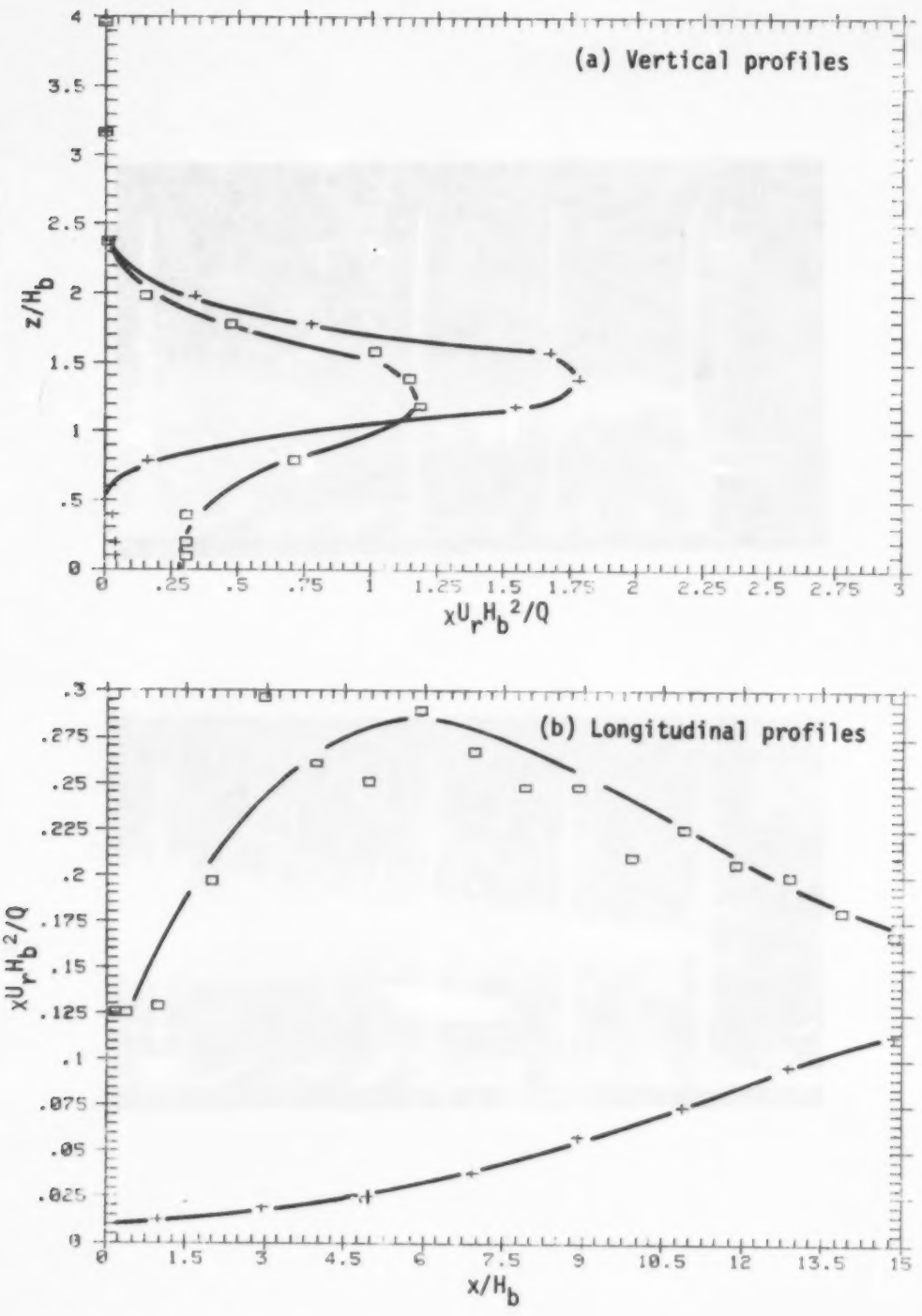

Figure A-30. Case No. 16 concentration measurements.

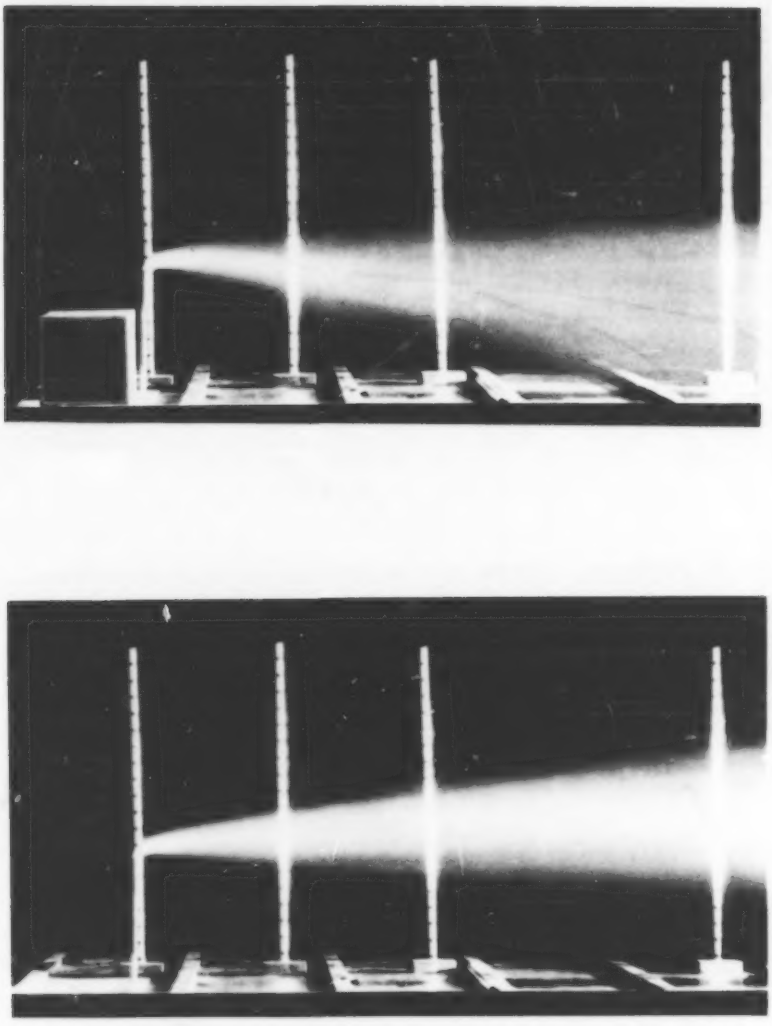

Figure A-31. Case No. 17 smoke visualization (1.5, 0.042, 1.5, 1.0, ∞).

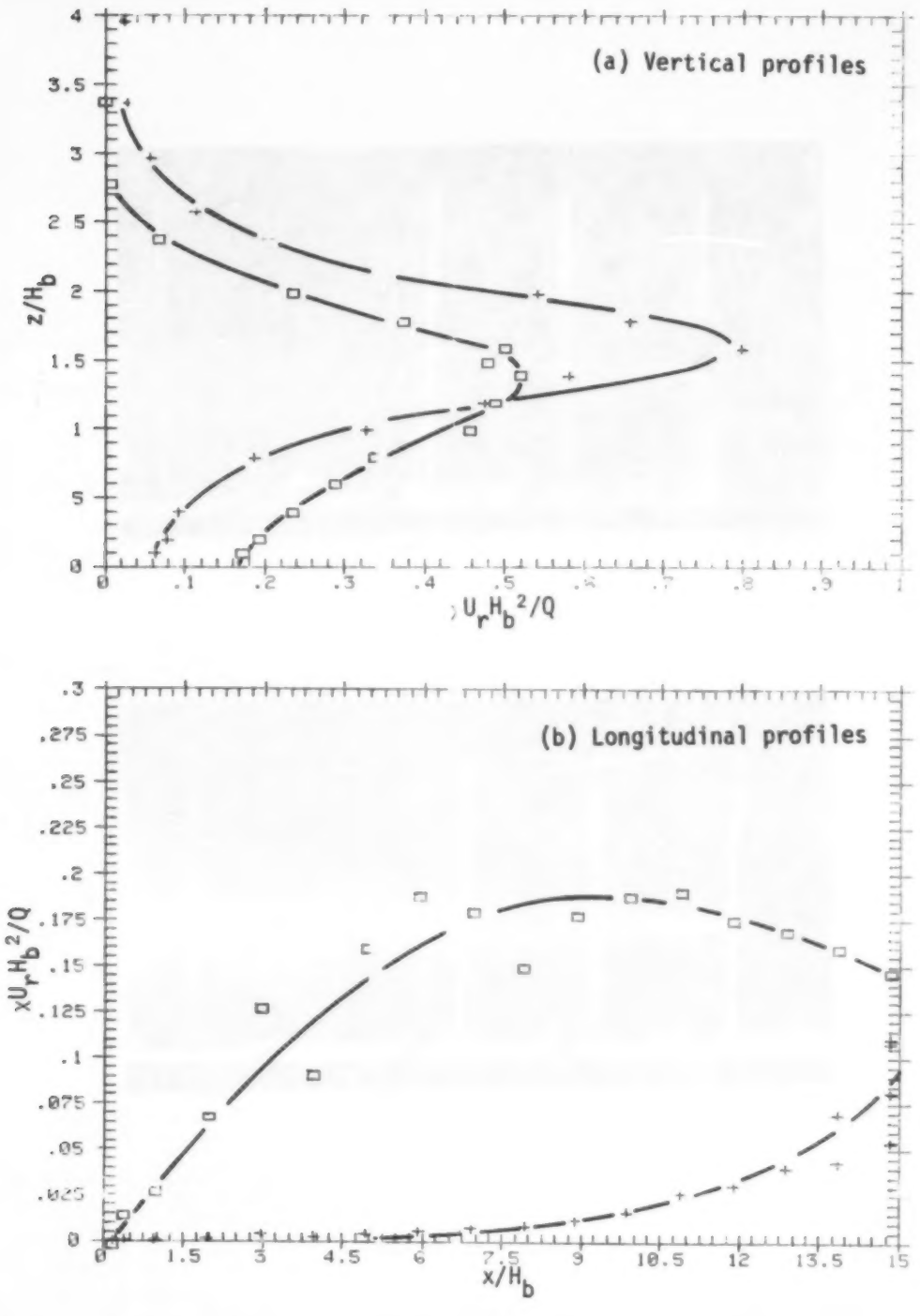

Figure A-32. Case No. 17 concentration measurements.

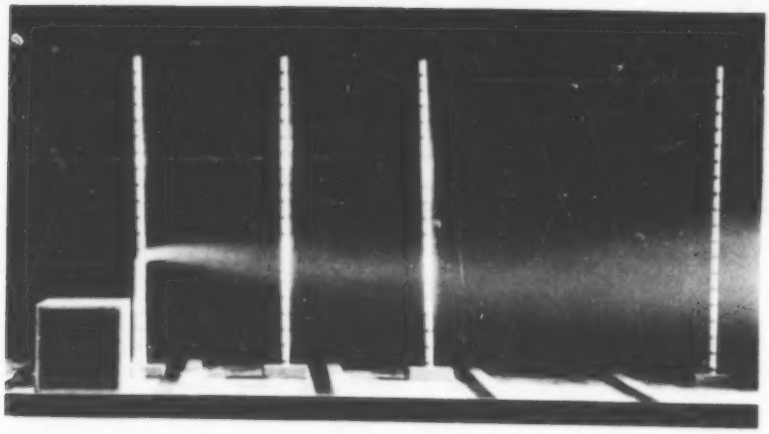

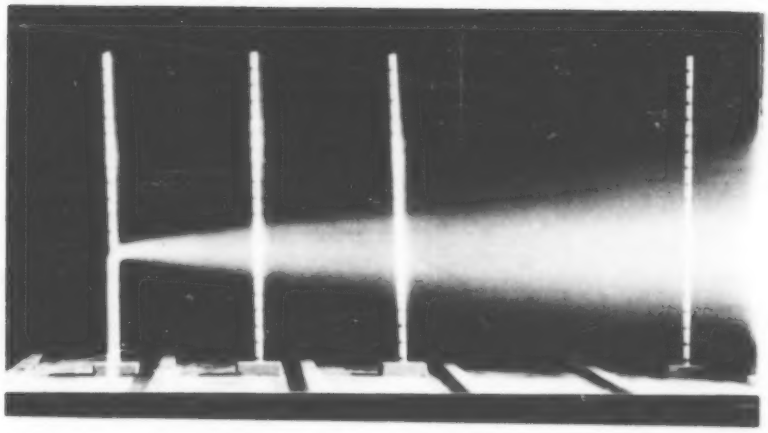

Figure A-33. Case No. 18 smoke visualization (1.5, 0.042, 1.5, 0.5, 13.0).

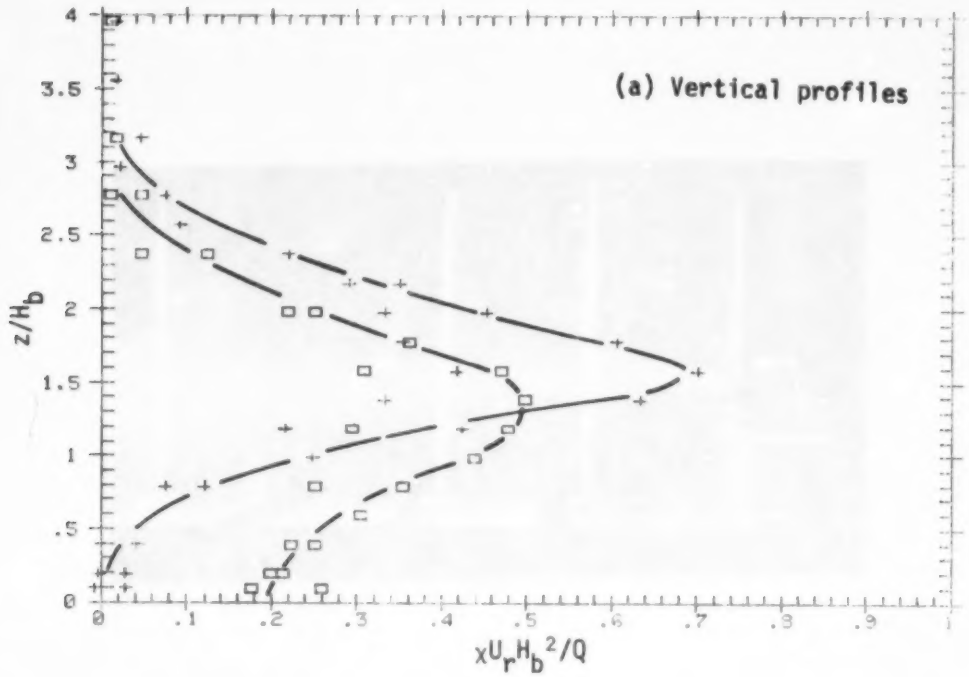

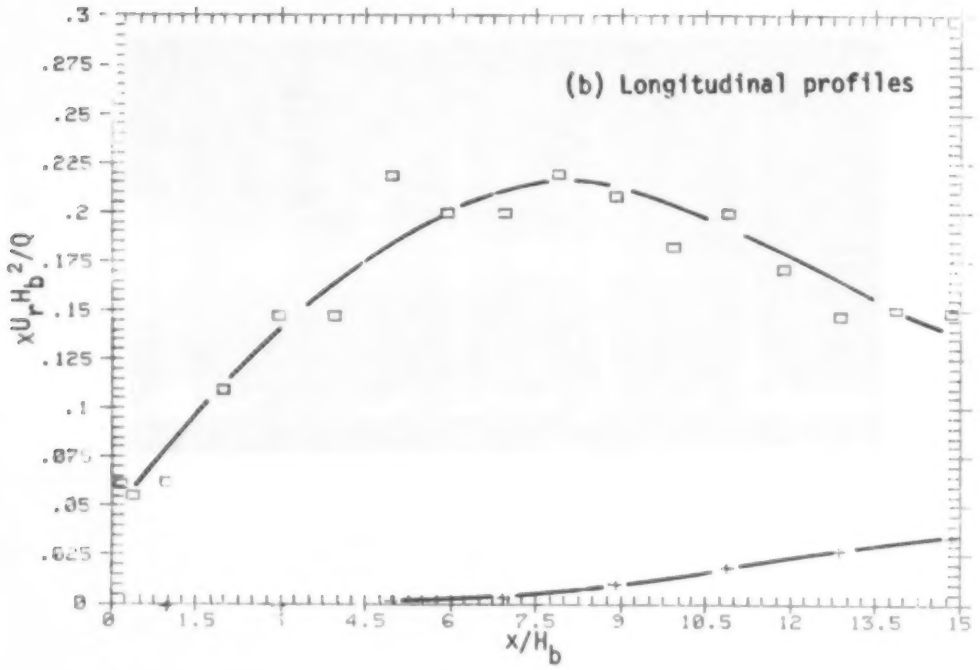

Figure A-34. Case No. 18 concentration measurements.

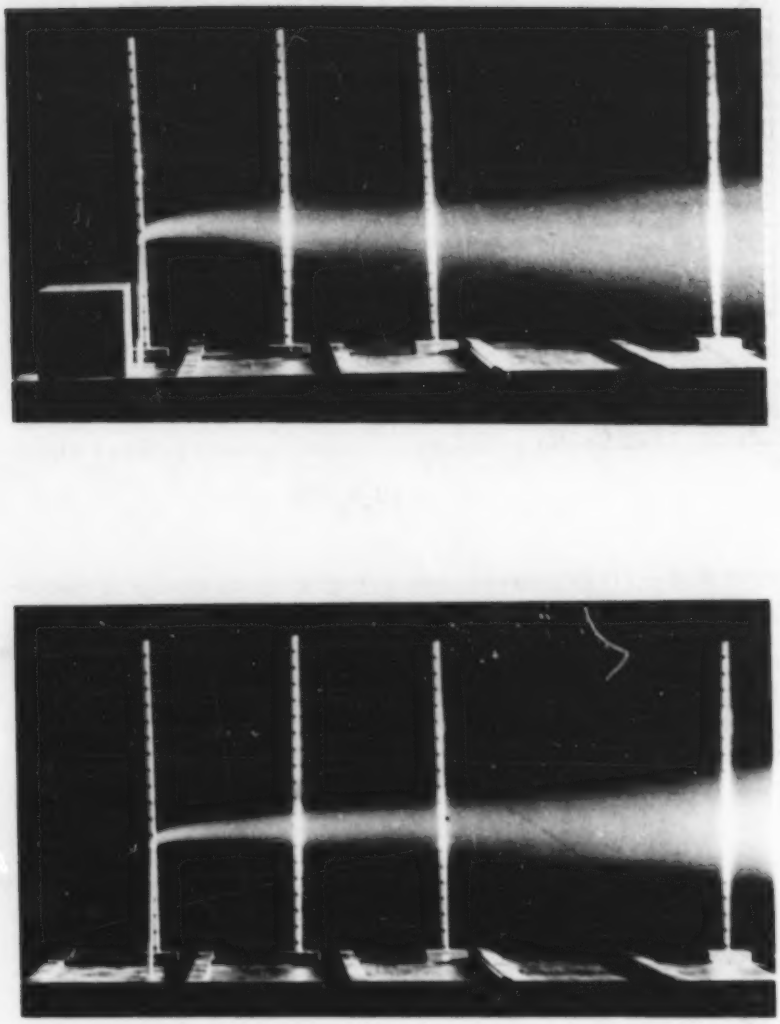

Figure A-34. Case No. 19 smoke visualization (1.5, 0042, 2.2, 1.0, ∞).

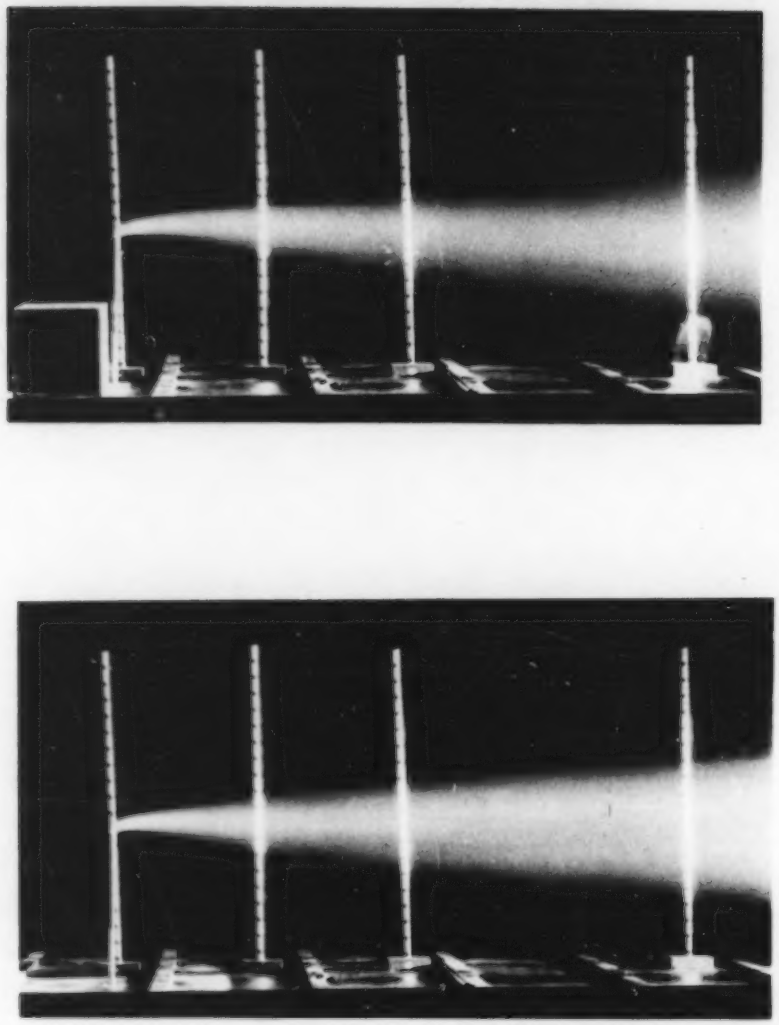

Figure A-36. Case No. 20 smoke visualization (1.8, 0.035, 0.7, 1.0, ∞).

Preceding page blank

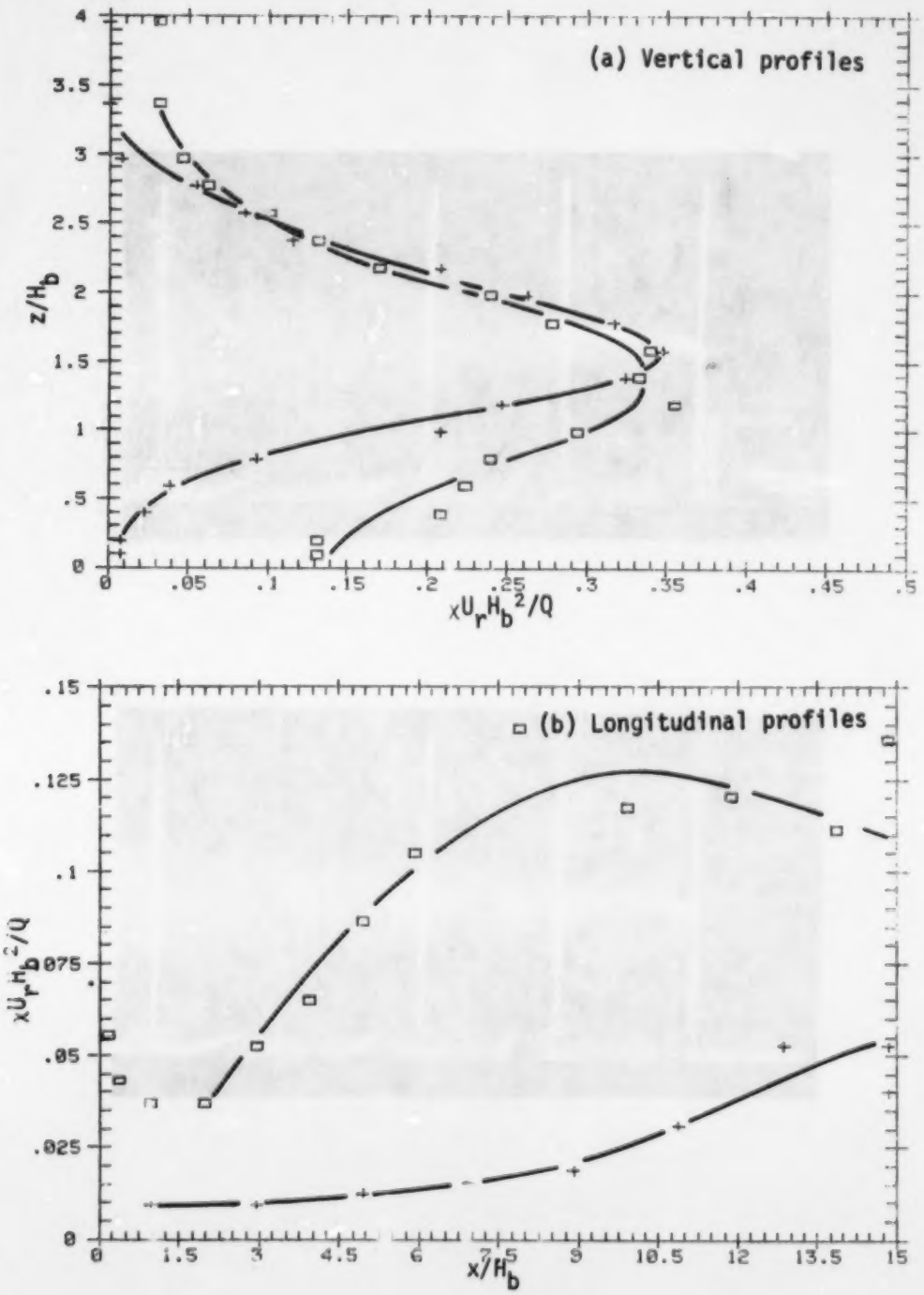

Figure A-37. Case No. 20 concentration measurements.

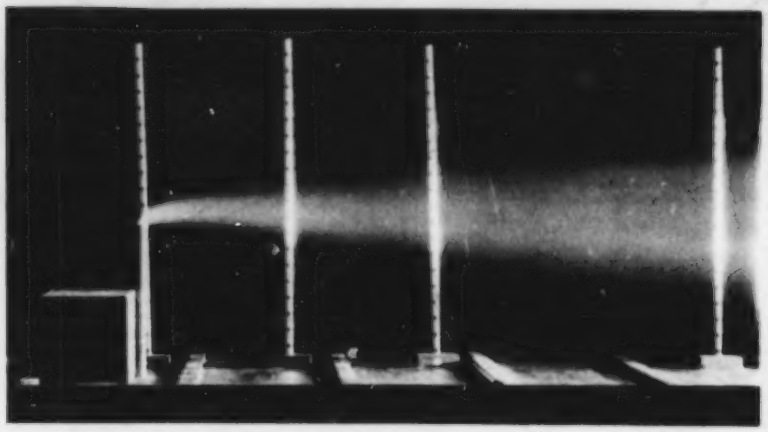

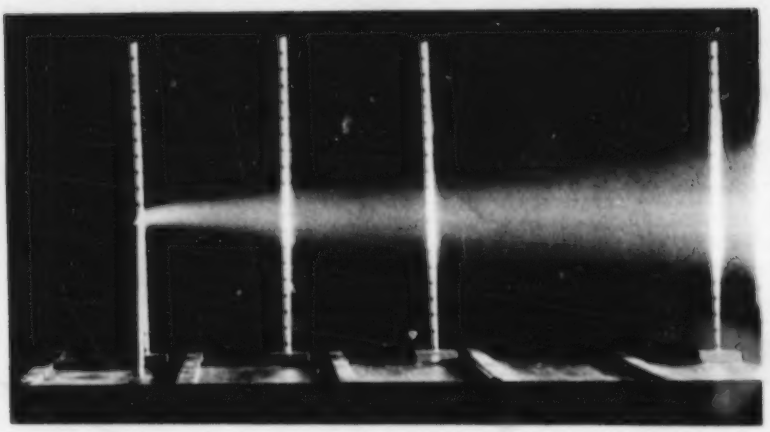

Figure A-38. Case No. 21 smoke visualization (1.8, 0.059, 0.7, 1.0, -).

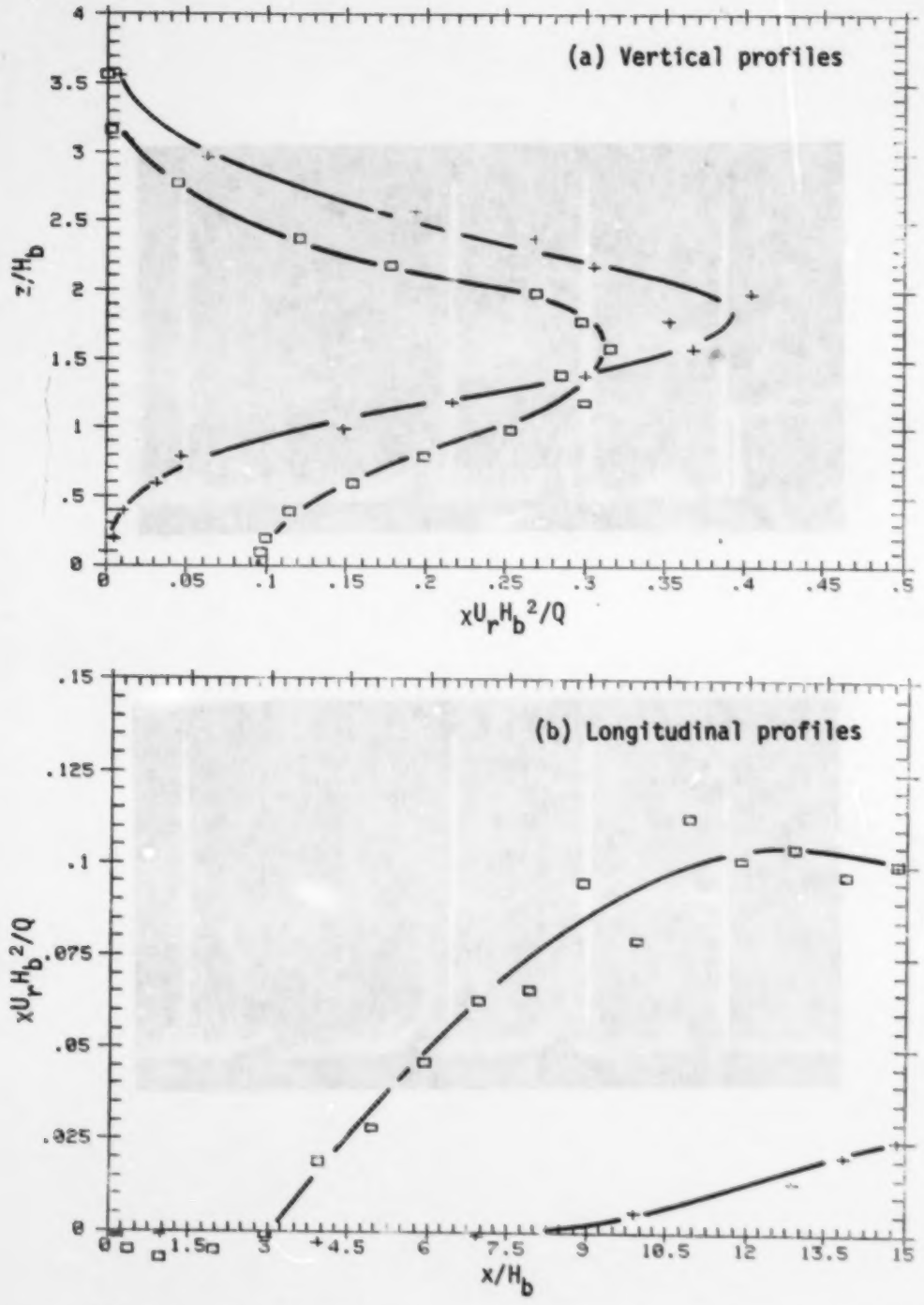

Figure A-39. Case No 21 concentration measurements.

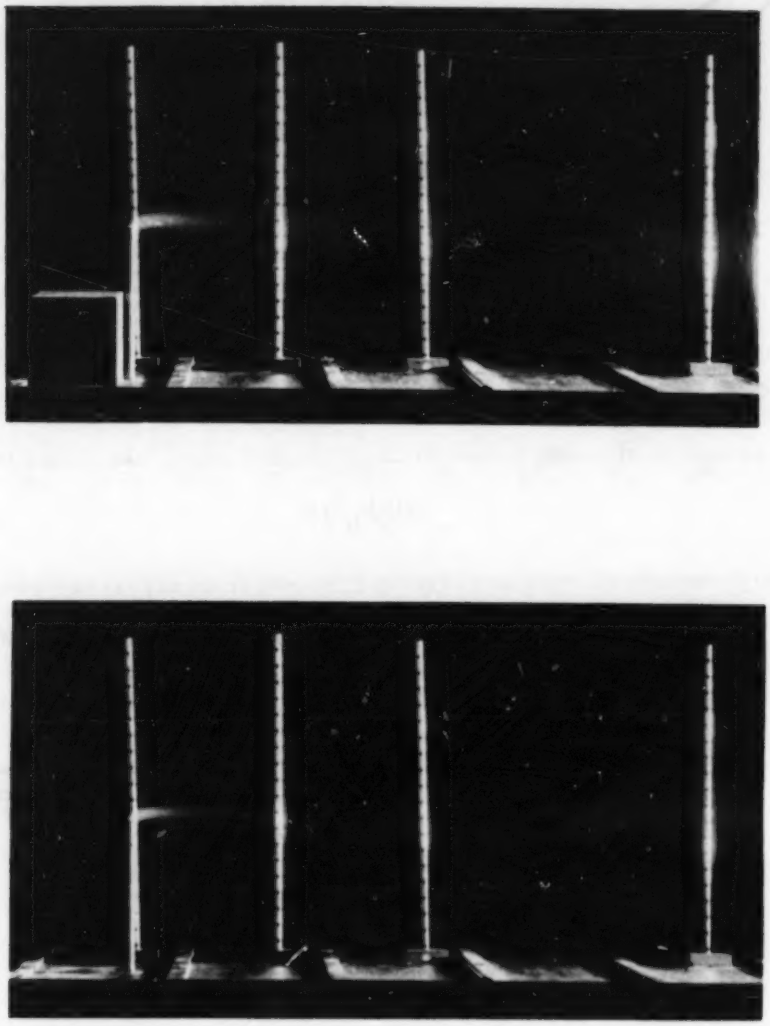

Figure A-40. Case No. 22 smoke visualization (1.8, 0.059, 0.7, 0.5, 4.5).

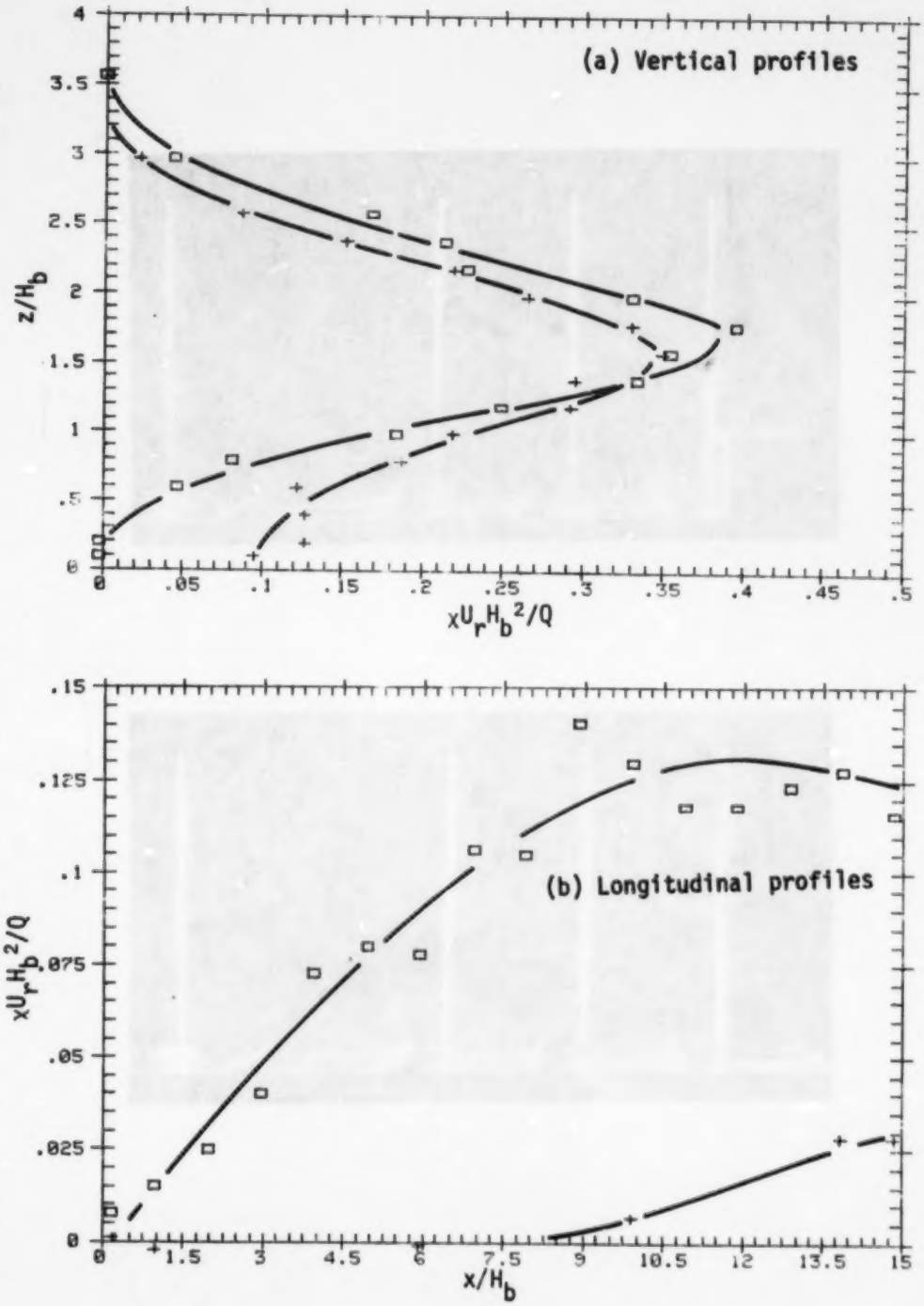

Figure A-41. Case No. 22 concentration measurements.

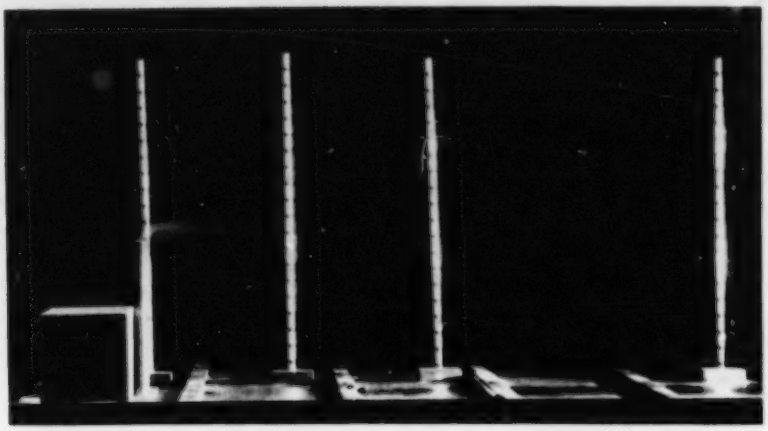

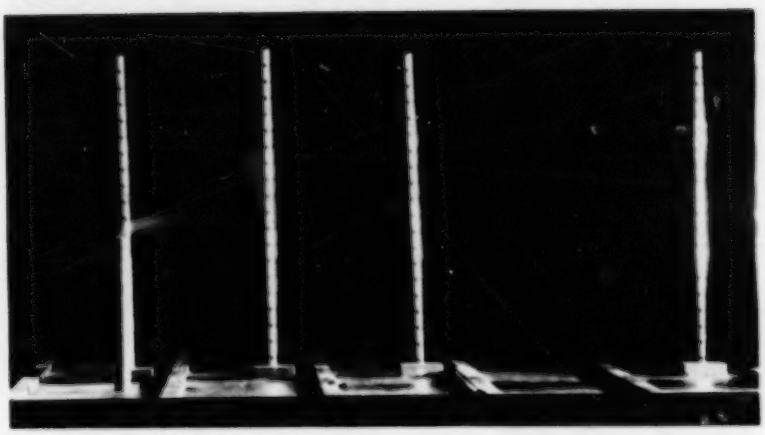

Figure A-42. Case No. 23 smoke visualization (1.8, 0.091, 0.7, 1.0, ∞).

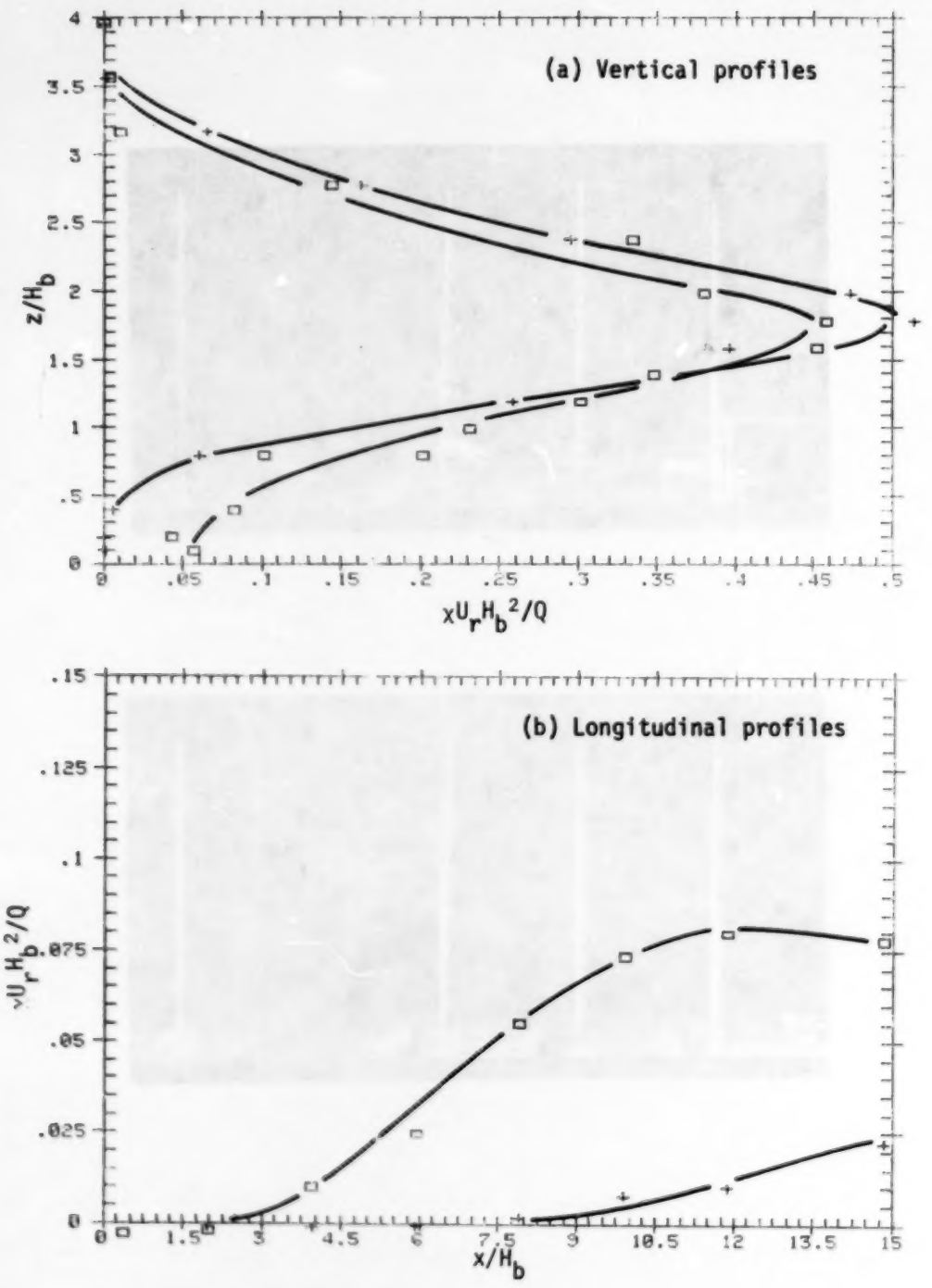

Figure A-43. Case No. 23 concentration measurements.

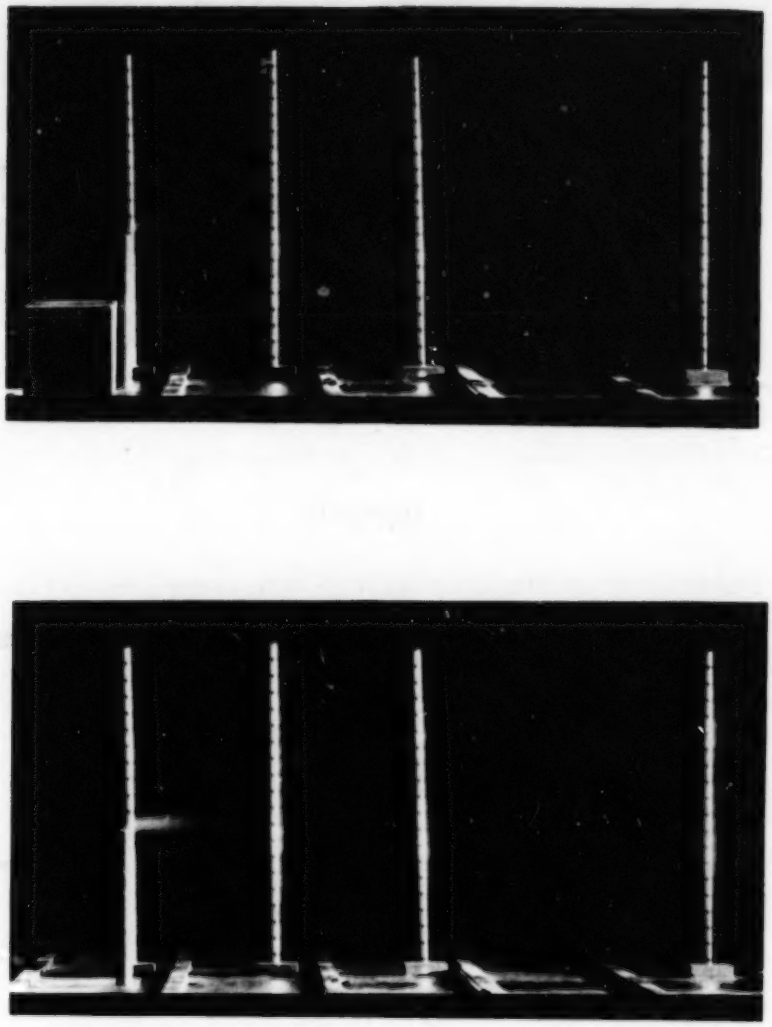

Figure A-44. Case No. 24 smoke visualization (1.8, 0.091, 0.7, 0.5, 4.2).

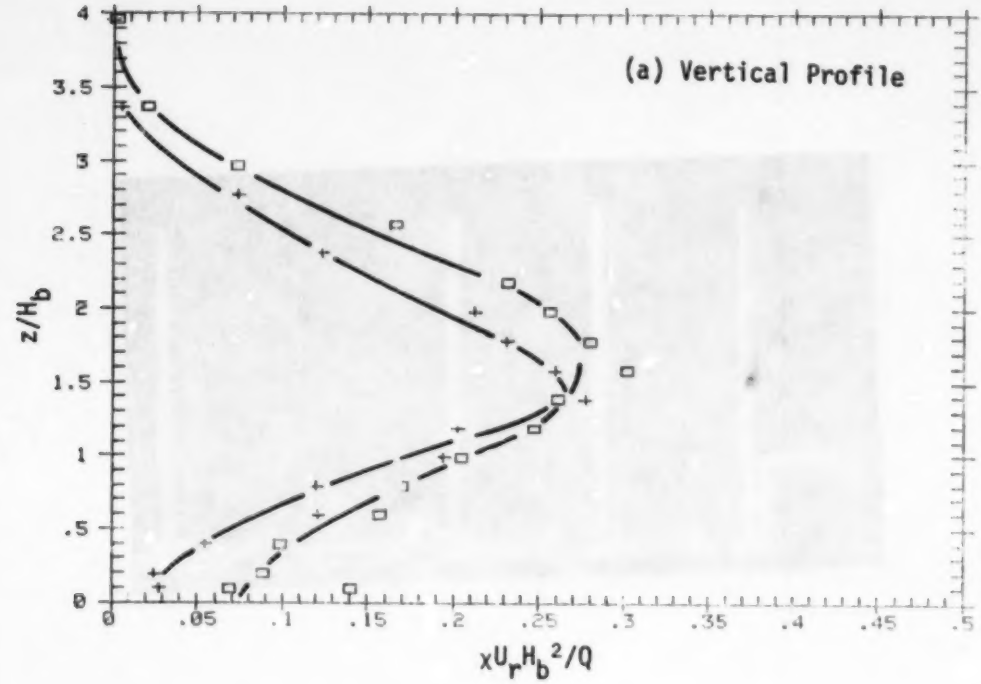

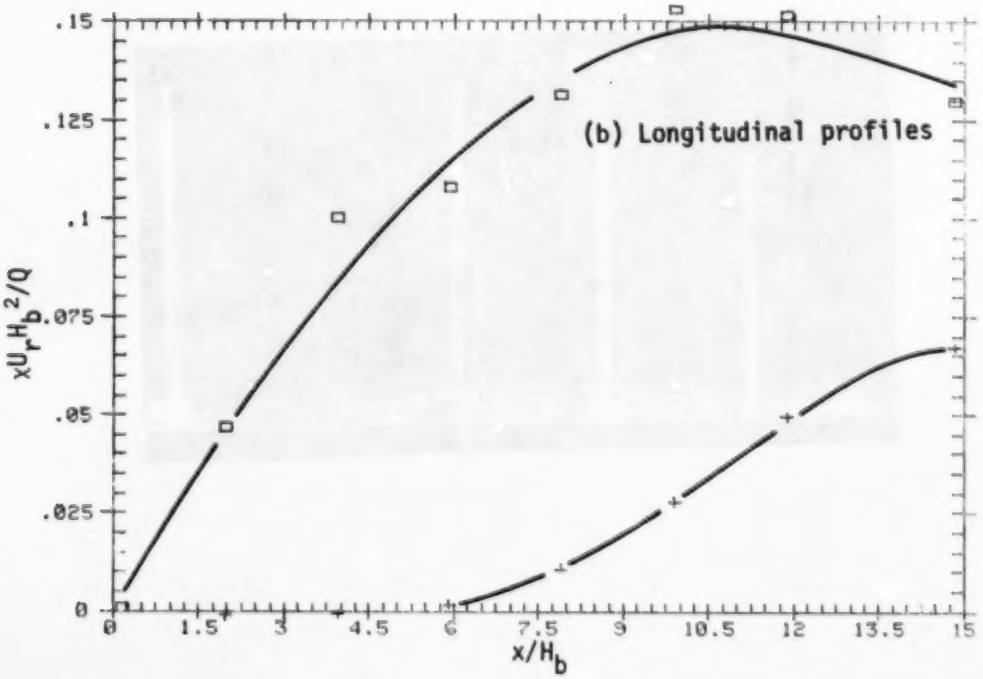

Figure A-45. Case No. 24 concentration measurements.

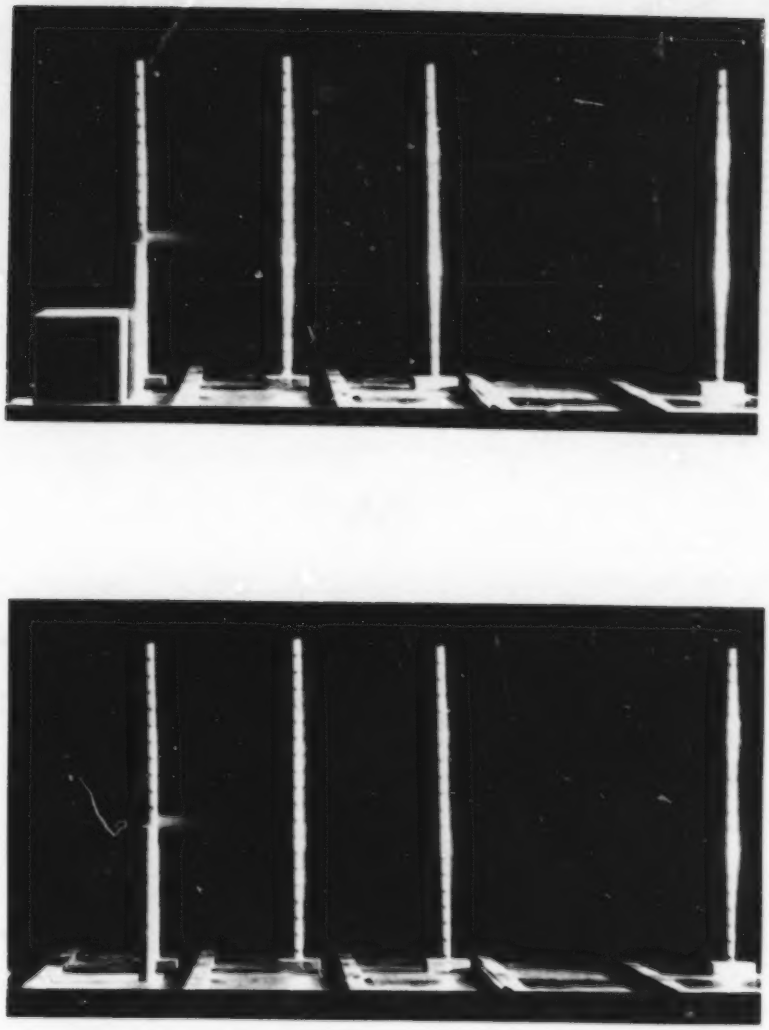

Figure A-46. Case No. 25 smoke visualization (1.8, 0.091, 0.4, 1.0, ∞).

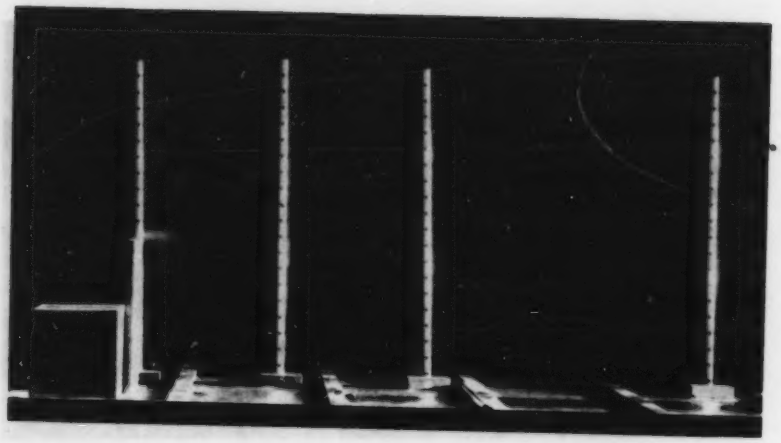

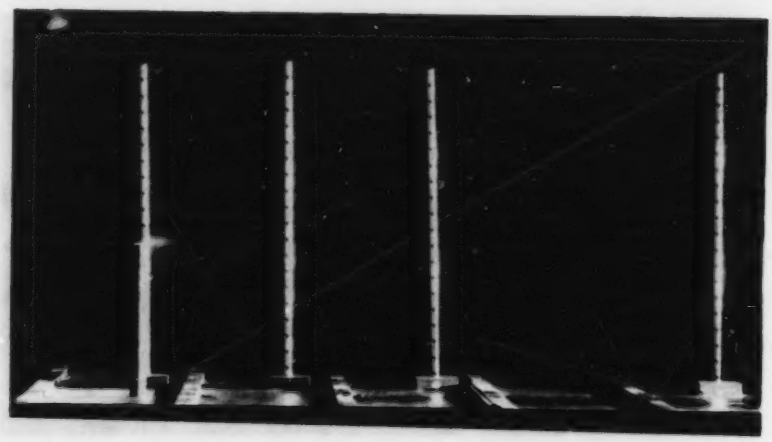

Figure A-47. Case No. 26 smoke visualization (1.8, 0.091, 0.4, 0.5, 4.2).

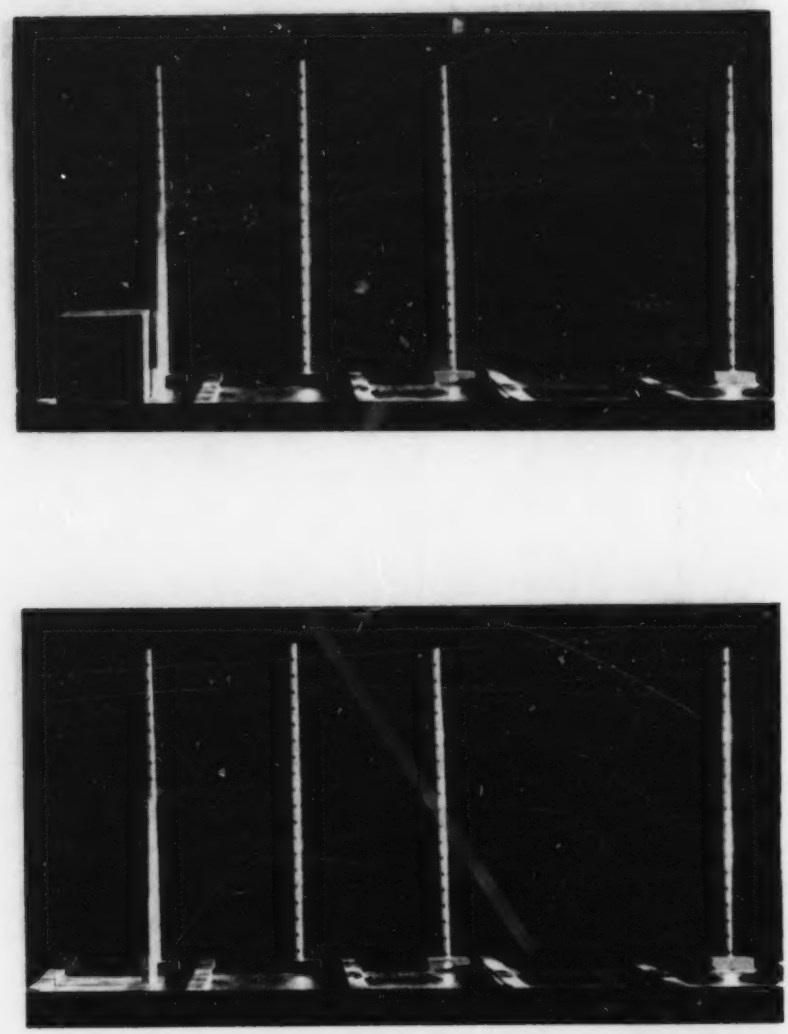

Figure A-48. Case No. 27 smoke visualization (2.15, 0.076, 0.7, 1.0, ∞).

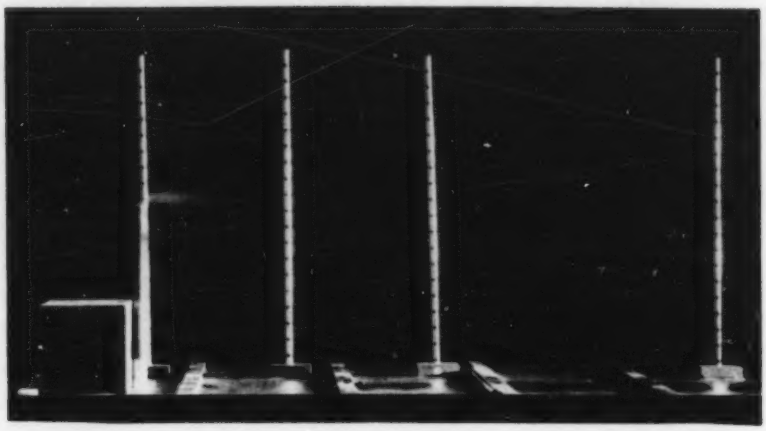

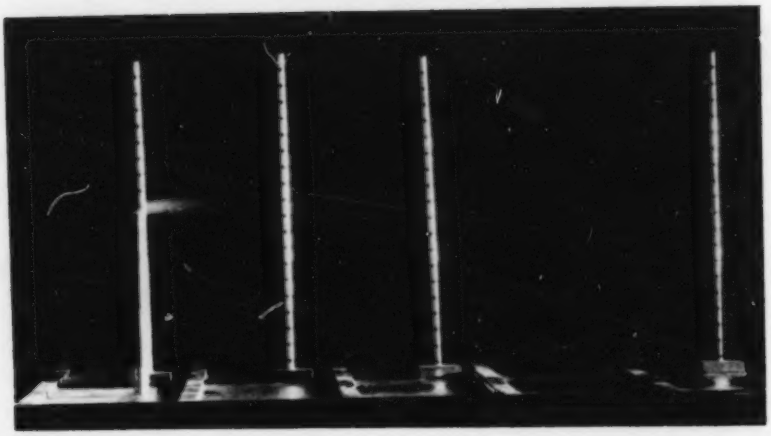

Figure A-49. Case No. 28 smoke visualization (2.15, 0.076, 0.7, 0.5, 4.2).

Preceding page blank

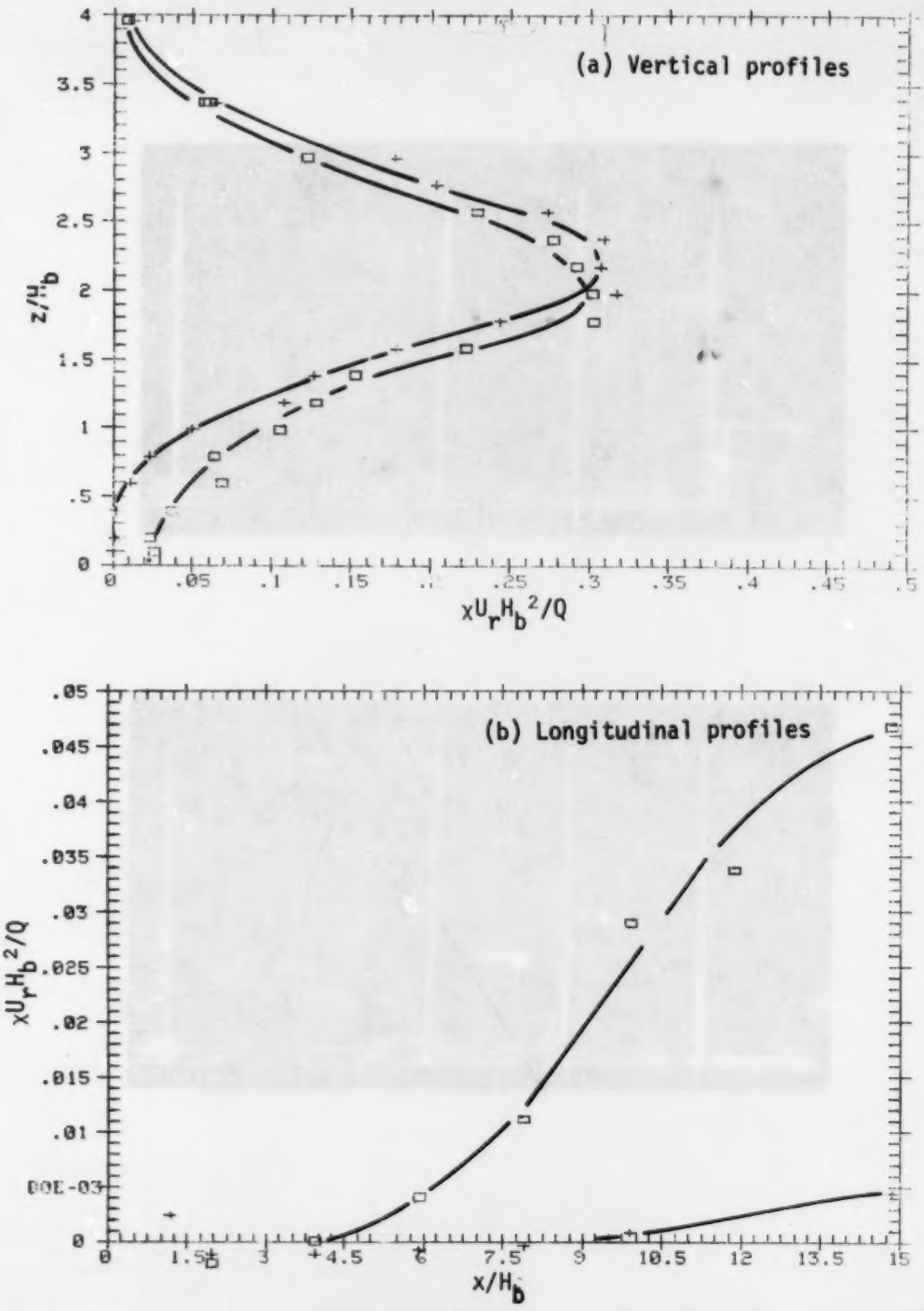

Figure A-50. Case No. 28 concentration measurements.

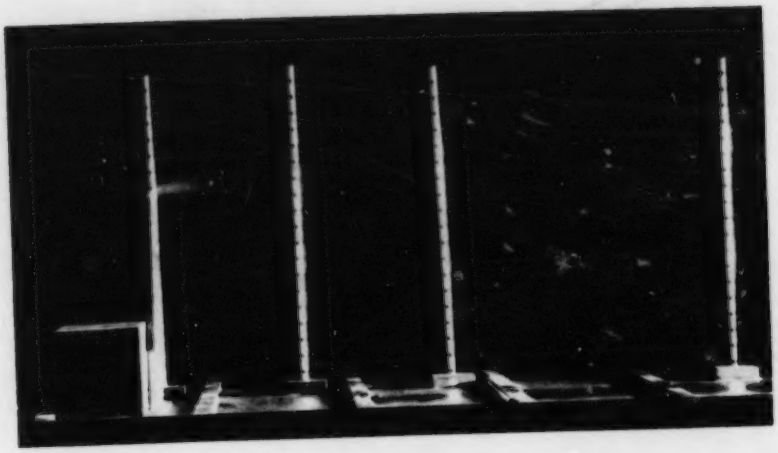

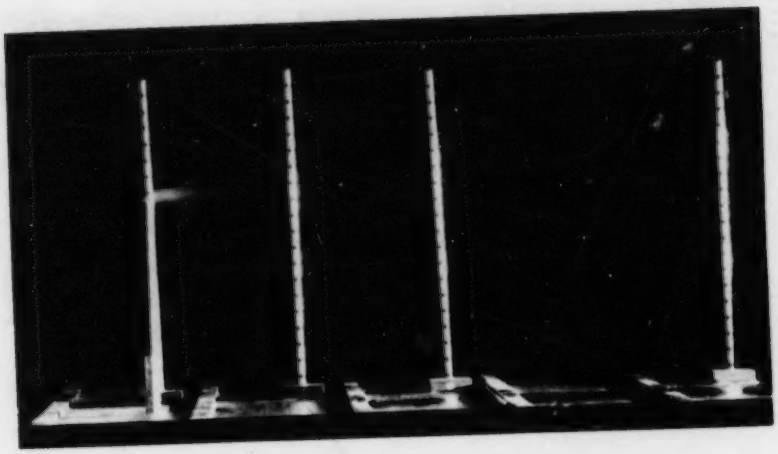

Figure A-51. Case No. 29 smoke visualization (2.5, 0.065, 0.7, 1.0, ∞).

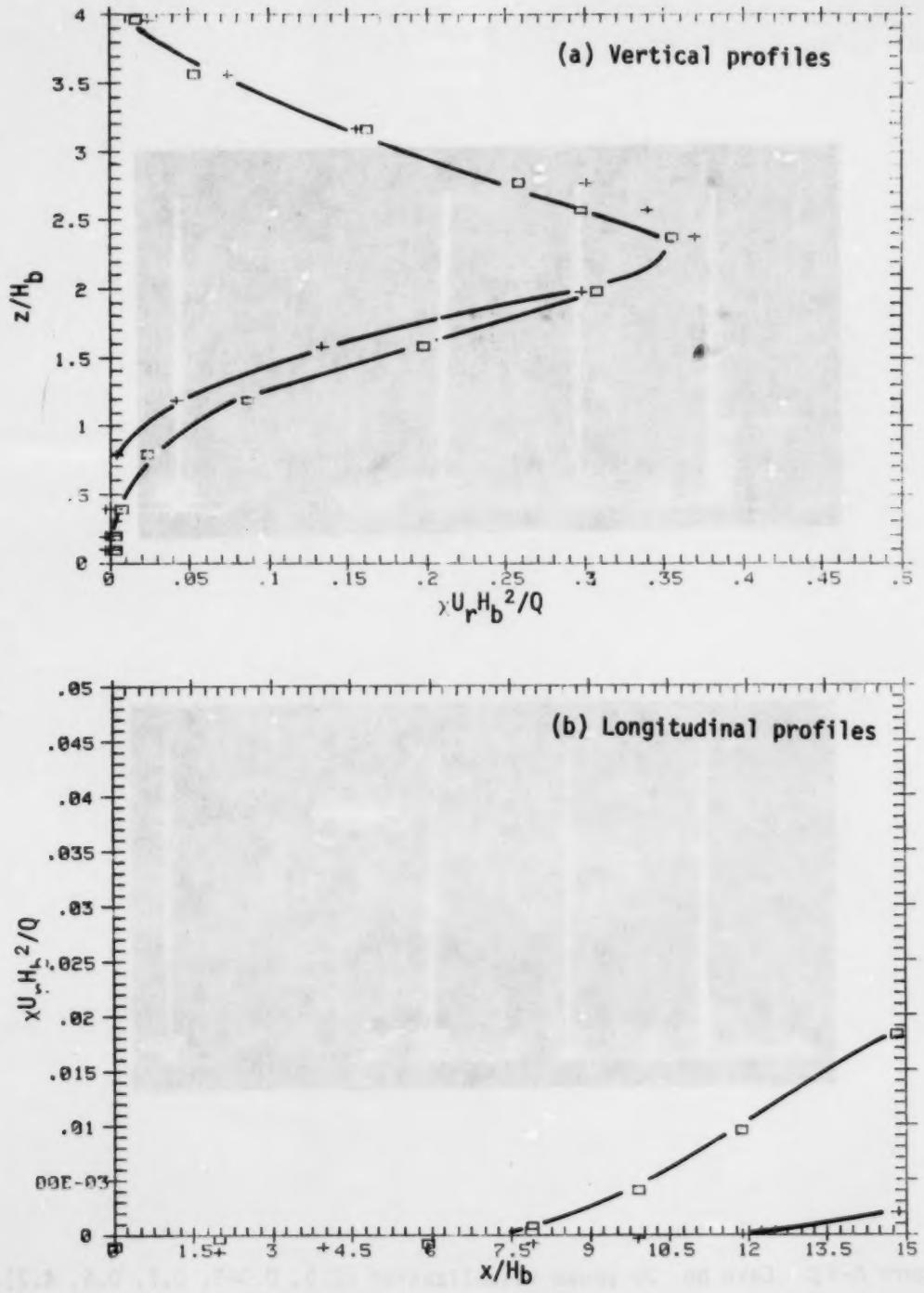

Figure A-52. Case No. 29 concentration measurements.

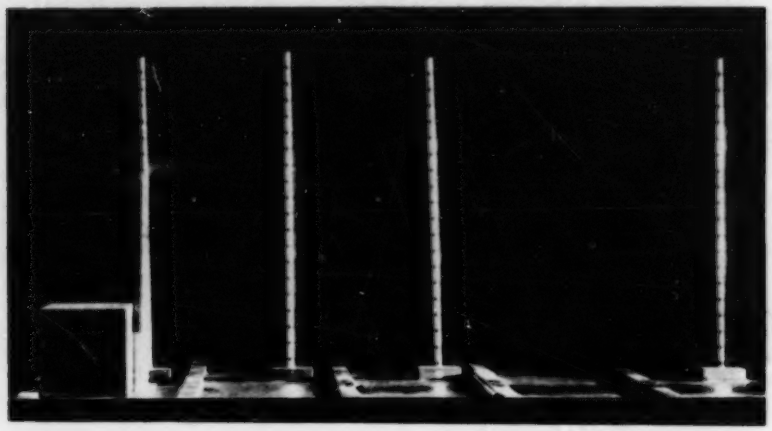

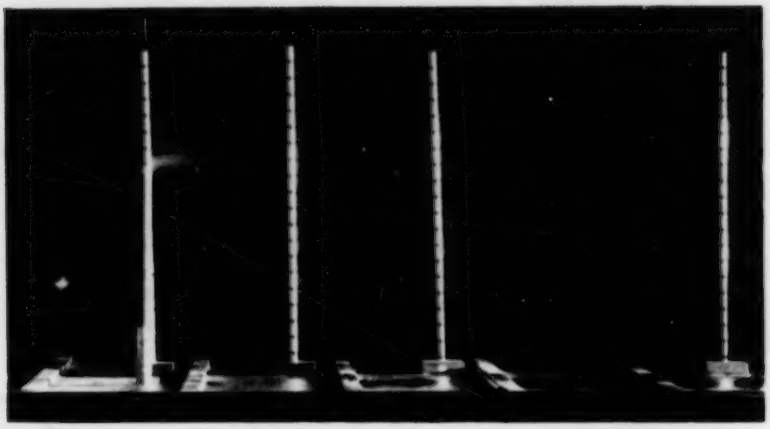

Figure A-53. Case No. 30 smoke visualization (2.5, 0.065, 0.7, 0.5, 4.2).

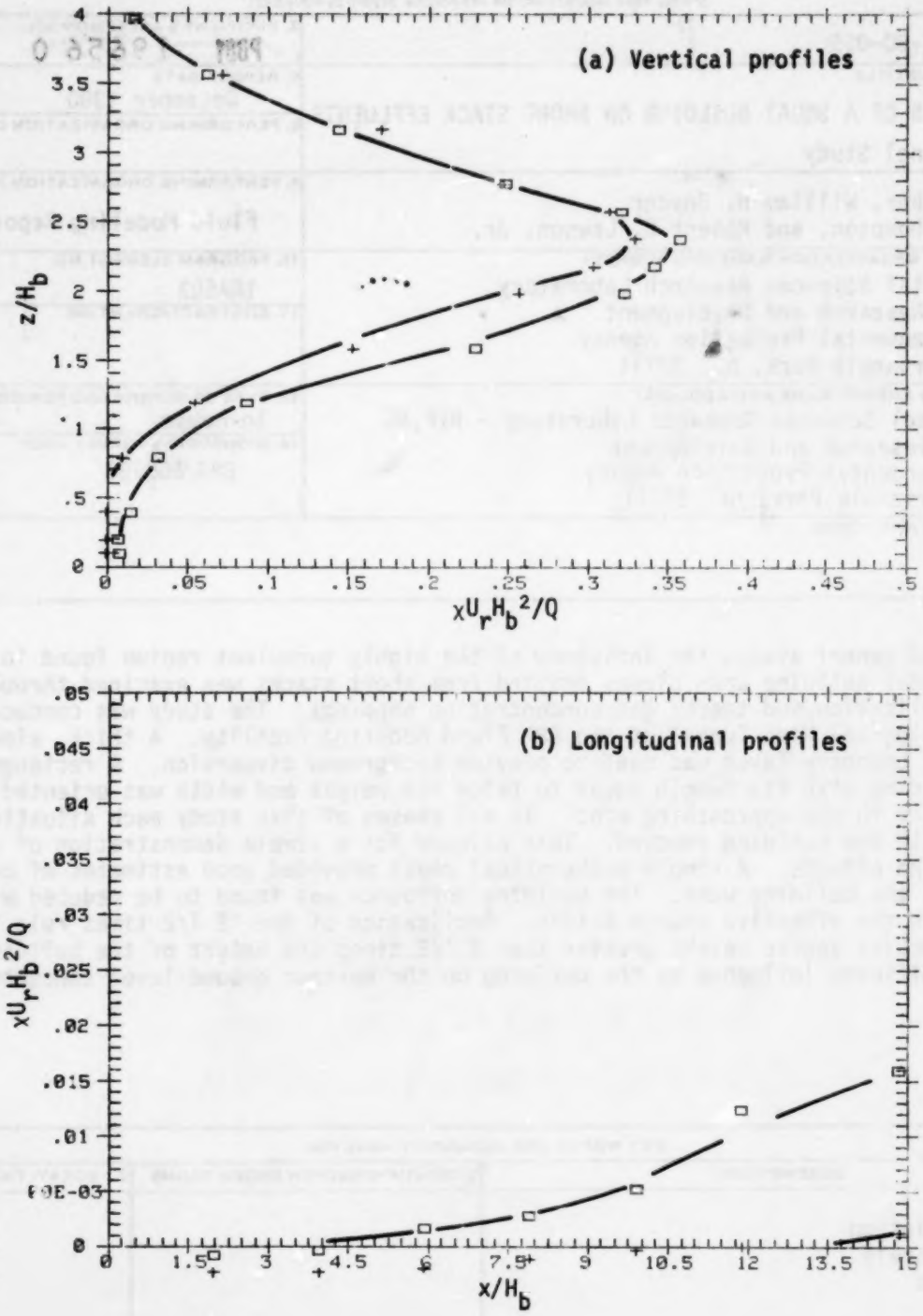

Figure A-54. Case No. 30 concentration measurements.